EXPERIMENTAL ANGULAR DISTRIBUTIONS FOR LOW ENERGY ELECTRONS SCATTERED BY ARGON, HELIUM, ATOMIC AND MOLECULAR HYDROGEN.

by

Kevin G. Williams, B. Sc. (Hons.)

Department of Physics.

A thesis submitted for the degree of

Doctor of Philosophy

in the

University of Adelaide

February, 1969.

TABLE OF CONTENTS

SUMMARY

This thesis describes the measurement of angular distributions for electrons scattered by argon, helium, and atomic and molecular hydrogen, using a modulated beam apparatus. Angular distributions for electrons elastically scattered from argon were measured at incident energies of 50, and 100 eV, from helium at 25, 50, 100, and 200 eV, and from molecular hydrogen at 30, 50, 100 and 200 eV. Inelastic angular distributions were also measured for the combined 2^1S, 2^3P, 2^1P excitation of He at incident energies of 100, and 200 eV, and the combined 2s, 2p excitation of H at 50, 100 and 200 eV. Excitation of the b $\left(^3\Sigma_u^+\right)$ state of H_2 was observed at 50, 100 and 200 eV. The angular range covered in these measurements extended generally from 20^o to 130^o.

A parallel plate electron spectrometer energy analysed the electrons scattered through a particular angle in a region which included the intersection of a crossed electron and modulated atomic/molecular beams. Phase sensitive detection was used to distinguish the beam signal from the background gas signal. Atomic hydrogen studies were performed using a partially dissociated H_2 beam. Mass spectrometer analysis of the beam was used to determine the H_2 contribution to the inelastic spectrum produced by the atomic/molecular beam. A data handling system was developed which displayed the energy spectrum of scattered electrons and recorded their elastic and inelastic angular distributions. By accumulating the beam signal in the store of a multi-channel analyser and repetitively scanning over the energy and angular range selected, errors produced by slow

drifts in experimental conditions were minimised.

Angular distributions measured for electrons elastically scattered by argon are compared with both recent calculations, and results that were obtained by others using a different experimental technique.

Excellent agreement has been obtained between the present measurements of the angular distributions of electrons elastically scattered by both helium and molecular hydrogen and the calculations of Khare and Moiseiwitsch. In particular the discrepancy at large angles between the measurements of Webb and the calculations of Khare and Moiseiwitsch are not observed.

The shape of the differential cross section calculated for the combined 2s, 2p excitation of H at 54 eV using the close coupling approximation is shown to be in good agreement with the shape of the observed angular distribution. However there is considerable discrepancy between the measurements reported here and the shape of the differential cross section in the Born - Oppenheimer approximation, the difference being greatest at the highest energy for which measurements were obtained (200 eV).

Implications of these observations are discussed.

PREFACE

This thesis contains no material which has been accepted for the award of any other degree or diploma in any University. To the best of the author's knowledge and belief it contains no material previously published or written by any other person, except where due reference is made in the text.

Kevin G. Williams.

February, 1969.

ACKNOWLEDGEMENTS

The vacuum system and mass spectrometer designed by Dr. P.J. Teubner has been modified for the present series of experiments. Both the electron spectrometer and electron gun discussed in this thesis were developed in collaboration with Dr. E. Weigold and Dr. P.J. Teubner.

The apparatus was constructed by the staff of the Physics Department Workshop. Their work, and in particular that of Mr. E. Connock and Mr. P. Schebella is gratefully acknowledged.

The author would like to express his appreciation for the many helpful discussions with Dr. K.H. Lokan and Mr. P. Leigh-Jones during the development of the electronic data handling system.

Thanks are due to Dr. B.L. Scott for providing tables of values of the differential cross section for elastic and inelastic (2s and 2p excitation) scattering of 54 eV electrons from atomic hydrogen, and to Dr. S.P. Khare for tables of values of differential cross sections for elastic scattering of electrons from helium and molecular hydrogen.

The author would also like to thank both Dr. L. Torop for helpful discussion during the writing of this thesis, and Dr. D.G. McCoy for drawing the diagrams.

Finally, the author would like to thank his supervisor, Professor J.H. Carver for his guidance throughout the course of this work.

This investigation was carried out while the author was holding a Commonwealth Postgraduate Award and a University Research Grant.

CHAPTER 1. HISTORICAL REVIEW

1.1 General.

The scattering of electrons by atoms and molecules has been of widespread interest for many years. With the development of quantum mechanics in the mid-1920's, a description of collision processes became available in which the probability of a system being in a particular state was related to the solution of the Schrodinger equation for the system. Considerable effort has been devoted to the solution of the Schrodinger equation at non-relativistic energies for which the only significant interactions present are due to the coulomb potential. Unfortunately, except for the hydrogen atom, exact wave functions for atoms and molecules are not known, and in no actual electron scattering problem (even the simplest, namely scattering of electrons by atomic hydrogen) is Schrodinger's equation solvable without approximation. The theoretical uncertainties stem solely from these as yet unavoidable approximations.

Therefore, it has become necessary to rely on a comparison between laboratory measurements of some of the simpler collision processes and predictions based on theoretical calculations to establish the range of validity of the various approximations used to solve the Schrodinger equation.

The simplest approximation (introduced by Born in 1926) is the first in a series of successive approximations, in which the zero order wave function of the unbound electron (substituted in the matrix elements for the collision) is a plane wave. This first Born approximation provides a

satisfactory solution to most collision phenomena when the incident particle's velocity is large compared with the velocities of the bound electrons in the target system. For this reason energy dependent relative cross sections are often normalized to Born approximation calculations at high energies.

Symmetrization of the wave function to include the effect of exchange was first introduced by Oppenheimer (1928). However, calculations based on the Born - Oppenheimer approximation do not always lead to an improved result (Bates, Fundaminsky, Leech and Massey, 1950).

The first Born approximation both with and without exchange, retains only those terms in the Born series which are linear in the interaction. Including terms which are quadratic in the interaction yields the second Born and related approximations. In these approximations, matrix elements between all states are included thus allowing for distortion and polarization of the atom by the incoming electron. The importance of allowing for the polarization in some collisions was demonstrated by Massey and Mohr (1934) in their use of the second Born approximation to account for the rather sharp rise of the differential cross section for the elastic scattering of electrons by molecular hydrogen at small angles.

However, the validity of all Born approximations for electron scattering at low energies is limited by their neglect of the distortion of the incident and outgoing electron wave by the atomic field. By substituting incoming and scattered waves which had been distorted by the field of the

atom in the Born - Oppenheimer approximation, Massey and Mohr (1932b) were able to obtain good agreement between the shape of the differential cross section for large angle scattering and experimental angular distributions for the collision of slow electrons with molecular hydrogen and helium.

During the decade prior to 1934, a wide range of experiments involving electron collisions with atoms and molecules had been performed which were considered to be in satisfactory agreement with calculations based on the wave mechanical treatment of the scattering problem. Thus by 1934 "it was widely felt that the field was completely understood in principle and that a limited number of then impossible experiments and calculations would tie up the entire matter" (Fite and Gerjuong, 1965). Subsequently the cultivation of the newer and then more fertile field of nuclear physics and the personnel requirements of such fields as radar and the atomic bomb during the Second World War resulted in the abandonment of the study of atomic processes. However, since the early 1950's there has been an ever increasing interest in this subject until "now it excites far more attention than it has ever done", (Massey, 1964). This is particularly true for electron scattering at low energy where quantitative application of detailed cross section information is required in a number of important areas - for instance the control of thermo-nuclear blast phenomena, the study of the ionosphere, stellar atmospheres and laboratory discharges, (Massey, 1956a). A further stimulus to the theoretical study of low energy collision processes is the advent of high speed computers,

which have enabled a large number of studies of various approximate methods and calculations to be performed on some simple processes. Unfortunately, the nature of the problem is such that with present experience it is still difficult to know with accuracy the errors of the various approximations in a given specific case (Wu and Ohmura, 1962) the range of validity of an approximation being determined generally by comparison with experimental results.

The most promising theoretical approximation for the study of electron collision processes at incident electron energies above that necessary to excite the target atom, is the expansion of the appropriately symmetrized wave function for the collision in terms of some chosen set of eigenfunctions of the atom. The finite number of coupled integro - differential equations resulting are known as the close coupling approximation. With the computational facility provided by computers, there has been the tendency to include more and more states in the close coupling approximations, so that it begins to resemble an exact rather than approximate treatment. In particular, at energies close to threshold, it has been suggested that the close coupling approximation is valid for all energies which are insufficient to excite resonances and eigenstates associated with the lowest levels excluded from the expansion (Burke, Ormonde and Whitaker, 1967). The experimental results of Chamberlain, Smith and Heddle (1964) on the behaviour of the 2p excitation cross section in the vicinity of threshold are consistent with this suggestion.

Major advances in experimental techniques over the last decade have made possible the measurement of low energy collision processes for which calculations will most readily reveal important features of the various approximations employed. Among the recent experimental developments have been the use of microwave probing of afterglows, crossed beam techniques and high energy resolution instruments. In particular the crossed beam technique using modulation, in conjunction with selective amplification has made it possible to observe cross sections for collisions with atoms such as hydrogen and oxygen which are normally bound in diatomic molecules. Furthermore the development and application of digital methods for detecting scattered particles as well as computer orientated data handling systems has permitted experiments to be performed on atomic hydrogen which observe fine structure in excitation cross sections close to threshold, (Williams and McGowan, 1968) as well as measuring the very small scattered signals associated with angular distributions of electrons scattered through large angles.

1.2 Electron Scattering by Atomic Hydrogen.

Since the impact of electrons with hydrogen atoms offers the simplest three body problem in collision theory, it has been the subject of many theoretical investigations. Furthermore the knowledge of exact wave functions for atomic hydrogen, permit the use of electron - hydrogen atom collision processes as a sensitive test of the various approximations used in low energy collision theory.

However, experimental results on atomic hydrogen

were severely restricted to such measurements as those provided by Ornstein and Lindeman (1933) on the excitation functions of Hα, Hβ, and Hγ, until Lamb and Retherford (1950, 1951) demonstrated the usefulness of performing experiments on the highly dissociated beam of molecular hydrogen which diffuses from a slit in a hot low pressure tungsten furnace. In 1958, Fite and Brackman (1958a) applied the modulated crossed beam technique of Boyd and Green (1958) to the study of thermally dissociated molecular hydrogen beams, and measured the ratio of the atomic to molecular ionization cross sections. Reviews of experiments and the various theoretical calculations that have been performed on atomic hydrogen are given by Burke and Smith (1962), Burke, Schey and Smith (1963), Moiseiwitsch and Smith (1968a), Fite (1962) and others.

In particular the cross section for elastic scattering below the first excited state of atomic hydrogen has been measured a number of times, and the results found to be consistent with a number of theoretical calculations (references to these results are given by Burke and Smith, 1962).

Inelastic scattering processes are often studied by measuring the energy dependence of the cross section for producing photons of a particular frequency. Such experimental photon-excitation cross sections generally cannot be directly compared with excitation cross sections for transitions between 2 states produced by theoreticians because the laboratory measurement includes cascading from higher levels excited by the electron impact. The term optical excitation function is therefore used extensively to identify experimental photon

excitation cross sections (Moiseiwitsch and Smith, 1968d). Comparison is often made between the laboratory results and a theoretical optical excitation function obtained by combining theoretical estimates of all the contributing processes.

The optical excitation function for the 2p→1s transition of atomic hydrogen has been determined by observing the Lyman-α flux produced in a region free of electric fields. The original measurements of Fite and Brackman (1958b) were subsequently improved in the low energy range by Fite, Stebbings and Brackman (1959), and are in good agreement with the recent measurements of Smith (1965). The 1s, 2s, 2p close coupling calculations of Burke, Schey and Smith (1963), agree with experimental results for the 2p→1s optical excitation function for energies greater than above 50 to 60 eV, but not below these energies except in the immediate vicinity of threshold..

Three measurements of the electron impact excitation of the metastable 2s state of atomic hydrogen have been performed. The first measurement to be made (Lichten and Schultz, 1959) was based on the detection of free electrons ejected from a platinum surface on which the metastable atoms were incident. The two subsequent measurements by Stebbings, Fite, Hummer and Brackman (1961), and Hils, Kleinpoppen and Koschmieder (1966), differed in principle from the earlier measurements, for they relied on the detection of the Lyman α photon emitted due to electric field quenching of the metastable atoms after they had moved out of the field free collision region. Whereas Stebbings et al normalized their excitation cross section using the 2p optical excitation function, Hils et al used a

different procedure by normalising their 2s optical excitation function data to the Born approximation at high energy. Although the general shapes of the three measurements are in general agreement their absolute values differ widely and the situation requires further experimental investigation.

The experiments performed to determine the cross section for excitation of the 2s and 2p states of atomic hydrogen by measuring their optical excitation functions have all relied on the Born approximation for both normalization of their results and allowance for the signal contributed by cascading from higher excited states. An alternative procedure which does not have these problems is to measure the differential cross section for excitation of a particular state and then to integrate over all angles to obtain the total cross section. Although this is a useful application of differential cross section data, the direct comparison of observed and calculated differential cross sections at all angles provides a far more sensitive test of the accuracy of the approximations used to solve Schrodinger's equation. Furthermore, the growing requirement for accurate differential cross sections (Altshuler, 1963) exphasises the need for a thorough examination, at all angles, of the accuracy of the various approximations used, and for this, experimental data is required. However, the very lack of data with which to compare calculations accounts for the comparatively few theoretical differential cross sections published in the literature. (Scott, 1965).

In the case of atomic hydrogen the only two measurements of angular distributions reported for electron

scattering have been concerned with elastically scattered electrons. Gilbody, Stebbings and Fite (1961) have reported angular distributions at four energies below the first excited state of atomic hydrogen. Their results are consistent with the shape of the close coupling calculations of Burke and Smith (1962). The second experiment has been performed by Teubner (1967), whose measurements at 75, 100 and 200 eV agree with the shape of the Born approximation angular distributions, while at 50 eV, agreement is obtained with the shape of the close coupling differential cross section calculations of Scott (1965) only at angles greater than 60^{o}.

This thesis extends the experimental information available on the angular distributions of electrons scattered by atomic hydrogen by presenting the shape of the differential cross section for the combined 2s, 2p excitation of atomic hydrogen at the incident electron energies of 50, 100 and 200 eV, over the angular range extending from 20^{o} to 130^{o}. Comparison of these results with recent calculations provide information on the validity of the approximations used and indicate the need for additional calculations. Moreover, further development of experimental techniques used to obtain the present results should contribute to the production of equipment which will measure directly differential and total cross sections for electron scattering from atomic hydrogen.

1.3 Electron Scattering from Molecular Hydrogen.

1.3.1 General.

Since the study of atomic hydrogen usually requires the use of gaseous beams containing a mixture of both

atoms and molecules it is often necessary to possess reliable data on electron - molecular hydrogen collision processes. Furthermore, the study of molecules is important because of additional effects which arise when electrons collide with molecules rather than single atoms. In particular, interference occurring between electron waves scattered from the individual atoms during elastic collisions is apparent in the angular distribution of the scattered electrons (Massey and Burhop, 1952a). Also, inelastic collisions include the possibility of molecular dissociation and the excitation of molecular rotation and vibration.

Because of its relative simplicity, much work has been done on electron collision processes with molecular hydrogen. Rozsnyai (1967), Miller and Krauss (1967), and Cartwright and Kuppermann (1967), report recent calculations on a number of electron - molecular hydrogen collision processes, whilst experimental studies have been concerned with dissociation (Corrigan, 1965), ionization (Briglia and Rapp, 1965 and Leventhal, Robiscoe and Lea, 1967), resonances (Golden and Bandel, 1965), and vibrational excitation processes (Heideman, Kuyatt and Chamberlain, 1966).

1.3.2 Elastic Scattering.

Measurements of angular distributions for the elastic scattering of electrons by molecular hydrogen were performed a number of times by the early experimentors in the field of atomic collisions. In particular, investigations were performed by Arnot (1931), Hughes and McMillen (1932b), and Webb (1935b), for electron impact energies ranging up to 900 eV and by

Bullard and Massey (1931a) at low energies. Calculations carried out by Massey (1930), and Massey and Mohr (1932a), neglecting both exchange and polarization effects were found to be in good agreement with experiment except at low energies and small angles. The rather sharp rise in the laboratory angular distribution data occurring at small scattering angles was attributed by Massey and Mohr (1934), to the polarization of the target molecule by the incident electron. Better agreement with experiment was obtained by Massey and Mohr (1934), using calculations based on the second Born approximation in which the effects of polarization can be allowed for. However, Kingston and Skinner (1961) have drawn attention to an inconsistency in the terms previously retained in the second Born scattering amplitude. A fresh study made by Khare and Moiseiwitsch (1965) found that even with the inclusion of exchange and polarization of the target molecule, experimental data tended to exceed calculated values of the angular distributions at both small and large angles. This discrepancy between theoretical and experimental angular distributions for electrons elastically scattered by molecular hydrogen has motivated the reinvestigation of this scattering process - for which preliminary results have been given by Teubner (1967).

1.3.3 Excitation of the b $\left(^3\Sigma_u^+\right)$ state Molecular Hydrogen.

Historically, the lowest triplet state b $\left(1s\sigma\ 2s\sigma\right)^3\Sigma_u^+$ of molecular hydrogen is of special interest because its existence was predicted by Heitler and London (1927) at the introduction of their quantum theory of valency. Also,

Winans and Stuekelberg (1928) were able to provide the correct explanation for the well established continuum stretching approximately over the wave length range from 4,000 to 2,000 A in the emission spectrum of molecular hydrogen as due to transitions from the a $\left({}^3\Sigma_g^+ \right)$ state to the unstable repulsive b $\left({}^3\Sigma_u^+ \right)$ state.

There have only been a limited number of observations of transitions to the b $\left({}^3\Sigma_u^+ \right)$ state of molecular hydrogen in the energy loss spectrum of electrons incident upon molecular hydrogen. Jones and Whiddington (1928), using a photographic film to detect magnetically analysed electrons which had been scattered in the forward direction, observed energy losses in two comparatively narrow ranges whose main energy loss was 9.1 eV and 12.6 eV. The latter energy loss included transitions to the B $\left(1s\sigma\ 2p\sigma \right)^1\Sigma_u^+$ and C $\left(1s\sigma\ 2p\pi \right)^1\Pi_u$ states (Heideman, Kuyatt and Chamberlain (1966), and are the principle transitions observed at all energies. It is now clear (see Section 7.2) that the former energy loss centred around 9.1 eV is due to the excitation of the hydrogen molecule to the b $\left({}^3\Sigma_u^+ \right)$ state, for which the maximum probability of excitation was observed by Jones and Whiddington to occur around incident electron energies of 17 eV. The probability of exciting the b $\left({}^3\Sigma_u^+ \right)$ state as a function of energy was observed to decrease rapidly on either side of its maximum value until it was no longer detectable with Jones' and Whiddington's apparatus at electron energies below 13 eV and above approximately 26 eV.

Kuppermann and Raff (1963), using more sensitive apparatus, observed the excitation of the $b\left(^3\Sigma_u^+\right)$ state from the ground state in the energy loss spectrum of electrons transmitted through molecular hydrogen, for electrons whose incident energy was 60 eV.

Recent high resolution studies of the energy loss spectrum for low energy electrons incident on molecular hydrogen however have not observed the $b\left(^3\Sigma_u^+\right)$ state, since they have been concerned with scattering angles of less than 0.1 radians and energy losses greater than 11.0 eV.

Investigation of the angular distribution of the inelastic spectrum of electrons scattered by molecular hydrogen was performed by Hughes and McMillen (1932b) for incident electron energies between 35 eV and 200 eV. These authors reported energy losses ranging from a minimum of about 12.0 eV, through a sharply defined most probable loss at 12.6 eV (thought by Hughes and McMillen to be due to either the $b\left(^3\Sigma_u^+\right)$, B or C state), and continues into the ionization continuum with decreasing probability. The spread of the hydrogen peak towards the elastic peak was noted by Hughes and McMillen, who pointed out that the spread did not exceed that of the energy loss peak of the first excited state of argon obtained using the same apparatus (Hughes and McMillen 1932a), and accounted for in their paper on argon as being due to a "blurring" of the sharpness of the curves at energies below 100 eV by the accelerating field at the entrance to their electron spectrometer. The analysis of their results was also difficult because of the uncertainty in the position of the $b\left(^3\Sigma_u^+\right)$ potential curve,

(see Figure 7 in Hughes and McMillen, 1932b), and the implication based on the Born - Oppenheimer approximation calculations of Massey and Mohr (1932a), that suggested the probability of exciting the $b\left(^3\Sigma_u^+\right)$ transition to be 10,000 times larger than the probability of exciting the B state.

It is now known that for circumstances in which exchange effects appear to give large cross sections according to the Born - Oppenheimer approximation, (in particular the $b\left(^3\Sigma_u^+\right)$ excitation of molecular hydrogen), the accuracy of the approximation is very poor (Bates, Fundaminsky, Leech and Massey, 1950) and the peak observed by Hughes et al corresponds to excitation of the B and C states of the hydrogen molecule (Kare, 1966).

Recent calculations by Cartwright (1967) for the electron impact excitation of the $b\left(^3\Sigma_u^+\right)$ state of molecular hydrogen, indicates a cross section that has a maximum in the vicinity of threshold and that decreases rapidly with increasing energy. The maximum is close to the value predicted by Khare for the sum of the B and C state excitations and is therefore in qualitative agreement with the observations of Jones and Whiddington (1928).

In the present investigation, the inelastic spectra for electrons scattered by molecular hydrogen has been observed to possess a continuous energy loss (within the resolution of the apparatus) which starts at approximately 8.5 eV and extends into the B state excitation part of the spectrum. This continuum has been interpreted as arising from electron excitation of the unstable $b\left(^3\Sigma_u^+\right)$ state. Since the study of

atomic hydrogen requires the use of partially dissociated molecular hydrogen beams, a preliminary investigation of the angular distribution of electrons exciting the b $\left({}^3\Sigma_u^+ \right)$ state of molecular hydrogen has been made to enable the total beam signal (observed at that part of the energy loss spectrum corresponding to the combined 2s, 2p excitation of atomic hydrogen), to be corrected for the molecular contribution.

1.4 Outline of Thesis.

Experimental techniques commonly used to measure angular distributions of scattered electrons are evaluated and the main principles for the successful application of the modulated beam technique to the study of atomic hydrogen are discussed in Chapter 2. Chapters 3 and 4 describe the mechanical and electronic equipment used in the present investigation to obtain the raw data, whose analysis to produce angular distributions is explained in Chapter 5. The theoretical formalism required for a discussion of the results is outlined in Chapter 6. Angular distributions for elastic and inelastic scattering from molecular hydrogen and for the combined excitation of the 2s, 2p states of atomic hydrogen are presented and discussed in Chapters 7 and 8 respectively. Finally, conclusions suggested by the present investigation are given in Chapter 9.

CHAPTER 2. EXPERIMENTAL METHODS

Introduction.

In Chapter 1, it was explained that even though the basic interaction between electrons and atoms (namely the Coulomb field) is known, and the quantum theory provides an accurate means of formulating electron scattering processes at non-relativistic energies, the equations obtained cannot be solved exactly, and the errors introduced by the various approximations used to obtain numerical solutions cannot generally be determined from theoretical grounds (Burke and Smith, 1962). The ever increasing need for quantitative data on numerous scattering processes has led to the development of a number of experimental techniques to obtain laboratory results, for use both in practical applications and as a source of information with which to compare calculations based on the various theoretical approximations. Since the accuracy of the approximations used can often be assessed most conveniently by studying electron scattering from atomic hydrogen (this being the only atom for which the wave functions are known exactly), the techniques commonly used for measuring angular distributions of the scattered electrons are discussed in this chapter with particular attention being paid to their possible application to the study of atomic hydrogen.

2.1 D C Techniques.

2.1.1 Static Gas Technique.

The only method used by early experimentors to measure the angular distributions of scattered electrons and one which is still important today, uses a scattering chamber

in which the gas studied fills the chamber throughout at a constant pressure - typically between 0.0005 torr and 0.003 torr. A detailed review of particular static gas arrangements used before the Second World War is given by Massey and Burhop (1952a).

Features which are common to all equipment used to study angular distributions include the projection of a parallel electron beam (produced by an electron gun) through a field free region of a scattering chamber into an electron collector (or Faraday Cup). Some of the electrons scattered out of the main beam by the gas in the chamber are collected by a scattered electron detector whose entrance aperture is generally restricted so that only those electrons which have been scattered into a small solid angle about a particular angle θ with respect to the main beam are observed. The scattered electron signal is studied as a function of scattering angle by rotating the scattered electron detector in a circle about an axis which passes through the centre of the electron beam in the field free interaction region, and is perpendicular to the beam. The scattered electron detector usually has the facility to velocity analyse the electrons entering it so that a particular energy loss process can be studied.

The static gas technique has the advantage that high gas pressures are generally easy to produce. However, to obtain the angular distribution from the observed angular dependence of the scattered signal, it is necessary to multiply the observed signal by $\sin\theta$ to compensate for the change in effective scattering path length with angle (Massey & Burhop, 1952b). This results in the accuracy of the angular

distribution becoming increasingly susceptible to errors in the correction factor as the scattering angle approaches both 0^{o} and 180^{o}.

The seriousness of possible distortion of observed angular distributions due to double scattering processes, (particularly at the high pressures available in the static gas technique), has been emphasised recently by Chamberlain, Simpson, Milczarck and Kuyatt (1967), who draw attention to the rapid decrease, with increasing angle, of differential cross sections for optical transitions compared with the more slowly varying elastic differential cross sections. The principle contribution to observed inelastic angular distributions from double scattering processes comes from large angle elastic scattering in or near the geometrically defined scattering volume which is proceeded, or followed, by small angle inelastic scattering along the electron path through the chamber. The presence of double scattering has limited the range of angles for which angular distributions of inelastic scattering processes could be determined by a number of investigators (for example Vriens, Simpson & Milczarck, 1968) who have used the static gas technique.

In the experimental study of electron scattering processes, there is usually a background component to the observed signal which arises from at least two sources other than impurities in the gas supply. First there is the incomplete trapping of electrons by the Faraday cup which results in the production of stray electrons that may be scattered by the walls of the chamber into the detector, and second, the presence of

foreign gases due to outgasing of the apparatus. The background signal contributed by these later two sources is usually determined by repeating the experiments with the chamber evacuated. The signal arising from the gas to be studied is then obtained by subtracting this background measurement from the signal observed when the gas to be studied is present in the chamber. Rather large uncertainties may be introduced into the final result however, if the background signal is a significant fraction of the total signal observed when the gas to be studied is present. Further error may also be introduced because of possible variations in the background signal with gas pressure, due to the shape of the electron beam depending on the positive ion density along it.

The static gas technique is not applicable to the study of electrons scattered by chemically unstable atoms (such as atomic hydrogen), because of the problems raised by the dissociation of the molecules and the rapid recombination of the atoms on the walls of the chamber.

2.1.2 Unmodulated Neutral Beam.

The problem of determining the background signal can often be simplified by directing a jet of the gas to be studied through a chamber in which it is intersected by an electron beam. This arrangement is commonly referred to as the crossed beam technique. The background signal (which for cross beam arrangements is usually defined as the component of the observed signal that does not arise from the neutral beam), is measured by performing the experiment with the gas admitted through an auxiliary port that directs the beam away from the

scattering region. The gas flow for the experiment to measure the background signal is adjusted so that the pressure observed on a gauge situated inside the chamber, but out of the neutral beam, reads the same value as observed when the neutral beam is on.

Although gas pressures in the neutral beam are usually lower than those used in static gas experiments, the crossed beam technique can be used to advantage for studying vapors or condensible gases (Porteus 1964). For example, the much lower pressures possible throughout the chamber if the neutral beam is at least partially condensed reduces the probability of double scattering. Also, subtraction of the background completely cancels signals produced by double scattering processes involving only the background gas. The crossed beam technique has the additional advantage that by making the shape of the neutral beam cross section circular, the $\sin\theta$ correction is eliminated from angular distribution measurements.

Although the study of electron collision processes using static gas methods are generally impractical for the study of chemically unstable atoms, low intensity beams of partially dissociated molecules have been successfully produced - for example hydrogen (Lamb and Retherford, 1950, 1951), nitrogen (Smith, Caplinger, Neynaber, Rothe and Trujillo, 1962), and oxygen (Neynaber, Marino, Rothe, Trujillo, 1961).

However, since the number density of the background gas present in a conventional high vacuum system (where pressures are typically about 10^{-6} torr at the region

in which the partially dissociated beam intersects an electron beam) may be as high as 40 times the number density of atoms in the neutral beam, the background gas contribution to the signal observed by a scattered electron detector is usually very much larger than the signal produced by the neutral beam. While this may not be a severe difficulty if the background gas pressure remains steady (say to within 1% or better), pressure drifts and fluctuations arising from unsteady operation of diffusion pumps generally makes D C experiments and subtraction techniques unsuitable for the study of partially dissociated beams.

2.2 A.C.Technique using a Modulated Neutral Beam.

2.2.1 General.

A solution to the problem presented by slow background pressure drifts in the study of low intensity beams of partially dissociated molecular gases, is the modulation of the neutral beam by a mechanical chopper (Fite and Brackman, 1958a). The very short time interval between the signals obtained with the neutral beam crossing and not crossing the electron beam enables the beam signal (which is the difference between these two signals) to be determined free of the influence of slow drifts in background pressure. The signal arising from the beam is then distinguished from the background signal as that component of the total signal which appears at the modulation frequency, with a specified phase with respect to a reference signal (which is produced by the mechanical chopper). However, rapid background pressure fluctuations may be introduced by chopping the neutral beam which will contribute to the beam signal. The use of the short term integrating

property of a vacuum system to average these fluctuations is discussed further in Section 2.2.3.

Since the background pressure is usually low (typically 10^{-6} torr) in a modulated beam apparatus, the probability of double scattering is reduced considerably - making the technique useful also for the study of large angle inelastic scattering from non-condensible gases.

2.2.2 Experimental technique.

The modulated crossed beam technique has been successfully applied to the measurement of a wide range of collision phenomena - involving a variety of projectiles and targets. (Examples are discussed in the detailed review by McDaniel, 1964.) The principle features usually found in a modulated beam apparatus are now described with particular reference to the application of this technique to measuring the angular distributions of scattered electrons whose incident energy is greater than the threshold energy for exciting the neutral beam.

The major device to minimise pressure fluctuations is the use of a three stage differentially pumped vacuum system. (See Figure 2.1). The first stage chamber (or oven chamber) containing the source of the partially dissociated beam is evacuated by a high speed pump. This pump quickly removes gas issuing from the source aperture which is not part of the neutral beam. After passing from the oven chamber into the second chamber (or chopping chamber), and being modulated by a mechanical chopper, the neutral beam moves downstream into a third chamber (or scattering chamber), where it is intersected

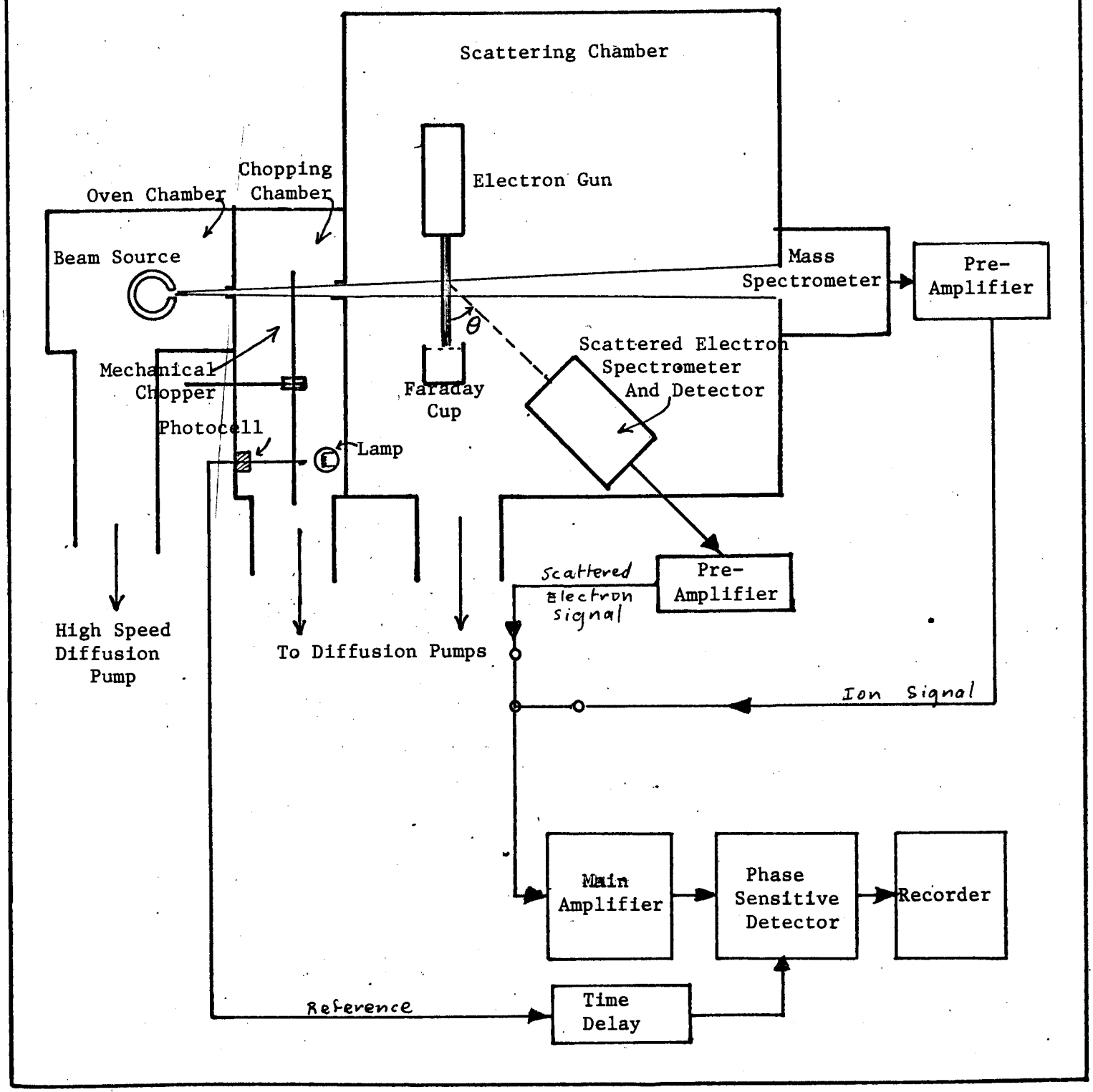

Figure 2.1 Schematic diagram of a possible modulated beam apparatus for measuring the angular distribution of electrons scattered by gases. The plane containing the electron beam and electron spectrometer is shown rotated from its true position (perpendicular to the neutral beam).

at right angles by an electron beam. Finally, the partially dissociated beam enters a mass spectrometer for the measurement of its degree of dissociation. The flow of background gas between chambers is reduced by the use of apertures in the vacuum chamber walls to pass the neutral beam from the first to the third chambers. Both the chopping and scattering chambers are evacuated by separate diffusion pumps.

Electrons scattered out of the main beam from a volume including the region of intersection of the crossed beams (referred to as the interaction region), are energy analysed by an electron spectrometer if they are scattered into a small solid angle about a particular angle θ in the plane perpendicular to the neutral beam. Electrons transmitted by the spectrometer, are amplified in an electron multiplier, whose output is converted to a voltage signal at the input of a preamplifier. If an analogue data handling system is used, the signal arising from the interaction of the electron beam with the background gas contributes a d.c. signal and can therefore be blocked by a condenser. The modulated neutral beam, however, contributes an a.c. signal, which after transmission by the preamplifier, can be further amplified (by an a.c. amplifier tuned to the modulation frequency), rectified, and integrated so that the beam signal can be displayed on a chart recorder. The phase of the reference voltage (taken directly from the chopper by means of a light-and-photocell monitor), which controls the rectification, is adjusted for maximum output from the phase sensitive detector. The angular distribution of electrons which have lost energy corresponding to a particular collision process is then obtained

by measuring the beam signal at a number of angles throughout the angular range to be studied.

2.2.3 Vacuum Systems.

A detailed analysis of the general properties of vacuum systems used in modulated beam equipment has been given by Fite and Brackman (1958a). Of particular importance is the background pressure dependence of any signal arriving from the background gas, which may produce both random and coherent contributions to the beam signal.

Random fluctuations occurring rapidly in the background pressure (produced by irregular pumping of diffusion pumps), will have Fourier components near the modulation frequency, which contribute to the noise of the beam signal. Since partially dissociated beams have low intensity, the magnitude of these random fluctuations is usually one of the factors determining the time required to reduce the noise component of the beam signal to a satisfactory level. In order to minimise random pressure fluctuations, differential pumping is provided along the neutral beam's path, and the pressure difference across chopping and scattering chamber vacuum pumps are reduced by backing both pumps with another diffusion pump.

A coherent modulation of the background pressure in the scattering chamber is produced by the introduction of the neutral beam during only half of each cycle. Now noting that the characteristic time constant of a vacuum system is given by the ratio of the chamber volume to speed of the the vacuum pump, it is evident that the choice of a modulation

frequency whose period is very small compared with the scattering chamber time constant, results in the coherent background pressure fluctuation being integrated in a manner completely analogous to integration by an R C electrical network, and therefore produces a coherent signal which is 90^{o} out of phase with the signal associated with the neutral beam. The signal arising from the interaction of the electron beam with the coherent modulation of the background gas is cancelled by phase sensitive rectification of the observed a.c. signal. An alternative procedure that can sometimes be used, considerably reduces the coherent modulation of the background pressure in the scattering chamber, by chopping the neutral beam in the scattering chamber.

A second possible coherent contribution to the beam signal arises from the net flow of background gas which moves down the neutral beam path from the oven chamber to the scattering chamber. Since this flow of gas is modulated by the mechanical chopper, the signal arising by its intersection with the electron beam is indistinguishable from the neutral beam produced by the oven. Neither of the coherent signals are usually important for the study of undissociated gases. However, in the study of partially dissociated beams the net flow of background gas will be almost entirely molecular, and therefore it is usually necessary to measure and subtract the contribution of the net background gas flow to the observed beam signal. Methods used to perform this measurement are discussed in Section 2.2.4.

2.2.4 Partially Dissociated Beams.

Since it is not possible to produce completely dissociated molecular beams, the molecular contribution to the observed beam signal must be determined. The following discussion is restricted to beam sources which rely on thermal dissociation inside an oven. The analysis given by Fite and Brackman, (1958a), shows that if there is a constant mass flow of gas per unit time and thermal equilibrium between the gas and walls of the oven, then the signal produced by the neutral beam would be inversely proportional to the square root of the oven temperature if no dissociation occurred. Therefore by experimentally determining the constant of proportionality between the molecular beam signal and temperature for conditions of no dissociation, the signal arising from the molecular fraction of the beam can be calculated when the beam is partially dissociated (from a knowledge of its degree of dissociation) and subtracted from the observed signal to yield the atomic beam signal.

This square root relationship between the undissociated beam's signal and oven temperature does not hold if there is significant net flow of molecular background gas directly from the oven chamber to the scattering chamber, because the temperature dependence of this gas flow is different from that of the beam from the oven. Fite and Brackman determined this correction to the observed beam signal by measuring the signal produced at the modulation frequency when a shutter blocked the direct beam in the oven chamber, (but did not interfere with the flow of background gas). An estimate of the signal produced by the background gas flow in the present investigation is determined

with a different technique. The method used introduces the gas into the oven chamber through an auxiliary port at a rate which produces the same background pressure in the oven chamber as observed when the highly dissociated beam is diffusing from the oven. The signal at the modulation frequency contributed by this gas flow never constituted more than a few percent of the total modulated signal.

With the present apparatus, it is found that the beam signal does not decrease as rapidly as the inverse of the square root of temperature for increasing temperatures when the source pressure (measured at room temperature by a gauge in the gas supply line) exceeds 0.5 torr. This departure from square root of temperature dependence is to be expected when the source pressure is too high to permit sufficient mean number of collisions between gas particles and oven walls for thermal equilibrium to be reached. Because of the rather low atomic hydrogen concentration produced in the neutral beam where it intersects the electron beam and the small differential cross section for inelastic scattering at large angles from the hydrogen atom, it is desirable to operate the source at room temperature pressures which are above 0.5 torr.

An alternative experimental procedure for determining the molecular contribution to the neutral beam signal is proposed which does not require a knowledge of the temperature dependence of the molecular beam, and therefore permits the use of higher source pressures.

Consider the experimental arrangement in which the volume including the intersection of the crossed neutral

and electron beams is used as the sourse of both scattered electrons whose angular distribution is to be measured and ions which are to be mass analysed to determine the composition of the beam. An extraction field is used to draw all ions formed in the vicinity of the interaction region into the mass spectrometer.

Then if the collecting and detecting efficiencies of electron and mass spectrometers are independent of the velocity of the gas particles, the probability P^i of a gas particle being ionized and detected at the output of a mass spectrometer, will be proportional to the probability P^e of a gas particle scattering an electron which is detected at the output of the electron spectrometer. That is

$$P^i = C P^e \qquad (2.1)$$

where C is a constant for a particular electron scattering angle θ, incident electron energy and gas species, and is independent of the degree of dissociation of the neutral beam.

If $I_m (T)$ and $E_m (T)$ represent the signals at the modulation frequency (produced at the output of the phase sensitive detector) from the mass and electron spectrometers respectively as a function of oven temperature T, then the molecular signals at two temperature are given by

$$I_m (T_h) = C E_m (T_h) \qquad (2.2)$$

and

$$I_m (T_r) = C E_m (T_r) \qquad (2.3)$$

where T_r and T_h represent room and high temperatures respectively. Taking the ratio of equations (2.2) and (2.3) and rearranging one obtains

$$E_m (T) = \frac{I_m (T_h)}{I_m (T_r)} \times E_m (T_r). \qquad (2.4)$$

When the temperature T_h is sufficiently high to produce a partially dissociated beam, the molecular contribution $E_m(T_h)$ to be subtracted from the rectified beam signal may be calculated from equation (2.4) In the remainder of this report, the term molecular beam signal will include the phase sensitively detected components of any signal produced by undissociated molecules, whether they be part of the neutral beam from the source or oven chamber, or coherent pressure fluctuations of the background gas in the scattering chamber. For the experiments reported here, the beam from the oven contributes all but a few percent of the molecular beam signal. When the neutral beam is partially dissociated, the molecular component of the beam signal is calculated using equation (2.4), from which it is clear that determination of $E_m(T_h)$ does not require the degree of dissociation to be known.

2.2.5 Crossed Beam Requirements.

The measurement of angular distributions of scattered electrons requires an electron beam which is parallel in the interaction region. A convenient neutral beam shape is one which has a circular cross section. Let r be the radius of cross section of the neutral beam where it intersects the electron beam and d be the distance from the centre of the interaction region to the entrance aperture of the electron spectrometer. Worst case calculations show that if the ratio of r/d is less than 7%, then for approximate cylindrical symmetry of the neutral beam and parallel electron beam, there is no significant distortion of the angular distribution as the

scattering angle θ is changed, due to small variations in the solid angle subtended at the electron spectrometer from each point in the electron beam. The ratio of r/d in the present apparatus is 5.5% and therefore satisfies this condition.

CHAPTER 3. DESCRIPTION OF APPARATUS

Introduction.

It was pointed out in Chapter 1 that even though the study of collisions between electrons and hydrogen atoms is the most fundamental many body problem, and the one for which theoretical predictions can be most easily and accurately calculated, there have been only a limited number of experiments performed on it, with which to compare the rather large variety of mathematical approximations employed. Until recently, measurements on atomic hydrogen had not been attempted because chemical instability of the atom precluded the use of conventional experimental techniques which usually employ static gases. The problem associated with instability can be solved by using a beam of partially dissociated molecules. However, the density of the atomic fraction of the beam is usually considerably less than the concentration of the background gas. Hence it is necessary to detect a signal which is at least an order of magnitude less than that produced by electron scattering from the background gas. In Chapter 2, a solution to this problem has been discussed in which the neutral beam is modulated by a mechanical chopper and the beam signal is recognised as the component of the total signal occurring at the modulation frequency with a specified phase with respect to a reference.

This chapter describes the modulated beam apparatus used in the present investigation to measure the angular distribution of electrons inelastically scattered from atomic hydrogen, and elastically scattered from a number of stable gases.

3.1 Production of Partially Dissociated Beams.

A review of the techniques used to produce beams of both stable and chemically unstable gases, and the principles involved, has been given by Lew (1967a). Partially dissociated beams of atomic hydrogen have been produced from a radio frequency discharge (Neynaber, Marino, Rothe and Trujillo, 1961), and more commonly by the thermal dissociation of molecular hydrogen inside a hot (3,000^{0} K) tungsten low pressure oven (Retherford, 1950, Fite and Brackman, 1958a). Since the thermal source has been reported to be capable of producing neutral beams whose degree of dissociation may be as high as 96% (Fite and Brackman, 1958a) as compared with 30% obtained by Neynaber et al from a radio frequency source, a tungsten oven was chosen in the present investigation. Details of the oven construction and also the dissociation processes have been discussed by Teubner (1967). In particular, the oven (which was made in the form of a hollow tube), was supported at both ends by water cooled copper rods which supplied the 300 amps alternating current required to raise the oven temperature to about 3,000^{0} K.

With slit dimensions (.008" x .12") and wall thickness (0.010") used in the present experiment, the gas flow was partially collimated in the forward direction if the source pressure was sufficiently low to satisfy the condition necessary for effusion, namely that the mean free path exceed the slit width (Lew, 1967b). However, to meet the need for an adequate supply of atomic hydrogen, a compromise between atomic hydrogen concentrations and the ability of the vacuum pumps to handle the

gas load was necessary, which in the present investigation resulted in the use of room temperature source pressures up to 10 torr, and therefore the conditions for effusive flow were not satisfied.

3.2 Vacuum Systems.

Unless otherwise stated, the vacuum system was the same as described by Teubner (1967). In order to minimise the effects of geometrical spread of the beam with distance from the source, it was desirable to place the interaction region as close as possible to the beam source. However, a compromise must be reached between this requirement and the need to differentially pump between the oven chamber and scattering chamber, and to provide room for the mechanical chopper. In the present apparatus the distance between oven and interaction region was approximately 5". To permit the measurement of the angular distributions of scattered electrons, the electron gun and Faraday cup were mounted on a platform which could be rotated (about an axis which lay along the centre of the neutral beam) by means of a rotating seal in the vacuum chamber wall. Electrical connections to the electron gun and Faraday cup were introduced first into the vacuum wall of the chopping chamber and then into the scattering chamber by means of electrical lead-throughs close to the neutral beam aperture.

The twelve toothed mechanical chopper (positioned in the chopping chamber) was replaced by a disc with 4 slots, and was rotated at a speed which produced a chopping frequency of around 116 cycles per second - making the time required for the beam to turn on and off a smaller fraction of each cycle

than with the earlier chopper.

A number of modifications to the original system were carried out to permit the measurement of angular distribution on both sides of zero scattering angle. These changes included the removal of a stray electron shield from the entrance aperture of the electron spectrometer and the use of a shorter Faraday cup, to permit the Faraday cup to move across the front of the electron spectrometer. With the additional flexing of electrical leads, (required by the electron gun and Faraday cup as a result of the additional angular range to be studied), the 2" diameter centre of the wall separating the chopping and scattering chambers was attached to the gun platform, so that the electrical leads could be held fixed in the scattering chamber and permitted to flex in the chopping chamber.

The migration of oil from diffusion pumps back into the scattering chamber was observed to result in unreliable behaviour of the electron gun beam, due to the buildup of electrical charges on insulating layers. This problem was overcome by maintaining traps filled with liquid air above the diffusion pumps at all times.

By reducing the temperature of a metal surface in the scattering chamber to that of liquid air a few hours after starting to evacuate the chamber, and maintaining the surface continuously at the liquid air temperature, the base pressure in the scattering chamber in the present experiments fell to less than 2×10^{-7} torr within 2 days of pumping after exposure to the atmosphere. A continuous record of the background pressure

in the scattering chamber was obtained on a chart recorder by monitoring the pressure measured by an ionization gauge situated in the scattering chamber. Typical pressures in the scattering chamber during experiments on molecular hydrogen were about 1×10^{-6} torr.

3.3 Electron Gun.

3.3.1 Requirements.

Since the present experimental investigations were concerned with particular energy losses by electrons scattered from gas particles, an approximately mono-energetic electron beam was required. Now the thermal spread in electron energies produced by thermionic emitters is given by the relation (Simpson, 1964)

$$\Delta E_T = \frac{2.54\ T}{11{,}600} \qquad (3.1)$$

where T is the temperature (^{o}K) of the emitter and ΔE_T the full width half maximum (F.W.H.M.) in electron volts. The higher the temperature of the emitting surface then, the greater is the energy spread.

Comparison of the various thermionic emitters available (for example in the review of Haas, 1967), reveals that electron beams produced by directly heated metal cathodes (such as tungsten) are unsuitable because of their large energy spread, resulting both from the high temperatures required and voltage drop across the wires. Indirectly heated oxide cathodes operating at much lower temperatures, have far narrower energy spreads than metal cathodes. However, oxide coated cathodes have the undesirable feature that once used, they must be

replaced after exposure to the atmosphere. Dispenser (or matrix) cathodes avoid this problem because of the possibility of reactivating their emitting surface with active material from within the matrix. A cathode of this type, consisting of a mixture of barium, calcium and aluminium oxides impregnated in an 80% tungsten matrix, was used in the present electron gun. The F.W.H.M. of the electron beam at the operating temperature of the cathode (approximately 1300° K) was, (according to equation 3.1), 0.3 eV.

The entrance aperture of the electron spectrometer used in the present investigation subtended a very small solid angle, (about 10^{-3} steradians), at the interaction region. This fact, coupled with the small concentration of atomic hydrogen in the beam, and the low differential cross section for excitation of atomic hydrogen to the 2s and 2p states at large angles, resulted in the need to produce intense beams of electrons at low energies. Therefore an electron gun was required which possessed a perveance of approximately 10^{-6}, (where perveance is defined as the ratio of beam current to the 3/2 power of the beam voltage).

3.3.2 Description.

Details of the multi-stage electron gun design used in the present investigation have been given by Teubner (1967). The first stage of the electron gun, (which uses the high perveance cathode - anode arrangement reported by Frost, Purl and Johnson, 1962), was designed to produce a high energy electron beam. The axially symmetric electron beam was

extracted from the vicinity of the cathode surface by a high anode potential and directed (through a circular hole in the anode) into the second stage, where focusing and fine adjustment to the beam's direction were performed. The electron beam was maintained at high energy in the second stage to reduce space charge repulsion within the electron beam (Simpson and Kuyatt, 1963), and was finally decelerated to emerge from the outer (grounded) electrode at an energy equal to the potential of the cathode measured with respect to earth.

A Faraday cup (which was maintained close to ground potential) collected the main electron beam. It was made from a hollow cylinder of diameter 0.75" and length 0.75" which was blanked at one end, and contained aluminium honeycomb ($\frac{1}{8}$" diameter holes) to improve the electron trapping efficiency. Further reduction of secondary electron emission was obtained by coating all conducting surfaces of the Faraday cup with aquadag.

3.3.3 Operation.

The operation of the electron gun during the present investigation was similar to that described by Teubner (1967), except for the method used to solve the problem presented by the wide range of signals produced when measuring angular distributions.

3.3.3 (a) First stage of the Electron Gun.

Even with the use of a high intensity electron beam, the combined beam and background count rate observed during large angle measurements on atomic hydrogen could be as low as several hundred electrons per second. An electron multiplier was therefore used to amplify this signal. There were two

methods for handling the electron pulse at the electron multiplier's output produced by a single electron at its input. Either the pulse could be integrated to produce an analogue signal or made to retain its pulse character until it was converted to a digital pulse of standard width and height. If most of the pulses could be amplified to a level which exceeded the noise generated within the amplifier, the digital technique was preferable to the analogue (for low count rates), since the observed signal was then less sensitive to gain variations.

In the present apparatus the maximum scaling rate was limited by the dead time of the discriminator to 1.3 megacycles per second. Actual scaling rates were generally restricted to less than 150 Kilocycles per second to reduce the dead time correction necessary. Whilst the scaling rate obtained at large angles for the high intensity electron beams used never exceeded 150 kilocycles per second, signals obtained at small angles greatly exceeded this value. Teubner (1967) maintained a constant electron gun current during the measurement of each angular distribution and reduced the observed signal rate at small angles by decreasing the gain of the pulse amplifier, so that only the largest pulses were detected. However, because of the much larger difference between small and large angle differential cross sections for inelastic collisions than elastic collisions, the amplification was held constant in the present investigation and a range of electron beam currents were used instead to measure a single angular distribution. This facility to be able to control the electron beam current

over a wide range of values at each energy was also useful since it provided a means of investigating the reliability of observed angular distributions.

The cathode arrangement of Frost et al used in this investigation was designed for space charge limited operation with large potentials between anode and cathode (for example one Kilovolt), and its operation was found to be unreliable at the very low voltages required to produce currents of a few micro amps. However, by operating the gun under temperature limited emission conditions and several hundred volts difference between anode and cathode, stable operation of the electron beam was obtained by using the Faraday cup current to stabilize the output of the d.c. cathode filament power supply.

A chart record obtained by continuously monitoring the Faraday cup current revealed a maximum time variation (over a period of 10 hours) of 2% of the electron beam current for all currents used.

3.3.3 (b) Focus Conditions.

Space charge repulsion between electrons in the main beam, limited the maximum current that could be directed through the neutral beam at a particular energy. If E is the energy of an electron beam that passes through a region defined by two apertures of diameter $2r_o$ separated by a distance d (Figure 3.1), then space charge repulsion limits the maximum current I_{max} to the value (Simpson 1967)

$$I_{max} = 38.5\ E^{\frac{3}{2}} \left(\frac{2r_o}{d}\right)^2 \qquad (3.2)$$

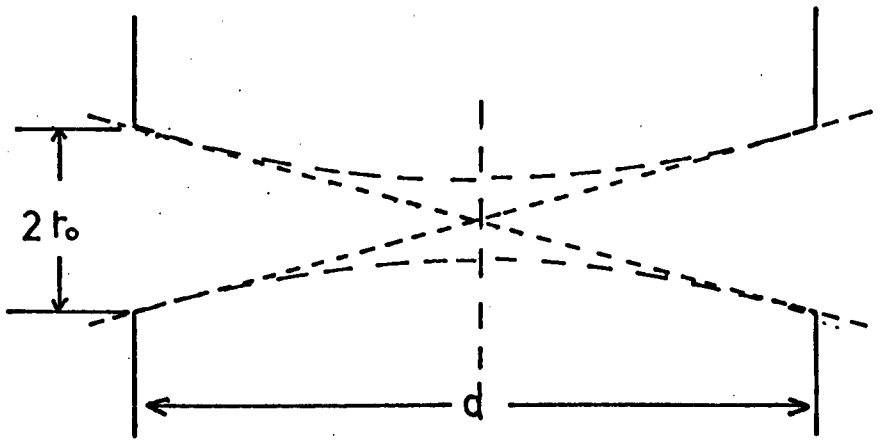

Figure 3.1 Idealized space charge - limited beam profile (dotted line) to saturate a given space.

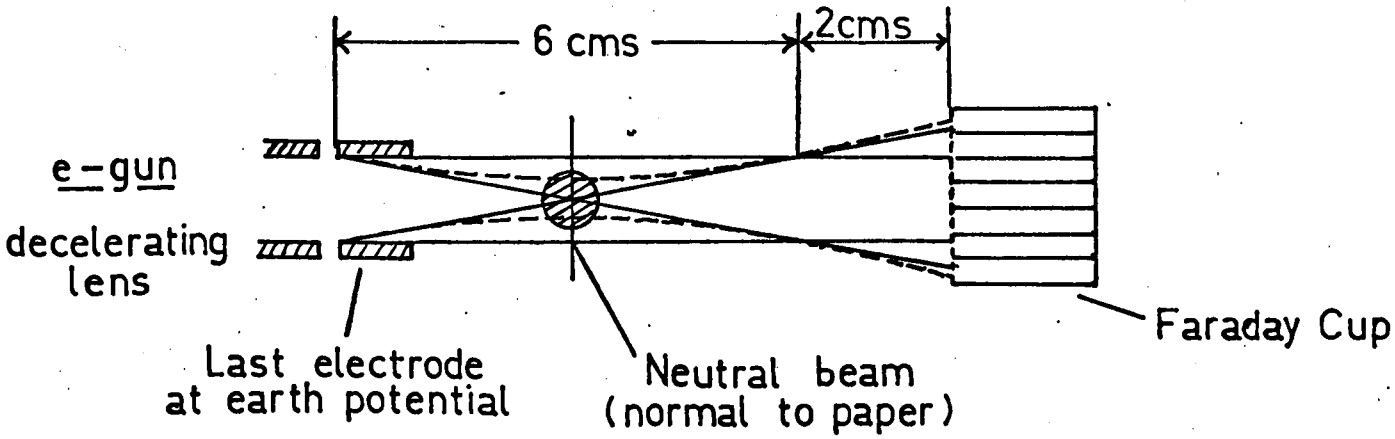

Figure 3.2 Position of the electron beam for space charge - limited flow in the present apparatus.

This maximum current is only possible, if the launch angle with which the edges of the beam enter the space between the apertures, is such that in the absence of space charge these extreme rays would cross over in the middle of the space. With the further assumption that the electron paths do not cross, then space charge repulsion spreads the beam so that at the centre of the space, the beam becomes a disc of diameter $2r_0/2.35$, and all electrons move parallel to the axis.

Numerical values of I_{max} corresponding to the dimensions of the present apparatus (shown in Figure 3.2) for the energies at which angular distributions were measured, are given in Table 3.1, as well as the range of gun currents actually used.

Table 3.1

BEAM ENERGY (e.V)	MAX CURRENT (μA) (Space Charge limited)	RANGE OF CURRENTS USED EXPERIMENTALLY (μA)
30	170	2 - 25
50	370	5 - 100
100	950	10 - 300
200	2700	9 - 700

Distortion of the angular distributions were observed at scattering angles less than 30^o if beam currents approaching I_{max} were used. This was probably due to non-ideal operation of the second stage of the electron gun at high space charge densities because of lens aberrations. Supporting this hypothesis was the observation that distortion could be significantly reduced by increasing the background pressure when

performing scattering experiments on argon, since the large ionization cross section of argon results in the production of sufficient positive ion concentration along the main beam to partially neutralize the negative space charge of the electron beam. Experiments were therefore performed using non-space charge saturated electron beams at currents ranging from a few percent of I_{max} for small scattering angles,(where the cross section changes most rapidly),to 30% of I_{max} at large angles. A Faraday cup having a diameter twice that of the electron gun aperture improved the collection of electrons from the present gun and was situated 5 cms from the neutral beam to increase the angular range available for study.

To produce a suitable electron beam, the cathode filament supply was first operated with the stabilization provided from the voltage at its output, and the electrode supplies adjusted to obtain the maximum Faraday cup current available from the cathode at that particular temperature. After correcting the filament power supply to obtain the required electron beam current and further adjustments to the electrode potentials to optimise the beam current, negative feed back control of the filament supply was changed over to the recorder output provided by the meter* measuring the Faraday cup current. Fine adjustments to the electrode potentials then optimised the Faraday cup current. Discussion of the reliability of this procedure for producing electron beams which were sufficiently parallel in the interaction region is given in Chapter 6 Section 6.

* Hewlett Packard, D C Microvolt-ammeter Model 425A.

3.4 Electron Energy Analyser.

3.4.1 Requirements.

Since the present investigation was concerned with the study of electrons which had been both elastically and inelastically scattered from atoms and molecules, it was necessary to velocity analyse the scattered electrons to select the process to be studied. Energy analysers which use magnetic field were precluded because of the difficulty of controlling low magnetic fields (Marton and Simpson, 1958). Design of electrostatic analysers have been considered by Simpson (1961, 1964), Kuyatt and Simpson (1967), and Harrower (1955). The parallel plate electron spectrometer discussed by Harrower was chosen for the present investigation because of its ease of construction and compactness (see Figure 3.3).

3.4.2 Description.

A description of the construction and operation of the electron spectrometer has been given by Teubner (1967). The instrument used the uniform field created between two parallel plates when one plate was earthed and a negative potential applied to the second (deflector) plate. Electrons passing through a slit in the earthed plate at an angle of 45^{o}, travelled in parabolic paths and were refocussed upon returning to the earthed plate. The energy of electrons E falling on a second slit situated a distance x_o from the first slit is proportional to the potential V applied to the deflector plate and is given by (Harrower)

$$E = \frac{x_o}{2d} V, \qquad (3.3)$$

where d was the separation of the plates. The value of the

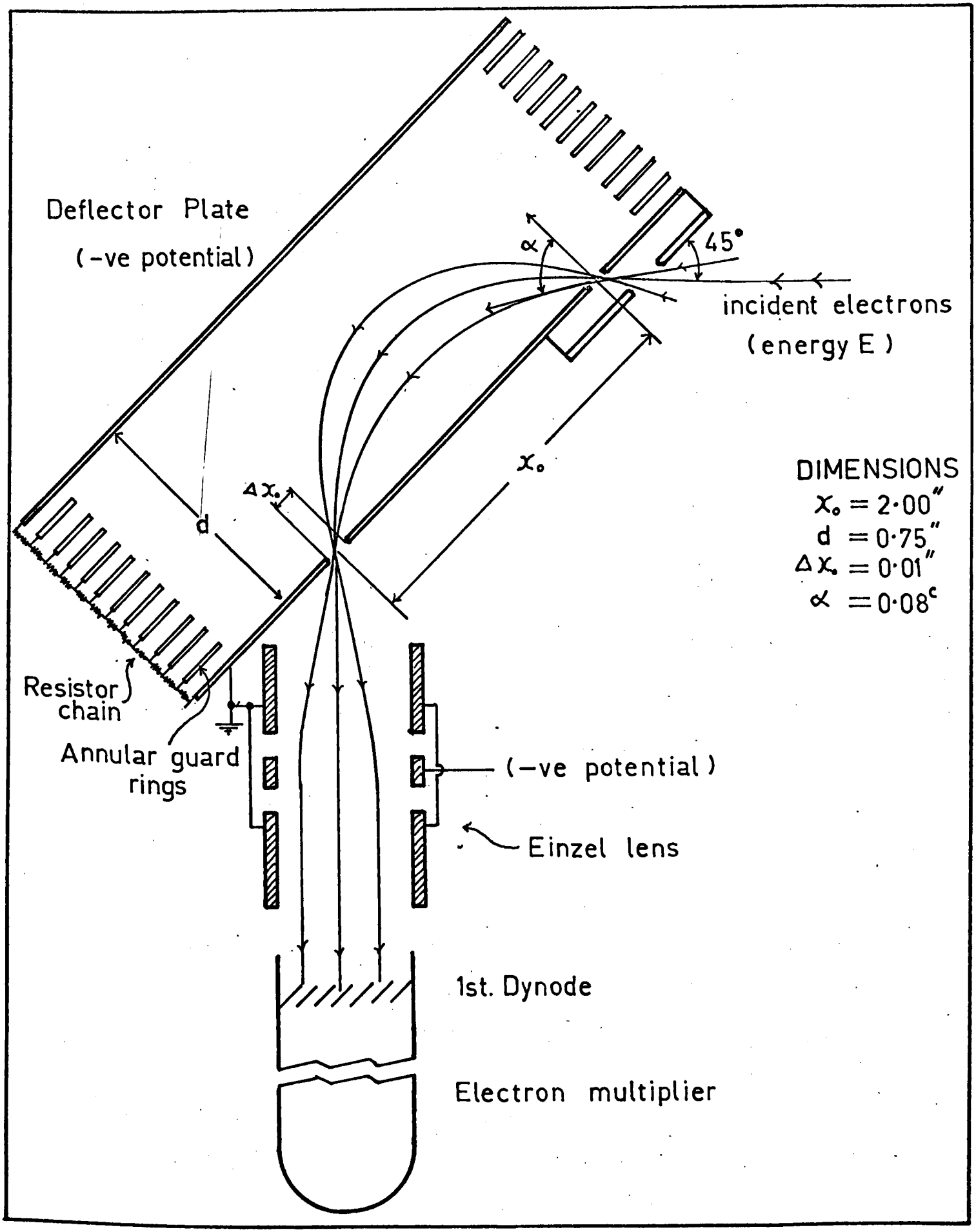

Figure 3.3 Electron Spectrometer and electron multiplier arrangement.

constant of proportionality between E and V determined experimentally agreed with the theoretical value of 1.32 electron beam before it entered the parallel field region. Then the resolution depended on the range of energy ΔE which electrons of average energy E possessed and still passed through the two slits of the analyser for a given value of the deflecting voltage. Harrower has shown that a linear relation exists between ΔE and the energy of the transmitted electrons. That is

$$\Delta E = k E \qquad (3.4)$$

where k is a constant and is given by

$$k = \frac{\Delta x}{x_0} (1 + \sec \alpha) - 1 + \sec \alpha \qquad (3.5)$$

Since increasing the entrance angle and slit widths to obtain larger beam signals resulted in a reduction of the resolution, the compromise chosen in the present apparatus for the theoretical value of k was 0.013 - sufficiently small to resolve electrons exciting the combined 2s, 2p states of atomic hydrogen for incident electron energies up to 200 eV. Aberrations in the electron optics and the thermal spread of the main electron beam however, resulted in an experimental value for k of approximately 0,017.

An example is given in Figure 3.4 of the inelastic spectrum of 200 eV electrons scattered through an angle of 25° from an approximately 75% dissociated beam of molecular hydrogen, showing the overlap of the prominent peak of electrons which had excited the combined 2s, 2p states of atomic hydrogen, with higher excited states of atomic hydrogen and the lower vibrational levels of the B state of molecular hydrogen. The combined 2s,

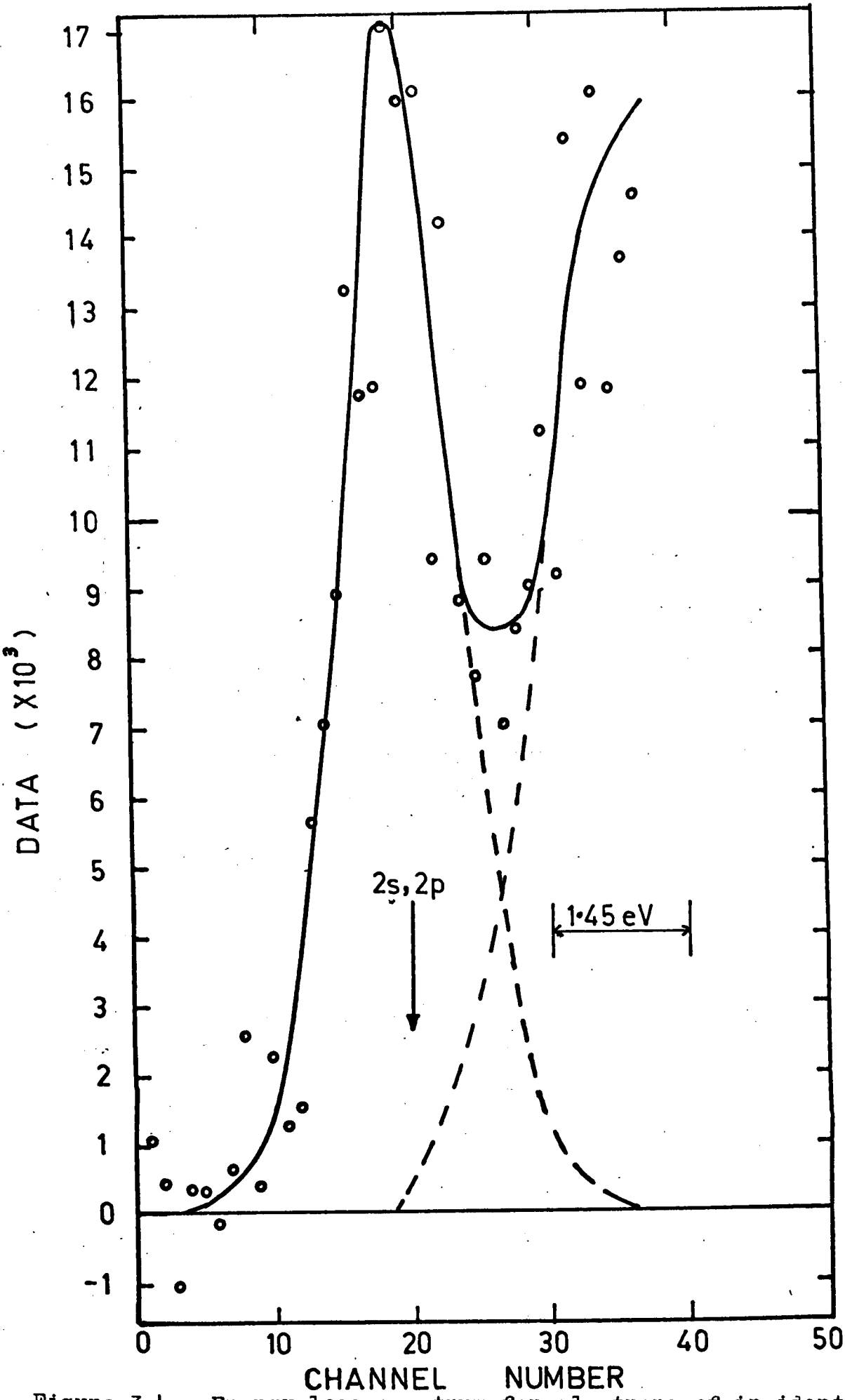

Figure 3.4 Energy loss spectrum for electrons of incident energy of 200 eV scattered through 25° from a highly dissociated molecular hydrogen beam

2p peak of atomic hydrogen was completely resolved from electrons exciting the higher states of atomic hydrogen and the B state of molecular hydrogen at incident electron energies of 50 and 100 eV.

The einzel lens situated between the exit slit of the spectrometer and electron multiplier, was operated with the outer pair of electrodes earthed. The centre electrode was maintained at a negative potential, (to suppress very low energy stray electrons), which never exceeded 40% of the energy of the electrons selected by the spectrometer. The beam signal was observed to be independent of the centre electrode over the range extending from 20% to 70% of the energy selected.

3.5 Mass Spectrometer.

Since the study of atomic hydrogen required the use of partially dissociated molecular hydrogen beams, a mass spectrometer was necessary to determine the composition of the beam. The theory and operation of the magnetic (60^{o} sector type) mass spectrometer used in the present system has been discussed by Teubner (1967). The only change to Teubner's arrangement was the inclusion of an ion extraction system and linear accelerator before injecting the ions into the electrostatic optics used to focus them on the entrance slit of the mass analysis stage. Since only very weak fields could be tolerated in the interaction region, it was necessary to perform the angular distribution measurements and mass analysis of the neutral beam in separate experiments, with the ion extraction field being removed whilst the signal from the electron spectrometer was accumulated. Figure 3.5 provides a schematic

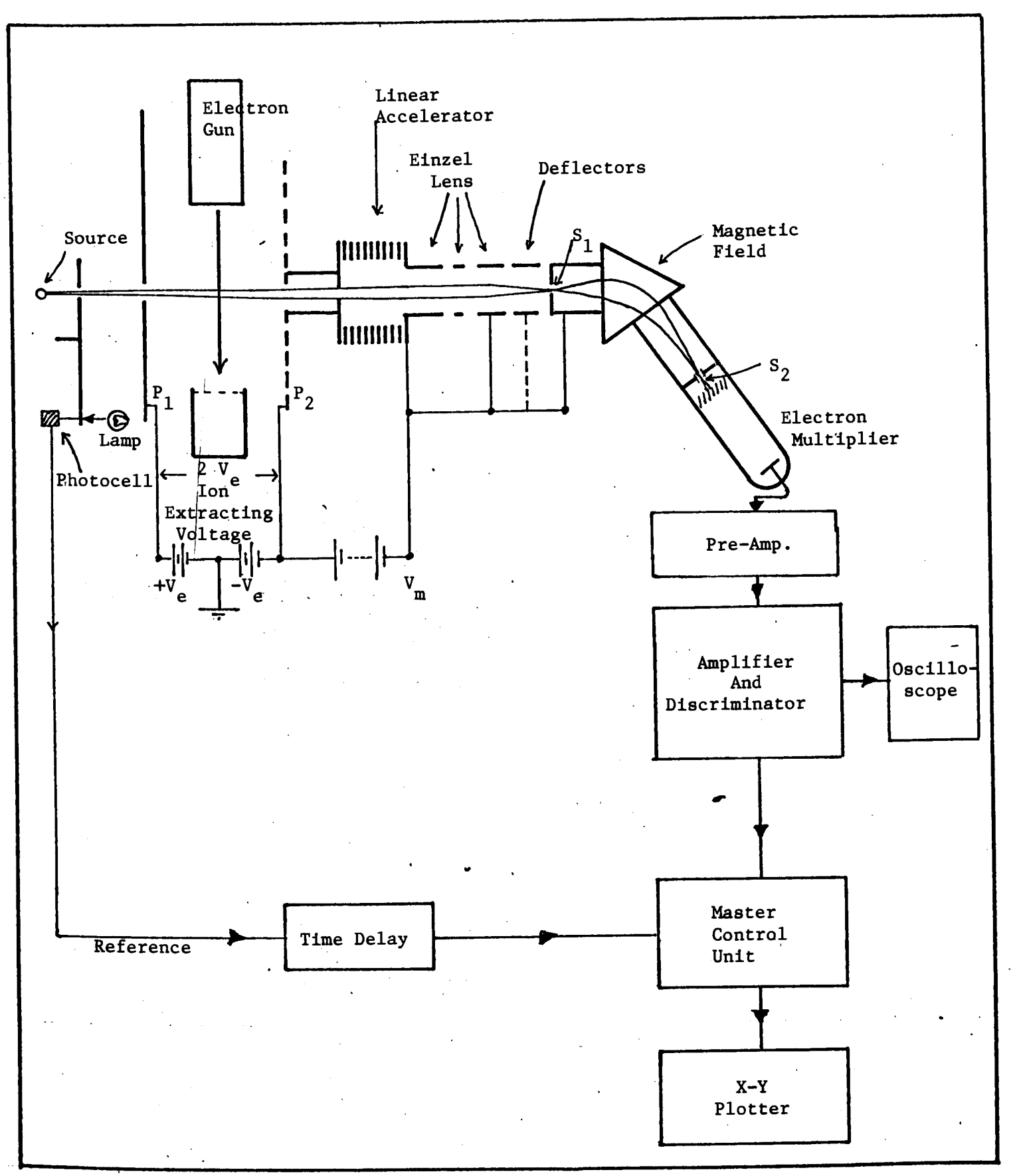

Figure 3.5. Schematic diagram for operation of the ion extraction field and mass spectrometer used to measure the composition of partially dissociated beams of molecular hydrogen.

diagram of the operation of the system when determining the composition of the neutral beam.

Ions produced in the volume including the intersection of the electron beam and neutral beam were extracted by an approximately parallel electrostatic field. This field was produced by applying the voltages $+V_e$ and $-V_e$ to two flat surfaces P_1 and P_2 respectively, which were symmetrically placed about the electron beam in a plane perpendicular to the neutral beam. (To remove the ion extraction field during the study of the scattered electrons, the extracting field surfaces P_1 and P_2 were earthed.) P_1 was a metal plate with an aperture to pass the neutral beam and P_2 a rigidly supported fine wire mesh (of 90% transparency). The ions were accelerated from their energy of approximately 7 eV, (gained during extraction from the interaction region), to 150 eV energy, by the linear accelerator. The parallel field of the linear accelerator was produced by placing 90% transparency copper mesh across the accelerator's input and output, and using a resistor chain to provide equal voltage increments between regularly spaced annular rings. The ion beam produced by the linear accelerator was first focussed on the slit S_1 and then analysed by the mass spectrometer. After mass analysis, the ion signal was amplified by an electron multiplier, digitized, and directed to the data handling system (discussed in the next section), where the beam signal was separated from the total signal and plotted on an X-Y recorder.

A study of the collecting efficiency of the extraction system as revealed by the change in beam signal (when the mass analysis was adjusted for a particular ion species

present in the neutral beam) with increasing extraction voltage 2Ve is shown in Figure 3.6. A plateau is obtained for extracting voltages above approximately 15 volts. The value of 2Ve used when determining the molecular hydrogen contributions to the total beam signal during the study of atomic hydrogen was 17 volts. Ionization of the neutral beam was performed by a high energy electron beam (200 eV) to prevent serious deflection of the electron beam by the ion extraction field.

3.6 Signal Handling Method.

3.6.1 Introduction.

The only experimental angular distributions that have been reported for electron scattering from atomic hydrogen (Gilbody et al 1961), were performed at energies below the first excitation threshold, and were therefore concerned with elastic scattering only. The analogue detection method previously described was therefore adequate for Gilbody's et al's experiment because no energy analysis was necessary, and an adequate signal could be obtained from the scattered electron detector by providing it with a sufficiently large entrance aperture. However, not only do experiments performed above the first excitation threshold require the use of an energy analyser (and therefore a small entrance aperture) to select those electrons with the required energy, but also the differential cross section at a particular energy rapidly becomes smaller with increasing angle. For example, at 122 eV, the Born - Oppenheimer value for the ratio of differential cross sections at 0^0 and 90^0 for exciting the 2s state is 1 : 10^5 (Wu 1960).

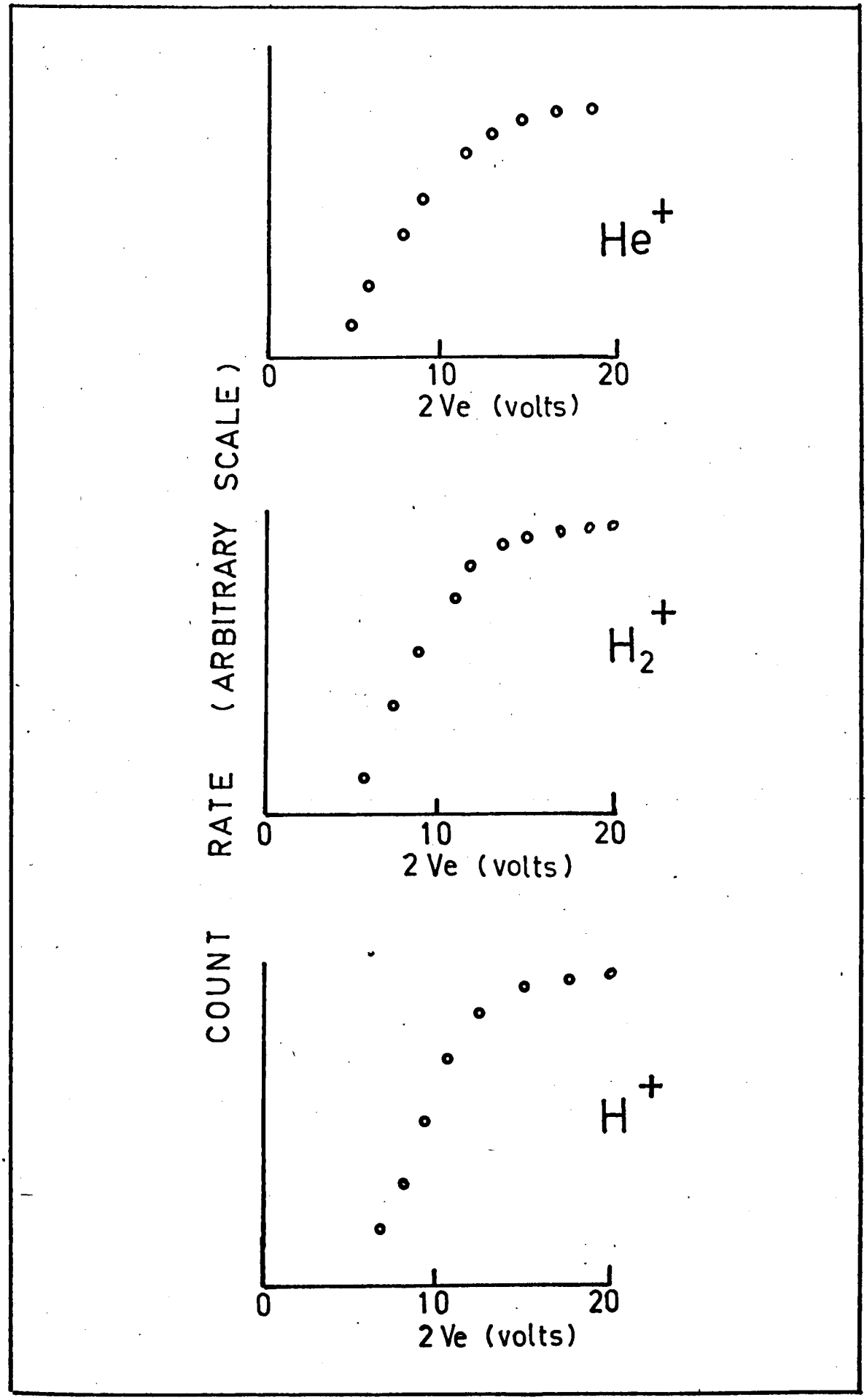

Figure 3.6 Studies of the collecting efficiency of the mass spectrometer as a function of ion extraction field 2 Ve for helium and atomic and molecular hydrogen.

Fortunately higher electron energies permit the generation of more intense electron beams, so that whilst the scattered intensity can still be studied as a function of angle for small angles using the previously described analogue techniques, this method is inadequate for large angle scattering, where the total signal produced by the neutral beam and background gas can be as low as several hundred electrons each second. It is therefore preferable to use digital techniques.

3.6.2 Analogue and digital techniques compared.

Arrechi (1966) has analysed the noise filtering properties of analogue amplifiers followed by phase sensitive detectors, and has shown that in principle digital detection and data handling is statistically equivalent to analogue systems provided the scaling rate can be adequately handled. Furthermore a digital system does not have the problems of avoiding unbalance effects and non-linear response in the rectification which are experienced with analogue systems. In digital systems, the output pulse from the electron multiplier is amplified, pulse shaped, and fed to the input of a pulse height discriminator whose threshold is adjusted so that it lies above all electrical noise present, (but below most of the pulses representing scattered electrons). These latter pulses are then converted to a standard pulse and counted in a scaler. Since the only noise pulses recorded originate in the electron multiplier at the very low rate of one every few seconds, the signal observed can be considered to be free of noise, while still maintaining a high detecting efficiency for electrons entering the electron multiplier.

3.6.3 Application of the Digital technique.

Scattered electrons transmitted by the electron spectrometer, and ions selected by the mass spectrometer, were initially amplified by separate electron multipliers.* After further linear amplifications,** all pulses above a threshold (adjusted to reject all electronic noise within the amplifier) were digitized by the discriminator unit.**

A number of experiments have been reported in the literature which employ digital techniques to handle the scattered signal. A common procedure (McGowan and Fineman, 1965) is to use the reference to switch the detector signal alternately between 2 scalers so that the beam plus background signal is accumulated in one scaler (while the beam is off). After scaling for sufficient time to reduce the fluctuations in the background signal to a small fraction of the beam signal, the latter is obtained by calculating the difference between the entries in the 2 scalers. Alternatively a single scaler can be used (Arrechi, 1966), in which all pulses received during the beam on period are added to the current entry, and during the beam off period are subtracted from the current entry. After equal numbers of beam on and beam off periods, the entry in this scaler (called the BEAM scaler) represents the sum of the beam signal and random walk of the background. A simple add - subtract scaler has been used in the present apparatus.

* E.M.I. Cu-Be venetian blind type 9603B.

** Dynatron Types 1430 and N101 for scattered electron pulses. Franklin Model 358 for ion pulses.

A representation of the energy loss spectrum for those electrons scattered through a particular angle by by atomic beam, can be obtained directly if the entry accumulated in the BEAM scaler during successive equal intervals of time, is recorded at regular increments of the peak voltage applied to the deflector plate of the spectrometer. This has been the method used in the present apparatus, with the deflector plate potential being provided by a STAIRCASE FUNCTION voltage generator. Since the increments were selected so that at least 12 steps were required to scan through a single energy loss peak at each of the incident energies studied, a graph of the data obtained represented the shape of the energy loss spectrum over the energy range covered.

3.6.4 Automatic Chart Recorder system.

A convenient recording system may be obtained by plotting the analogue voltage (representing the entry in the BEAM scaler at the end of the accumulation period) on the Y axis of an X-Y recorder*, whose X axis is controlled by the voltage applied to the spectrometer. Experiments can be performed more efficiently if the sequence of commands required to produce an energy loss spectrum are automated. Since none of the automatic recording systems described in the literature (Briglia and Rapp, 1965; St John, Lin, Stanton, West, Sweeney and Rinehart,

* Moseley Model 2D-2.

1962, and Rudd, 1966) provide the STAIRCASE FUNCTION generator** and sequence of operations required, a system was developed and is described in this thesis, which automatically performed these functions and therefore could be used for recording (on an X-Y chart recorder) the data obtained from experiments requiring only a single scan through the spectrum at each angle. An example of the chart record obtained is given in Figure 3.7.

** Instead of performing the energy analysis at discrete intervals, an alternative method is to apply a linear voltage ramp to the analyser and record the analogue voltage (representing the scaler entry) at regular intervals of time. Since (as will be explained later in this section) the fraction of each second during which data can be directed to the BEAM scaler is a function of the speed of the mechanical chopper, any variations in its speed result in the problem of synchronizing the data record and the average energy at which it is recorded - particularly towards the end of the ramp. Further-more linear ramps generated electronically using IC operational amplifiers (whose slopes are therefore simple to vary over a wide range), require very high values of input resistance and feed back capacitors if high linearity is to be combined with very small changes of voltage with time.

The method described in the text employing a STAIRCASE FUNCTION generator, not only avoids these problems, but is convenient for extending the system to multiple scanning, since the starting condition is obtained simply by resetting the scaler used in the production of the STAIRCASE FUNCTION.

Figure 3.7 Sample X - Y recorder points plot for elastic scattering of 200 eV electrons from molecular hydrogen at angles from 60^{o} to 130^{o}. Note: this data was obtained with a single scan through the elastic peak at each angle.

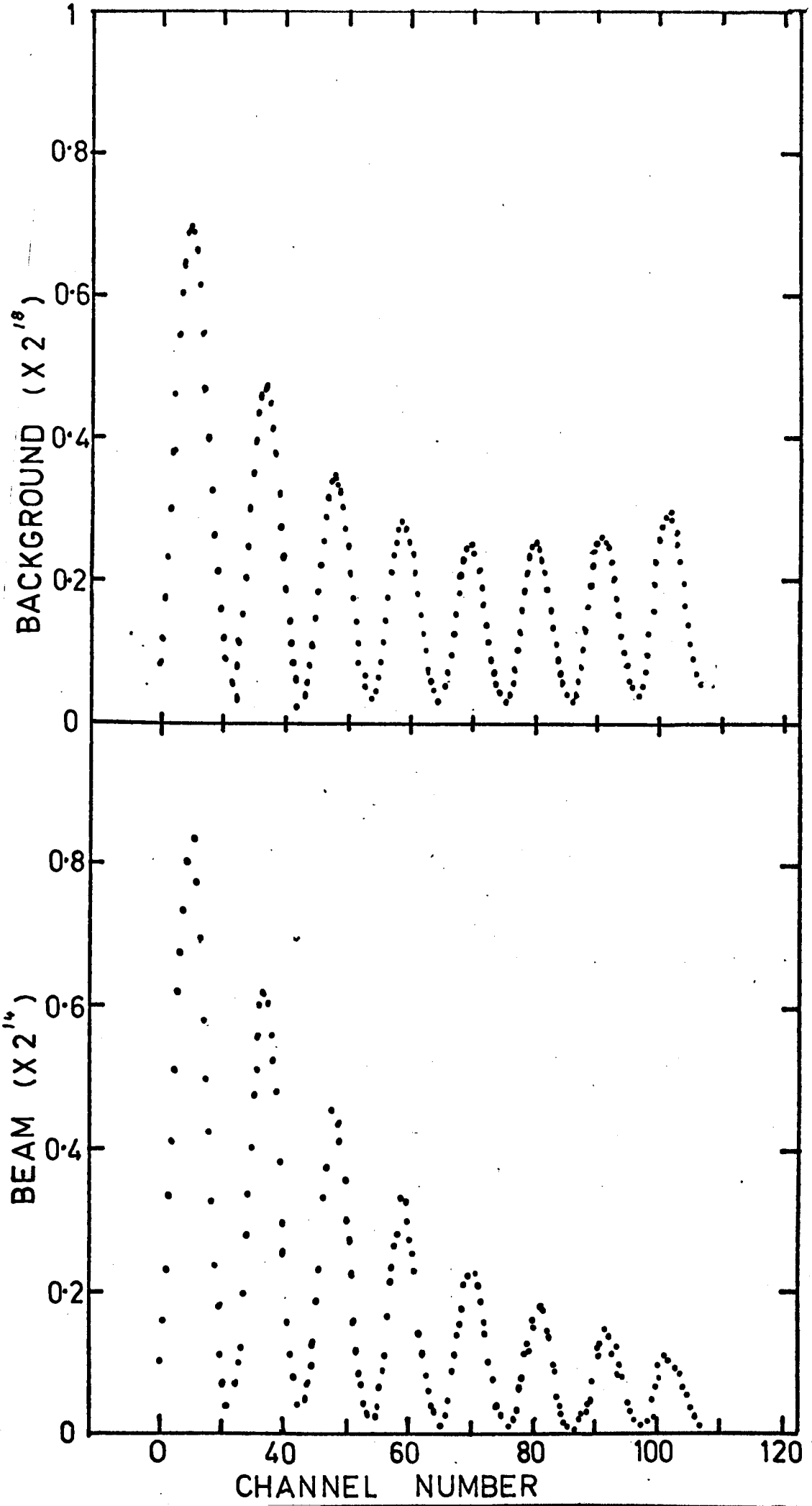
1
0·8
0·6
0·4
0·2
0
BACKGROUND (X 2^18)
0·8
0·6
0·4
0·2
0
BEAM (X 2^14)
0
40
60
80
100
120
CHANNEL NUMBER

3.6.5 Multiple Scanning.

Except at small angles, however, there was the further complication that the beam signal,(which was never more than eight per cent of the total scattered signal),was so low that up to six hours of data accumulation were necessary to record inelastic spectra at a number of angles with sufficient statistical accuracy to derive reliable scattered electron angular distributions. Even though the electronics used by digital detection and data handling techniques had good long term stability, drifts in experimental conditions could still occur during the long period of time separating the measurement of the first and last angle's spectra, which were difficult to allow for, and seriously limited the reliability of angular distributions so obtained.

Long term drifts could be averaged out however, if a single inelastic spectrum was produced for each angle by adding together a large number of records of each angle's spectrum obtained by repeatedly scanning rapdily over energy and angle. A more efficient method of summing the large number of scans produced at a given angle, was to record the beam counts on computer punch cards or tape (Heddle and Keesing, 1967a) and use a computer to perform the addition. This method had the disadvantage that the statistical accuracy of the data at any time was not readily available, unless there was on line access to a computer (Bowen et al 1967). The procedure adopted here avoided this problem by using a multichannel analyser* (operated in store mode) as a 400 channel multiscaler (Heddle and Keesing,

* RIDL Model 34-12B

1967b) with the beam data being stored in different channels for each voltage of the STAIRCASE FUNCTION and each angle studied. During subsequent scans over the same energy and angular ranges, data was added to the information previously stored, and the process continued until the fluctuations in the spectra were reduced to a satisfactory level. The display provided by the oscilloscope for typical data stored in the multichannel analyser was similar to the lower half of Figure 3.7. The contents of the multichannel analyser were then automatically plotted on an X-Y chart recorder, or transferred to either a printer for numerical read-out, or punch cards for subsequent analysis by computer.

Since the electron spectrometer was supported from the lid of the scattering chamber and always occupied the same position with respect to the vacuum system, the angle through which electrons must be scattered out of the incident beam to enter the spectrometer was varied by rotating the gun platform (to which the electron gun is mounted) about the atomic beam's axis. To permit automatic control of the angular scan, the detection of scattered electrons was limited to those angles at which a wiper (mounted on the rotating electron gun platform but insulated from it and maintained at 15 volts) made contact with one of a series of regularly spaced pins, which were attached to the base of the scattering chamber but electrically isolated from it. Wires connecting each of the pins to the electronics which controlled the angular scan control were introduced into the vacuum system through kovar seals.

Whilst the automatic chart recorder system was not essential if the data was stored in the multichannel analyser, it was still very useful when performing repetitive scans, since it provided on-line information and a permanent record of the data added to each channel during every scan.

A description of the data handling system is given in Chapter 4.

CHAPTER 4. AUTOMATIC DATA HANDLING SYSTEM

Introduction.

It was noted in Chapter 3 that while the modulated beam technique provides a means of performing experimental studies on atomic hydrogen, the small signals obtained when examining the electrons which have been inelastically scattered through large angles, requires the use of digital detection and data handling techniques. Furthermore, the many hours of data accumulation necessary to obtain inelastic spectra for even a limited number of angles, makes it desirable to sum the information obtained by repetitively scanning rapidly over energy and angles. Since none of the automatic recording systems described in the literature provide the sequence of operations required, a system is described here in which the beam data for each value of the STAIRCASE FUNCTION generator (used to control the energy analysis) and each angle studied, is stored in different channels of a multichannel analyser. A detailed account of the operations of this system has been given elsewhere (Williams 1968).

4.1 General.

The data handling system is divided into two units which perform separate functions. The first unit (called the MASTER CONTROL UNIT, M.C.U.) can be used independently of the second unit (the AUXILIARY CONTROL UNIT, A.C.U.), to produce X-Y recorder point plots of both the beam and background signals when the count rate is high enough to render multiple scanning unnecessary. Note however,

if used separately from the A.C.U., it is necessary to either duplicate the STAIRCASE FUNCTION generator (which is part of the A.C.U.) or provide a linear ramp to supply the voltage required by the electron spectrometer. The second unit (A.C.U.) is used in conjunction with the M.C.U. when it is necessary to multiply scan. The A.C.U. controls the flow of data to the multichannel analyser, synchronising its CHANNEL ADDRESS scaler with both the scattering angle viewed by the electron spectrometer and the voltage controlling the energy analysis. The operator need only select the scattering angles, energy range and interval of time spent in each channel at the appropriate controls on the front panels of the two units, and the energy and angular scanning sequence is automatically repeated until stopped by the operator.

The data system described here has been designed with the additional purpose of obtaining information which would enable atomic and molecular hydrogen angular distribution to be normalized to known differential cross sections (Vriens 1968a) for excitation of the 2^1P state of helium (See Appendix A). While the operation of the DOUBLE RANGE CONTROL unit, (which enables such experiments to be performed by including two energy ranges in the automatic scanning sequence), is not relevant to the present investigation, a description of the data handling system would be incomplete without its inclusion.

4.2 Master Control Unit.

The general operating functions of each of the sub-units which make up the MASTER CONTROL UNIT are drawn in Figure 4.1 and enclosed in dotted lines. Shown also are the principle interconnections between the sub-units. In the remainder of this description, the sub-units will be referred to as units. Outputs from the REFERENCE unit co-ordinate the functions performed by all other units of the M.C.U. The time during which data may be transmitted by the INPUT SIGNAL GATE to both BEAM and BACKGROUND scalers is limited to a specified fraction (or window interval) of each half cycle by the WINDOW TIME unit. The CHANNEL CONTROL unit restricts the period of time during which data is accumulated in a particular channel to a preselected number of window intervals (counted by the CHANNEL TIME unit). The sequence of operations required to plot (on an X-Y chart recorder), analogue values corresponding to the entries in the two signal scalers are produced by the PLOT CONTROL unit.

The reference signal is first converted to a square wave, and then provided with a variable delay to permit the phase sensitive detection of the beam signal. The DELAYED REFERENCE is referred to as REFERENCE A and its inverse as REFERENCE B. A short PREPULSE which preceeds each level change of the DELAYED REFERENCE is used as a "clock" pulse to synchronise the functions performed by the other units of the M.C.U.

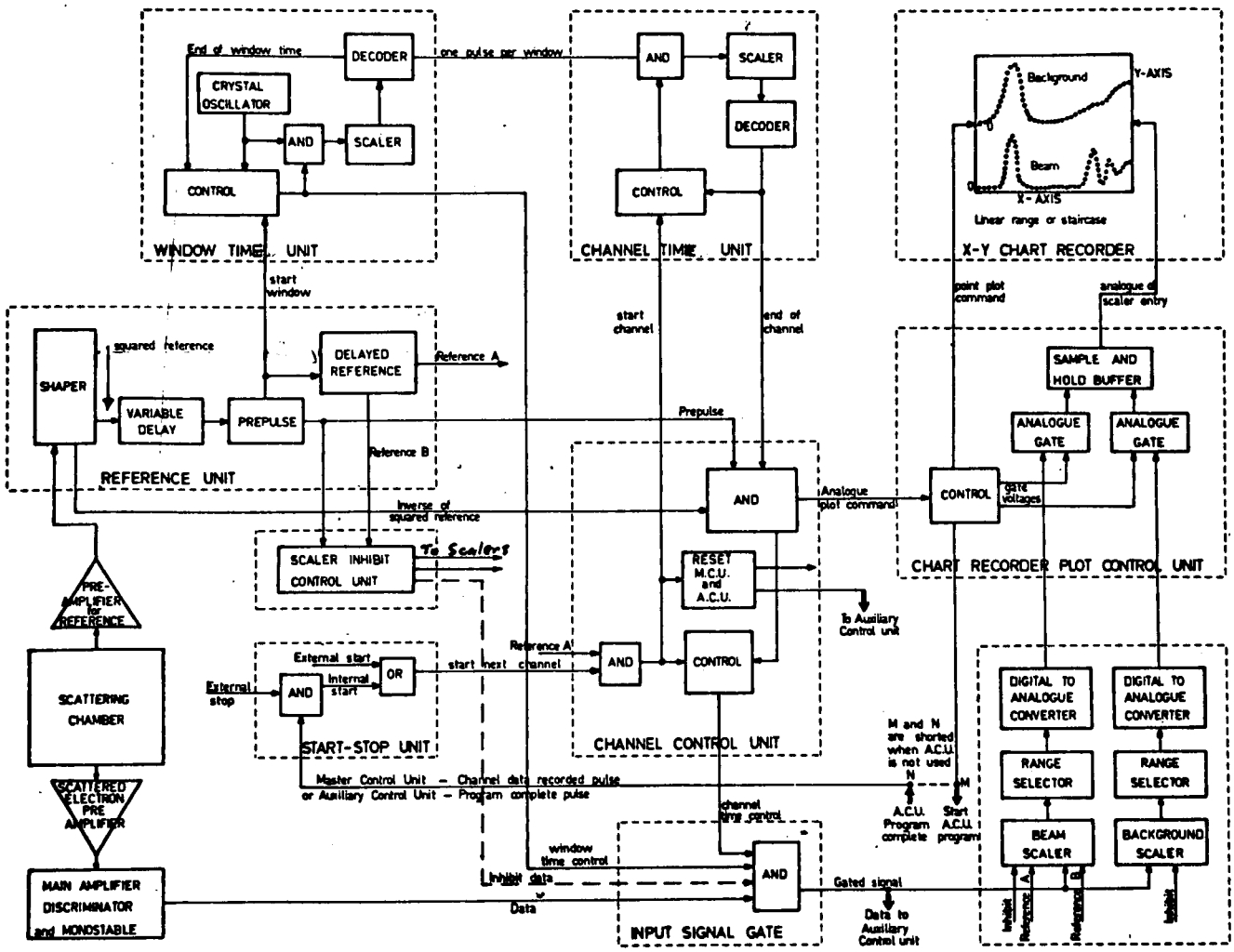

Figure 4.1 Schematic diagram showing the principle logic operations performed within the MASTER CONTROL UNIT. Dotted lines enclose the separate units of which it is made.

Two conditions must be satisfied for the production of useful beam signal records. Since the beam signal is usually only a few percent of the total signal, it is necessary to reduce any systematic error contributed by the background signal to the beam signal, to less than 0.01% of the background. The M.C.U. satisfies this condition by limiting the scaling period during each half cycle to a "window" period which is accurately determined by the interval of time required to scale a preselected number of oscillations produced by a crystal oscillator*. The timing of this interval (which usually occupies about 90% of each half cycle of the reference waveform) is performed by the WINDOW TIME unit. The second condition arises out of the need to accumulate data for a regular period of time before permanently recording the entry present in each signal scaler. The CHANNEL CONTROL unit performs this function by restricting the time between chart recorder plots of the data, to the period of time required to scale a preselected number of window intervals. Both WINDOW TIME and CHANNEL CONTROL units, (through their outputs to the INPUT SIGNAL gate) limit the flow of data from the apparatus to the signal scalers so that the data recorded satisfies the two conditions previously stated.

A third condition which must also be satisfied is the prevention of data from reaching the scalers during the last few micro-seconds before the reference changes state, to allow for the propagation delay in the signal scalers. This, however, is easily satisfied by a suitable restriction on the length of the window interval. If this system were used without

* A similar procedure has been used by Dance, Harrison, and Smith

the inclusion of the WINDOW TIME unit, the propagation delay could be allowed for by the inclusion of a third input (also shown on Figure 4.1) to the INPUT SIGNAL gate which is controlled by the INHIBIT SIGNAL output of the SCALER INHIBIT CONTROL unit.

Two scalers are used to record the experimental data transmitted by the INPUT SIGNAL GATE. One of these, the BEAM scaler, is directed by REFERENCE voltages A and B to operate in the add mode during the beam on half cycle and subtract mode during the beam off half cycle. The remaining signal scaler (called the BACKGROUND scaler) is inhibited (by an output from the SCALER INHIBIT CONTROL UNIT) during the beam on half cycle, and adds the data arriving during the beam off period to the background signal previously accumulated.

When the INPUT SIGNAL gate closes at the end of each channel accumulation period, the CHANNEL CONTROL unit starts the PLOT CONTROL sequence, which plots the DIGITAL to ANALOGUE CONVERTER output for each scaler alternately as points on separate halves of the chart recorder paper. Range selection is provided in the parallel output from each signal scaler to its DIGITAL to ANALOGUE CONVERTER (D.A.C.). Best use can then be made of the chart recorder plot by selecting the range for which the most significant bit of the entry in each scaler produces half of full scale deflection. After plotting the first point (from one D.A.C.) and buffering the output from the other D.A.C. until it can be plotted, the PLOT CONTROL unit produces a pulse which restarts the data accumulation sequence for the next channel.

Hence once the M.C.U. has been started, it will

continue to reset the signal scalers, accumulate data and plot the analogue beam and background signals regularly until stopped by an external command. The M.C.U. is started manually by simulating the CHANNEL DATA RECORDED pulse from the PLOT CONTROL unit, and stopped by preventing the CHANNEL DATA RECORDED pulse fromreaching the CHANNEL CONTROL unit and starting a new channel.

4.3 Auxiliary Control Unit.

The AUXILIARY CONTROL UNIT (A.C.U.) is used when it is necessary to scan repeatedly over the energy range and angles under study, and therefore preferable to accumulate the data in the store of a MULTICHANNEL ANALYSER (M.C.A.). The connections between the SCATTERING CHAMBER, DATA HANDLING system and MULTICHANNEL ANALYSER are shown schematically by Figure 4.2. Also shown are the principle connections between the various control units (drawn in block diagram form) which comprise the A.C.U.

The period of time for which beam signal is accumulated in the M.C.A. is determined by the WINDOW TIME and CHANNEL TIME control units of the M.C.U. Data which has been appropriately gated by the MASTER CONTROL UNIT (M.C.U.) is then directed first to the A.C.U. for buffering, and finally to the M.C.A. where it is accumulated in its ADD-SUBTRACT scaler. ADD and SUBTRACT COMMANDS are obtained from the M.C.U. (after buffering by the A.C.U.) so that the beam signal is accumulated under the same conditions as described for the M.C.U. BEAM scaler (see Section 4.2).

There are two main functions of the A.C.U.

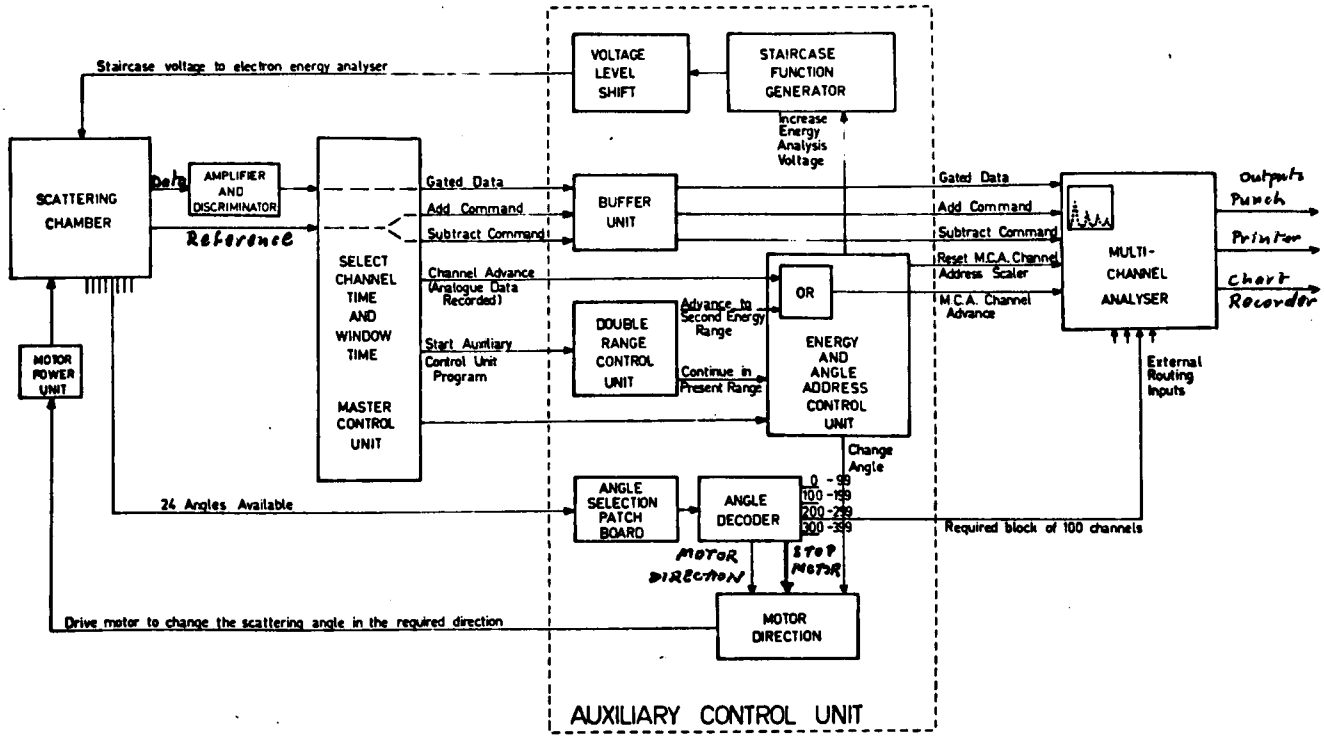

Figure 4.2 Schematic diagram of the arrangement used when performing multiple scans, showing the connections between the scattering chamber, Data Handling System and Multichannel Analyser. The principle connections between the various control units within the AUXILIARY CONTROL UNIT are also shown.

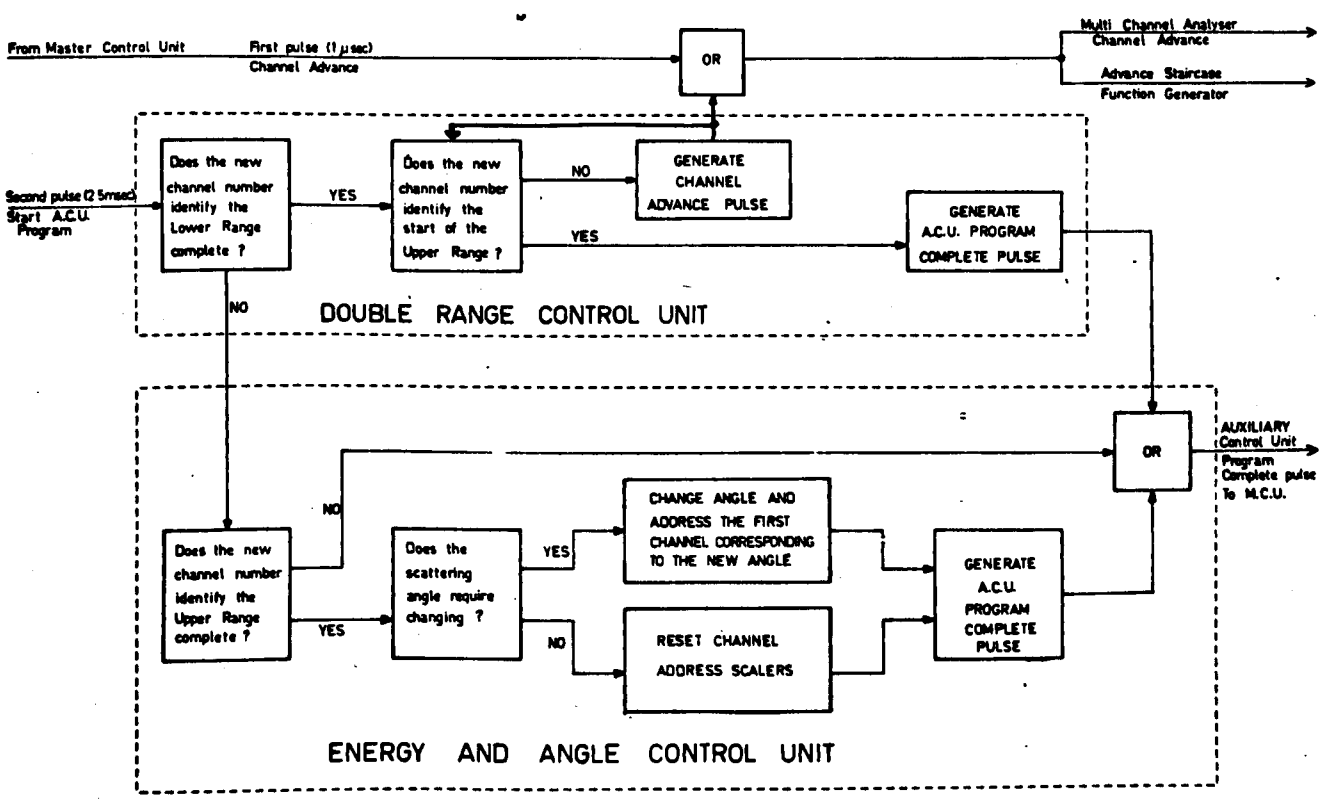

Figure 4.3 Block diagram form of the functions performed by the two pulses delivered to the AUXILIARY CONTROL UNIT from the MASTER CONTROL UNIT.

Firstly it synchronizes the channel in which the contents of the M.C.A.'s ADD-SUBTRACT scaler is stored with the particular energy of scattered electrons and angle at which they are observed. And secondly it automatically performs a single energy scan at each of the angles selected, and then repeats the sequence indefinitely - at each repetition, adding the new data to that previously accumulated.

External inputs to the M.C.A. permit the subdivision of its store into 4 blocks of 100 channels each. If 4 or less angles are included in the multiple scan, 100 channels can then be assigned to each angle. To extend the number of angles up to a maximum of 8, these blocks are further subdivided into 2 blocks of 50 channels each, with odd angles occupying the first half of the original blocks of 100 channels and the even angles occupying the second half.

To permit automatic control of the angular scan, the detection of scattered electrons is limited to those angles at which a wiper (mounted on the rotating electron gun platform but insulated from it and maintained at 15 volts) makes contact with one of a series of regularly spaced pins which are attached to the base of the SCATTERING CHAMBER but electrically isolated from it. A wire connects each pin to the ANGLE SELECTION patch board (at the front panel of the A.C.U.), from which the angles to be studied in any particular experiment are selected and connected to the ANGLE DECODER unit.

The particular angle selection input to the ANGLE DECODER corresponding to the current position of the electron gun, selects unambiguously the first channel at the

appropriate block of 100 channels by directing a suitable logic level to the required input of the 4 EXTERNAL ROUTING inputs at the M.C.A. If 50 channels are used at each angle, then for even angles, 50 CHANNEL ADVANCE pulses are automatically directed to the M.C.A. to advance the units and decade CHANNEL ADDRESS binaries to the entry value of 50. Separate blocks of channels are therefore assigned unambiguously to each of the angles studied.

Energy analysis of electrons scattered through a known angle is performed at regular increments of the STAIRCASE voltage which is applied to the deflection plate of the electron spectrometer. This STAIRCASE voltage is produced in the A.C.U. by converting the digital entry in a scaler to an analogue voltage. The A.C.U. then synchronises the units and decade CHANNEL ADDRESS binaries of the M.C.A. with the scaler of the STAIRCASE FUNCTION generator (and hence the energy of the detected scattered electrons), by resetting both scalers simultaneously (and directing the 50 channel advance pulses to the M.C.U. when addressing even angles) at the start of the data collection at each angle, and always directing subsequent CHANNEL ADVANCE pulses in parallel to both scalers when performing the energy analysis. Since the STAIRCASE FUNCTION generator operates at voltages close to earth, two variable floating power supplies (LOWER and UPPER VOLTAGE supplies) can be connected in series between the output of the STAIRCASE FUNCTION generator and the spectrometer, to provide the absolute voltage required by the analyser for transmission of electrons with the desired energy.

Figure 4.3 illustrates the decisions made by the DOUBLE RANGE CONTROL unit, whose function is to include either one or two separate energy ranges in the automatic energy scan sequence. Switches on the front panel of the A.C.U. permit the selection of the limits of the two (LOWER and UPPER) ranges or the end of the energy scan when a single range only is studied.

Changes in the A.C.U. are initiated by two pulses (generated by the M.C.U.) at the end of the data accumulation period for the current channel as directed by the CHANNEL TIME control unit of the M.C.U. Firstly an ANALOGUE PLOT COMMAND pulse, generated by the PLOT CONTROL unit of the M.C.U., is delivered to the A.C.U. where it generates CHANNEL and STAIRCASE FUNCTION generator ADVANCE pulses. These in turn advance by one the entry in the M.C.A. CHANNEL ADDRESS and STAIRCASE FUNCTION generator scalers respectively. A second pulse generated in the M.C.U., (where is restarts the data handling sequence when the A.C.U. is not used), is delivered to the A.C.U. 70 milliseconds after the first pulse. This second pulse (referred to as the START A.C.U. PROGRAM pulse), does one of three things (Figure 4.3), depending on the relation between the new channel and the channel numbers identifying the limits of the LOWER and UPPER energy ranges selected.

If the new channel corresponds to the limit of either the LOWER or UPPER energy range, the START A.C.U. PROGRAM pulse is transmitted by the ENERGY AND ANGLE CONTROL unit and produces an A.C.U. PROGRAM COMPLETE.

However, if the new entry corresponds to the upper limit of the LOWER energy range, then the START A.C.U.

PROGRAM pulse initiates a series of pulses which change the energy range from LOWER to UPPER range, after which it generates an A.C.U. PROGRAM COMPLETE pulse. If the new entry corresponds to the upper limit of the UPPER energy range there are two alternatives.

For multiple scanning over more than one angle, the START A.C.U. PROGRAM pulse commands the motor at the scattering chamber to change the scattering angle, and upon reaching the next angle selected, produces an A.C.U. PROGRAM COMPLETE pulse. If the multiple scanning is performed at one angle only, an A.C.U. PROGRAM COMPLETE pulse is generated immediately, and directed to the M.C.U. where (for all of the three possible previous operations), it restarts the data handling sequence. On returning to the first angle, the scanning sequence is automatically restarted, unless a manual command to stop has been given at any point in time during the previous scan over the selected angles.

The MOTOR DIRECTION unit ensures that no transient voltage spikes between wiper and pin can prevent the scattering angle changing to the next angle selected. It also reverses the direction of the motor to return the scattering angle directly to the first angle after completing the energy scan at the last angle.

When the experimentor considers that the statistical spread of the data has been reduced to an adequate level, outputs at the rear of the M.C.A. enable the contents of its store to be either automatically plotted on an X-Y chart recorder, or transferred to either a printer (for numerical read-out) or punch cards (for subsequent analysis by computer).

CHAPTER 5. DATA ANALYSIS

Introduction.

A data handling system has been described in Chapter 4 which enables ions or scattered electrons produced at the intersection of an electron beam and chopped neutral beam to be distinguished from the far greater signal produced by the background gas. It has been further explained how the raw data for the beam signal (in which each count represents the detection of a single ion or scattered electron) is accumulated in the store of a multichannel analyser.

This chapter is concerned with the procedures used to convert the raw data into angular distributions. Also possible sources of error are identified and evaluated and the quality of the results obtained from this apparatus is demonstrated by comparison with published results for electron scattering from helium and argon.

5.1 Data Reduction.

5.1.1 General Procedure.

To obtain all the information required to derive an angular distribution, it was necessary to perform the experiment in two parts. During the first part of the experiment, beam data only was stored in the multichannel analyser in accordance with the description given in Chapters 3 and 4, while the second part determined the total observed signal count at each channel so that the raw beam data could be corrected for dead time losses. This second part of the experiment was performed immediately following the printing* and punching** of the

* Hewlett Packard Model H23-562A.

** I.B.M. Model 026

raw beam data and was identical in all respects to part one except that all data was now added (in the multichannel analyser) during both halves of the reference cycle and only one scan was necessary to obtain satisfactory statistics.**

Printed and punched records of the results of part two were then obtained and the raw beam and total data submitted to the computer# for processing to produce an angular distribution.

The computer program processed the data in six stages. First, dead time corrections were made to the beam and background data for each channel - after which the raw data, corrected data and standard deviations of the corrected beam data were printed in tabular form. Graphs of the energy spectrum (obtained by graphing the corrected beam data against channel number) were then plotted at each angle by the computer to display the energy loss peak for the scattering process studied. The area under each peak was calculated next by summing the corrected beam from the appropriate channels. The fifth stage was concerned with calculating the standard deviation of the area, and the sixth stage printed the angular

---

** While fluctuations and drifts in the background signal made it preferable to accumulate the background signal simultaneously with the beam signal, this had been prevented by the lack of sufficient storage capacity in the multichannel analyser. However, the method described was satisfactory since the record of the background signal produced on the X-Y chart recorder during each scan always showed that the background signal never varied by more than 10%.

CDC 6400.

distribution and standard deviations in tabular form.

The formulae used to correct the raw data for dead time losses are derived in Appendix B. If the raw beam data N_o accumulated in each channel during a total time T_{beam}, is corrected for the dead time t_d of the discriminator, then the number of beam pulses N_e which entered the discriminator is given by (equation B.15 of Appendix B)

$$N_e = \frac{4\ N_o}{\left(2 - \frac{T_{beam}}{T_{total}}\ S_o\ t\right)^2 - (N_o\ t)^2} \quad , (5.1)$$

where $$t = \frac{2\ t_d}{T_{beam}\ f\ t_w} \quad , (5.2)$$

f was the modulation frequency, t_w the window interval, and S_o the raw data for the total count obtained during the second experiment and accumulated over a time T_{total}.

The total background count $2M_e$ is given by (equations B.16 and B.17 of Appendix B)

$$2\ M_e = \frac{2\ D_o}{2 - D_o\ t} \quad , (5.3)$$

where $$D_o = \frac{T_{beam}}{T_{total}}\ S_o - N_o \quad . (5.4)$$

If $(N_e + 2\ M_e)_n$ represents the sum of corrected beam and background data in channel number n, then the standard deviation σ of the area under the curve representing the total beam signal scattered into the electron spectrometer at a

particular angle is given by

$$\sigma^2 = \sum_{n=N_1}^{N_2} (N_e + 2 M_e)_n \qquad (5.5)$$

where N_1 and N_2 are the extreme channel numbers included in the energy loss peak at that angle. Since the beam data N_e was always a small fraction of the total background $2 M_e$, the major contribution to the random error of the beam signal was always due to the background signal. An example of the X-Y chart recorder point plot for two successive scans through the combined 2s, 2p inelastic peak of atomic hydrogen is shown in Figure 5.1. The random error of individual beam data points is observed to be large compared with the scatter of the background data points. The single spectrum obtained by summing the beam data for each channel (in the multi-channel analyser) from 8 scans is shown in Figure 5.2 (b).

Since the maximum number of angles for which data could be stored in the multichannel analyser was limited (by the present data handling system) to eight, it was not possible to adequately cover the full angular range in one experiment. Therefore, it was necessary to repeat the experiment for different ranges of angles and overlap them at common angles. Additional experiments were performed using different electron beam currents and neutral beam source pressures. To obtain a single angular distribution for a single incident electron energy and scattering process involving a particular gas, the results of all relevant experiments were plotted on separate graphs (using a logarithmic scale for the beam data) and superimposed to obtain the best fit of all the

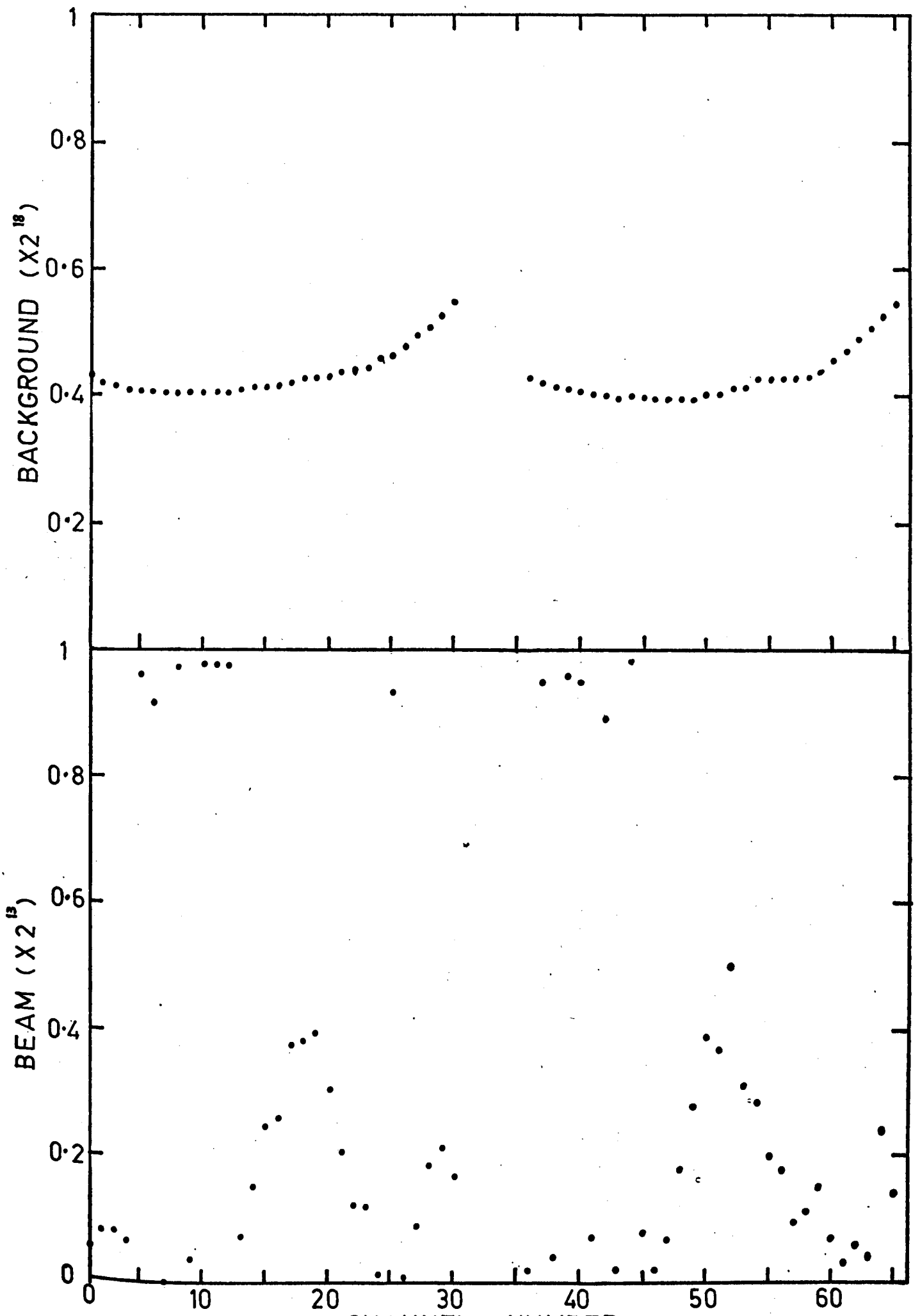

Figure 5.1 X-Y chart recorder plots of two successive scans for inelastic H.

data as judged visually. Account was taken of the standard deviation of each data point both when matching the results from all the experiments and when drawing the curve which represented the best visual fit to all the data points. This single curve is referred to as the experimental angular distribution obtained from the present experiment. It is believed that any subjective error introduced by this method of combining the individual experiments, is much less than the observed spread of data points around the experimental angular distribution.

5.1.2 Atomic hydrogen correction.

It was pointed out in Section 1.3.3 that electrons inelastically scattered by exciting molecular hydrogen to the $b\left(^3\Sigma_u^+\right)$ state, constituted a continuum in the energy loss spectrum, which was observed (in the present investigation) to extend from approximately 8.5 volts to at least 11 volts. Since the 10.2 eV of energy lost by electrons exciting the 2s and 2p states of atomic hydrogen lay within this energy range, electrons scattered from the molecular hydrogen fraction of the partially dissociated neutral beam, that excited the $b\left(^3\Sigma_u^+\right)$ state of molecular hydrogen, were indistinguishable from electrons producing hydrogen atoms in their first excited state.

Examples are shown in Figures 5.2 (a) and 5.2 (b) of the relevant part of the energy loss spectrum for 100 eV electrons inelastically scattered through 35^o by a molecular hydrogen beam and a highly dissociated beam respectively. The room temperature measurement was performed immediately following the high temperature experiment with all other parameters

Figure 5.2 Energy loss spectra for 100 eV incident electrons losing from 8 to 12.5 eV and scattered through 35^{o} by

(a) room temperature molecular hydrogen beam,

(b) highly dissociated molecular hydrogen.

The graphs are direct copies of graphical outputs from the computer, the statistical error is approximately the same (1,200) for each points, and the data was obtained by summing the signal from eight successive energy scans. The dashed line is a visual fit to the data.

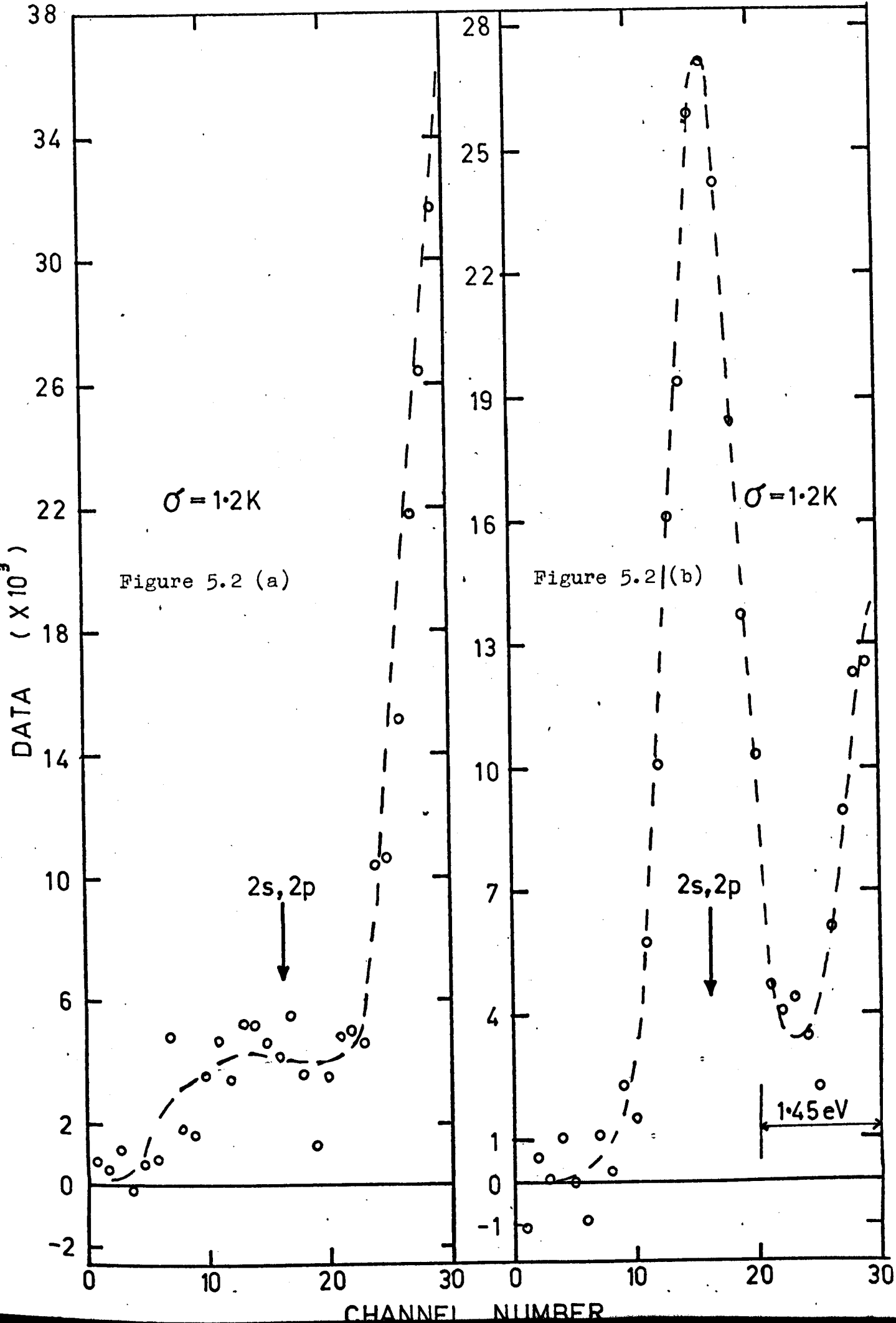

Figure 5.2 (a)

Figure 5.2 (b)

unchanged. The voltage increment of the STAIRCASE FUNCTION generator between channels was 0.11 eV, which (from equation 3.3) corresponded to a change in the peak energy transmitted by the electron spectrometer of 0.145 eV per channel.

In section 2.2.4 a method was proposed to determine the molecular hydrogen contribution to the beam signal from room temperature T_r measurements of the electron $E_m\ (T_r)$ and ion $I_m\ (T_r)$ molecular beam signals, and the molecular ion beam signal $I_m\ (T_h)$ at the high temperature T_h used to produce a highly dissociated neutral beam. In the present series of experiments $E_m\ (T)$ represented the sum over channels which extended approximately one half of the F.W.H.M. on either side of the top of the first inelastic peak of atomic hydrogen. Channels outside this range were excluded because they contributed only a small fraction (less than 20%) of the total area of the peak, while contributing substantially to the standard deviation of the beam signal. According to equation (2.4) the molecular signal $E_m\ (T_h)$ at the temperature T_h is given by

$$E_m\ (T_h) = \frac{I_m\ (T_h)}{I_m\ (T_r)} \times E_m\ (T_r) \quad . \qquad (5.6)$$

During the present investigation the molecular hydrogen correction to the neutral beam (equation 5.6) was calculated and subtracted from the neutral beam signal at each angle. This correction $E_m\ (T)$ to the total beam signal never exceeded 25% of the atomic hydrogen signal.

5.2 Discussion of Experimental Errors.

5.2.1 Digital Detecting Efficiency.

It was stated in Section 3.3.3 that by detecting

single electron pulses at the output of an electron multiplier using digital rather than analogue methods, experimental results would be less susceptible to variations in the gain of the various stages of amplification, if the threshold of the discriminator could be adjusted to provide high detecting efficiency whilst rejecting electronic noise in the amplifiers. The pulse height distribution of single electron pulses from the present apparatus has been measured with the discriminator unit* operated as a single channel analyser. The variation of the count rate with peak height (measured in volts) obtained using a 2 volt window is shown in Figure 5.3. In this experiment, electrons entering the electron multiplier had been elastically scattered from a 200 eV electron beam, and the voltage applied to the tube was 2.6 KeV. During angular distribution experiments, the threshold of the discriminator was always 5 volts - the gain of the main amplifier being adjusted so that all electronic noise was rejected. Examination of Figure 5.3 suggests that the detecting efficiency was greater than 90% and therefore insensitive to small gain variations.

5.2.2 Energy Analysis.

If the voltage applied to the deflector plate of the electron spectrometer were adjusted (at one angle) to transmit the maximum number of electrons for a particular scattering process, and this single channel beam signal were studied as a function of angle, the angular distribution obtained would be susceptible to small variations in both the contact potential at the cathode and the voltage supplied to the cathode

* Dynatron Model N101

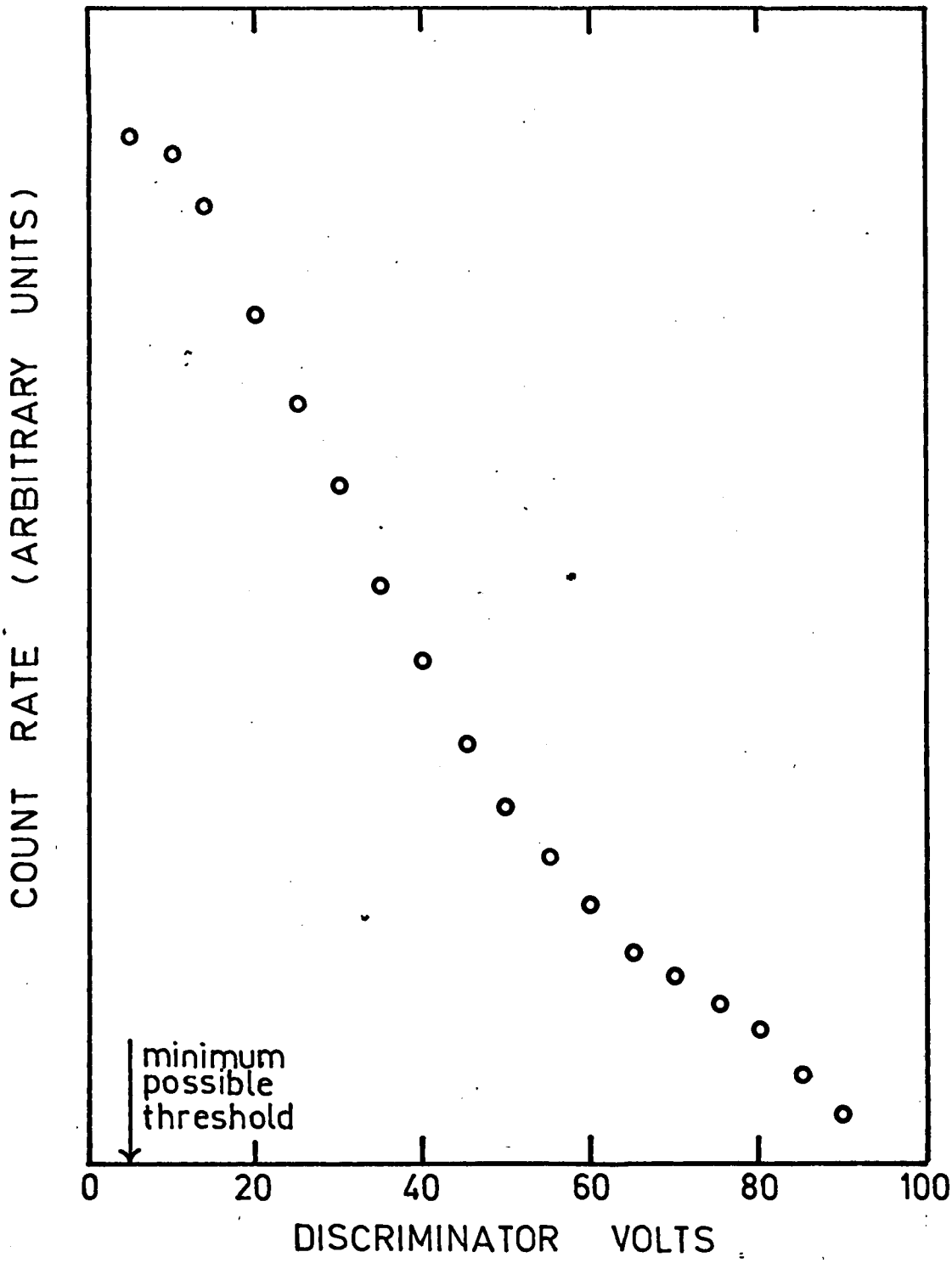

Figure 5.3 Pulse height spectrum of single electron pulses produced by an EMI 9603B electron multiplier, and measured using a Dynatron Single Channel Analyser unit with the window set to 2 volts. The voltage applied to the tube was 2.6 KV and a 200 eV electron beam was used.

and electron spectrometer. The present method of scanning across the whole peak and calculating the area under most of the peak, effectively eliminated this source of error.

Although the energy dependence of the F.W.H.M. of the electron spectrometer (equation 3.3) resulted in a 3% change of the F.W.H.M. when scanning completely across a peak, this did not introduce any significant inaccuracy since the same range of deflector plate voltages was used at all angles for incident electrons of a given energy.

5.2.3 Gas Purity.

Both the helium and argon used were stated (by their suppliers) to be greater than 99.99% pure. Since the commercial grade hydrogen had possible nitrogen and oxygen contents of up to 0.2% and 0.1% respectively, a palladium diffusion source (described by Haddad, 1967) was used to remove all impurities from the hydrogen. A schematic diagram of the gas supply to the oven is given in Figure 5.4. The pressure in the hydrogen cylinder was reduced to that required in the oven in four stages. Coarse control of the gas flow was obtained by adjusting the regulator and needle valve number 1. Pure hydrogen at an estimated pressure of several hundred millimeters was produced at the input to needle valve number 2 by adjusting the temperature of the palladium diffusion source. Final pressure reduction of the gas before entering the tube leading to the oven occurred through needle valve number 2. The room temperature pressure of the gas was measured between number 2 needle valve and the tungsten oven by a Baratron* gauge.

* M.K.S. Instruments Inc., Type 77.

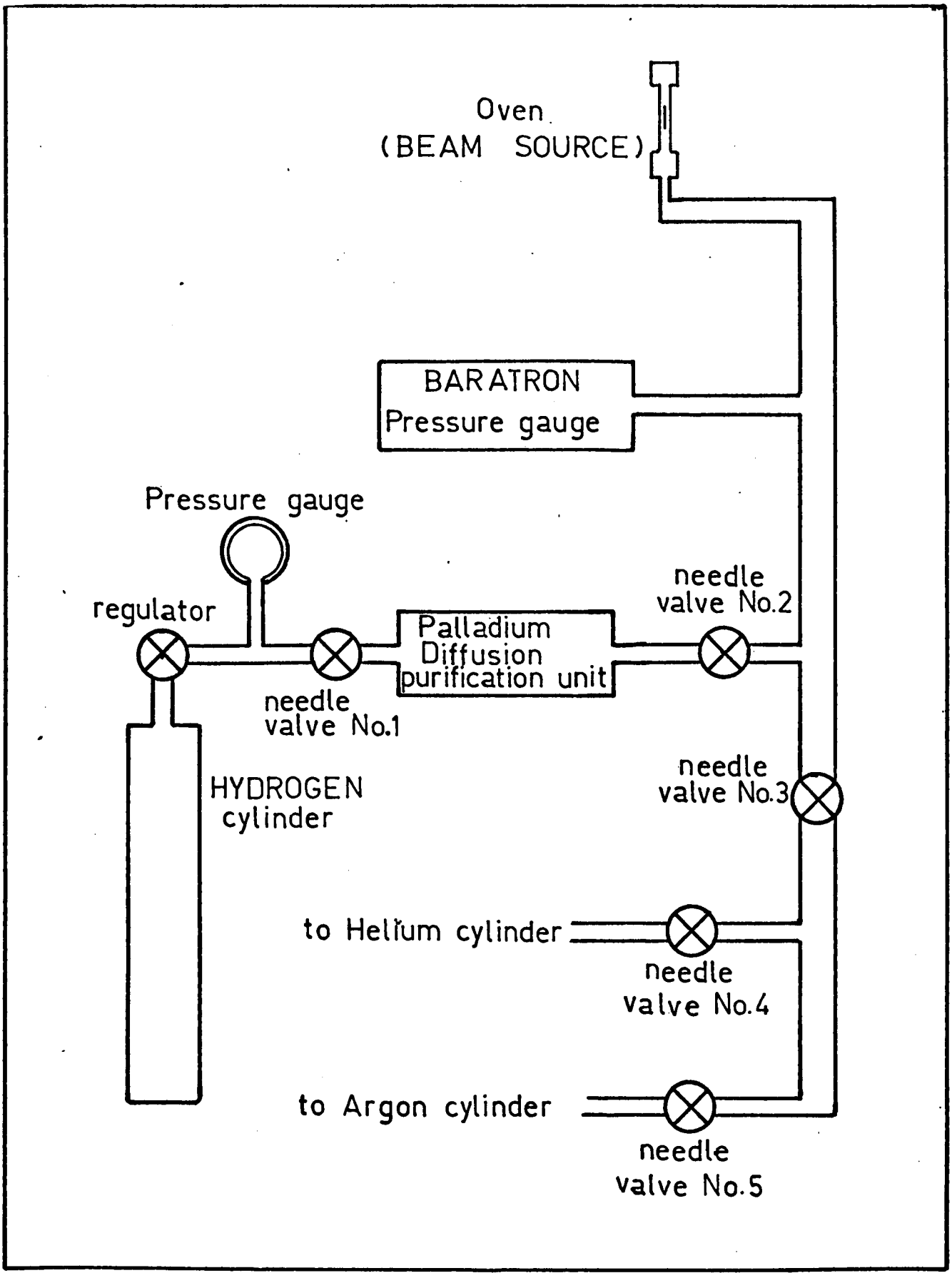

Figure 5.4 Schematic Diagram of the gas supply to the oven. Needle valve numbers 1, 4, 5 were supplied by Commonwealth Industrial Gases. Numbers 2, 3 were Edwards Type LBIA.

Since the resolution of this instrument was better than 0.01% of full scale, settings of the needle valves and purification unit were found which resulted in a maximum variation of the pressure (measured by the Baratron gauge) of 5% during a particular experiment.

Separate gas supply pipes were used to introduce helium and argon. Not shown on Figure 5.4 are vacuum connections by which the pipes could be evacuated by a diffusion pump when changing from one gas to another.

5.2.4. Background Contribution.

5.2.4 (a) Window Time.

In Section 4.2 it was explained that any systematic error contributed by the background signal to the beam signal (due to the beam on and off periods not being exactly equal), was reduced to less than 0.01% of the background by limiting the scaling period during each half cycle to a "window" period which was accurately determined by counting a preselected number of oscillations produced by a crystal oscillator. The accuracy claimed was verified periodically by observing that the beam signal produced when pulses were introduced into the Master Control Unit from a pulse generator never exceeded 0.005% of the total number of input pulses.

5.2.4 (b) Coherent Background Gas Fluctuations.

The concept of the characteristic time constant of a vacuum system was used in Section 2.2.3 to explain how the pressure fluctuation produced by introduction of the neutral beam into the scattering chamber during only half of each cycle could be discriminated against by phase sensitive detection of

the beam signal, if the period of the modulation frequency was a very small fraction of the scattering chamber time constant. The period used in the apparatus (0.0086 seconds) was demonstrated to be a sufficiently small fraction of the characteristic time constant (0.2 seconds) by observing that there was no change in the beam signal when the characteristic time constant was varied by a factor of 3.

The variation of beam signal with delay of the reference is shown in Figure 5.5 for electrons elastically scattered by argon. Note that a flat peak was produced because the window interval was less than (approximately 90% of) half a cycle. Similar graphs were obtained for helium and hydrogen and experiments were performed using the delay corresponding to the middle of the flat peak for the particular gas studied.

5.2.4 (c) Double Scattering.

The angular distribution observed at large angles for electrons exciting the 2s and 2p states of atomic hydrogen would be distorted if there were sufficient number of electrons suffering the double scattering process described in Section 2.1.1. In this process electrons are elastically scattered through a large angle by the atoms in the neutral beam, and inelastically scattered in the forward direction by the atomic hydrogen fraction of the background gas. An approximate formula has been derived in Appendix C (equation C.4), for the ratio of the probabilities of detecting electrons (at a particular angle) which have undergone single and double collisions. Using calculations based on the close coupling approximation, it has been shown in Appendix C that at 54 eV

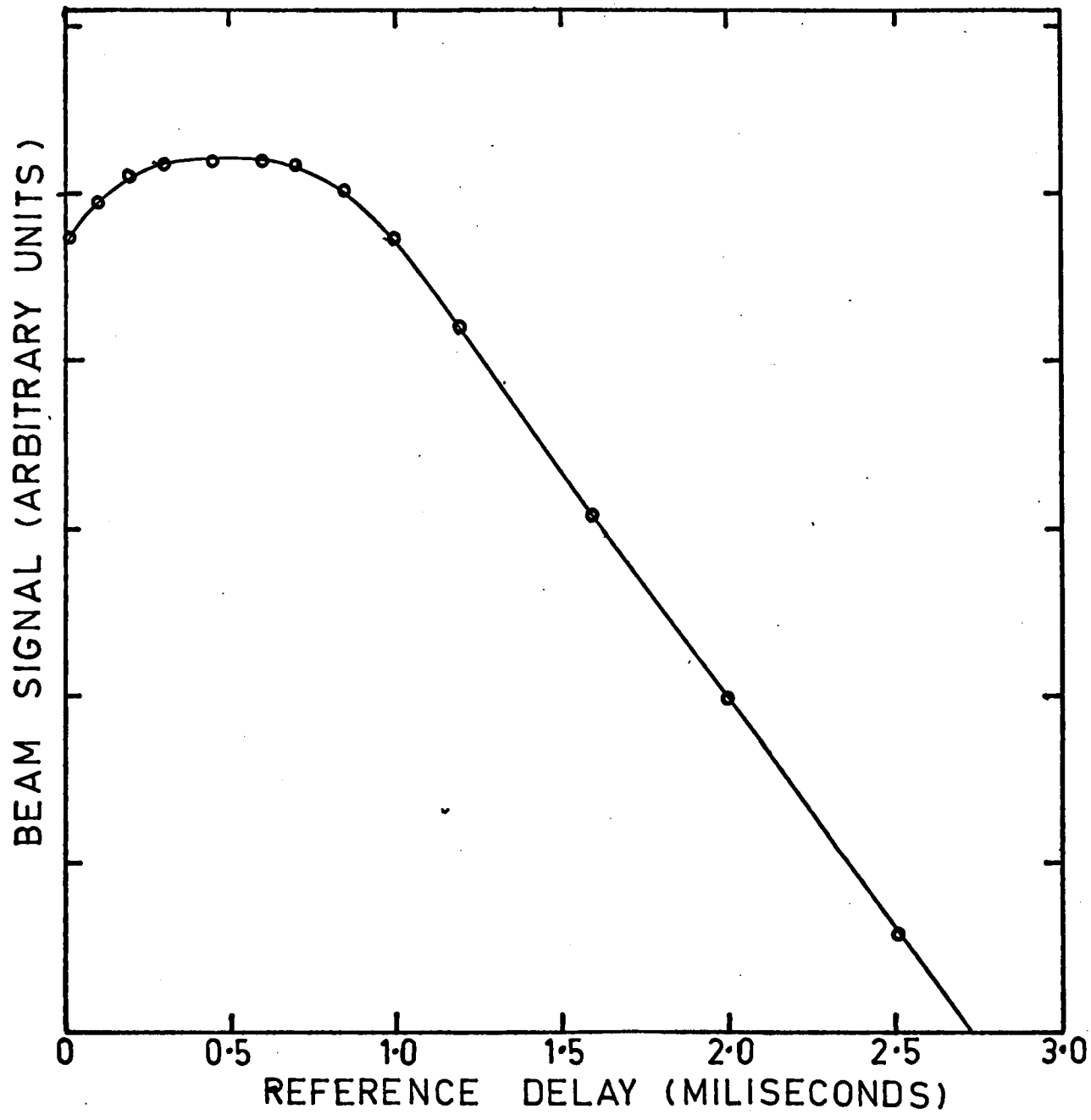

Figure 5.5 Variation of scattered electron signal with time delay of the reference (for electrons elastically scattered from argon). Data points are represented by circles.

the probability of detecting electrons scattered once only is at least 2,000 times greater than that of detecting electrons scattered twice. Even though calculations based on the Born - Oppenheimer approximation indicate that double scattering processes could be significant at large scattering angles for an incident electron energy of 200 eV, the discussion of the experimental results in Chapter 8 suggests that this is not so, and it is believed that double scattering processes did not contribute measurable error to the atomic hydrogen results.

5.2.5 Electron Beam, Neutral Beam and Electron Spectrometer Alignment.

The three dimensional mechanical alignment of both electron and neutral beams, with the field of view of the electron spectrometer is believed to be within 0.01". Some experimental evidence for the accuracy of the alignment was obtained by studying 50 and 100 eV electrons elastically scattered through 90° by argon. For it was observed that adjusting the electron gun deflecting voltages to maximise the Faraday cup current also produced maximum beam signal from the electron spectrometer.

Elastic scattering from argon at 90° was chosen for this test because the cross section is both large enough to give adequate signal in a short period of time, and the differential cross section is approximately flat (see Figure 5.8 and 5.9) near this angle. Results obtained by deflecting the electron beam along the direction of the neutral beam at small scattering angles were also consistent with the alignment claimed.

Identical settings of the deflectors were also

obtained for maximum beam signal and Faraday cup current at scattering angles of 90^{o} on both sides of 0^{o}.

5.2.6 Finite Angular Resolution.

For a particular position of the electron spectrometer, it was possible to detect electrons (with the required energy) which have been scattered through a range of angles $\Delta\theta$ about the geometrically defined scattering angle θ.

Among the factors determining $\Delta\theta$ were the finite size of the interaction region, imperfect collimation of the main electron beam, space charge repulsion of the scattered electrons within the main electron beam, and the angular resolution of the spectrometer itself.

5.2.6 (a) Space Charge Repulsion.

Electrostatic fields produced within the main electron beam by space charge can be estimated from the equation (Moiseiwitsch and Smith 1968b)

$$E_{av} = 0.2 \frac{I}{R\, E^{\frac{1}{2}}} \quad , \qquad (5.7)$$

where E_{av} (volts per cm) is the volume average of the electrostatic field within a homogeneous infinitely long unconfined beam of cross sectional radius R (m.m.), E (eV) is the electron energy, and I (microamperes) is the beam current. Values of E_{av} corresponding to the maximum beam currents used (from Table 3.1) are listed in Table 5.1 for an assumed electron beam radius of 4 m.m.

Table 5.1

ENERGY (eV)	CURRENT (μA)	E_{av} (volts per cm)
50	100	0.7
100	300	1.4
200	700	2.7

This field would have caused deflection of the scattered electrons. Worst case calculations indicated that the maximum deflection was about 1^{o} for electrons scattered through 15^{o}, (the smallest angle at which measurements could be made). The effect of space charge repulsion when averaged over all electron paths would therefore be much less than 1^{o}. Furthermore, the large currents listed in Table 5.1 were only used at large scattering angles, where differential cross sections usually vary only slowly compared with small scattering angles. The tendency of ions (produced along the electron beam) to neutralise the effect of the space charge of the electron beam also reduced the divergence of electron paths.

It is therefore believed that space charge repulsion did not significantly distort the observed angular distributions.

5.2.6 (b) Geometrical Factors.

The diameter of the neutral beam and the length of slits in the spectrometer were the same, and therefore both subtended equal angles ($3\frac{1}{2}^{o}$) with each other. Since differential cross sections are usually approximately linear over a few degrees, it is considered that no significant error was generally introduced by the detection of electrons which were in the possible 2^{o} or 3^{o} angular range either side of the geometrically

defined scattering angle.

5.2.6 (c) Electron Beam Shape.

Experimental checks on the accuracy of observed angular distributions due to non-ideal properties of the main electron beam, were made by measuring a number of angular distributions repeatedly for a range of electron gun currents and neutral beam source pressures, and observing that the results for a particular process agreed within statistical error. Data points for individual measurements are shown on the graphs of the angular distributions presented in this thesis, to demonstrate the agreement claimed. Attention may also be drawn to the fact that the depth of the minimum observed at approximately 70^{o} in the angular distribution for elastic scattering of 50 eV electrons from argon (Figure 5.8) is consistent with a well collimated electron beam.

Since measurements of atomic hydrogen angular distributions over the complete angular range possible with the present apparatus required at least 10 hours of data accumulation, it was preferable to perform experimental checks on the properties of the electron beam using another gas. It was not possible to perform elastic scattering at the electron gun current used to study atomic hydrogen because total count rates would be too high for the data handling system. Therefore, combined angular distributions for electrons exciting the $2^{1}S$, $2^{3}P$ and $2^{1}P$ states of helium were measured for a wide range of electron beam currents and shown to be independent of both the gun current and neutral beam source pressure. The experimental angular distributions obtained from these experiments for

incident electron energies of 100 and 200 eV are the curves labelled (a) in Figures 5.6 and 5.7 respectively. They have been normalized at 15^{o} to the sum of the experimental differential cross sections of Vriens, Simpson and Mielczarek (1968) for the $2^{1}S$ and $2^{1}P$ states. Omission of the $2^{3}P$ state in this normalization is not important since the contribution from this state is very small at 15^{o} (Vriens et al 1968). The results of individual experiments in which the standard deviation of data points exceeded 3%, are drawn (displaced from one another and labelled (c)) on Figures 5.6 and 5.7. The relation of the data points to the experimental angular distributions is also shown on curve (b) of Figure 5.6 and curve (a) of Figure 5.7.

Further confidence in the apparatus was gained by demonstrating that the results of measurements of a number of angular distributions measured repeatedly over a period of 5 months were reproducible.

5.2.7 Stray Magnetic Fields.

By constructing the scattering chamber walls out of mild steel and extensive use of magnetic shielding materials*, the residual magnetic field (measured by a Hall** effect probe) along the electron paths (except when close to the cathode) was reduced to less than 20 milligauss (the smallest field measurable with that instrument). In particular it was necessary to prevent magnetic fields from penetrating into the scattering chamber from both the mass spectrometer and the 300 ampere A.C. current used to heat the tungsten oven. The effectiveness of shielding from

* Perfection Mica Co. Netic for strong fields.
Conetic for weak fields.

** R.F.L. Model 1890

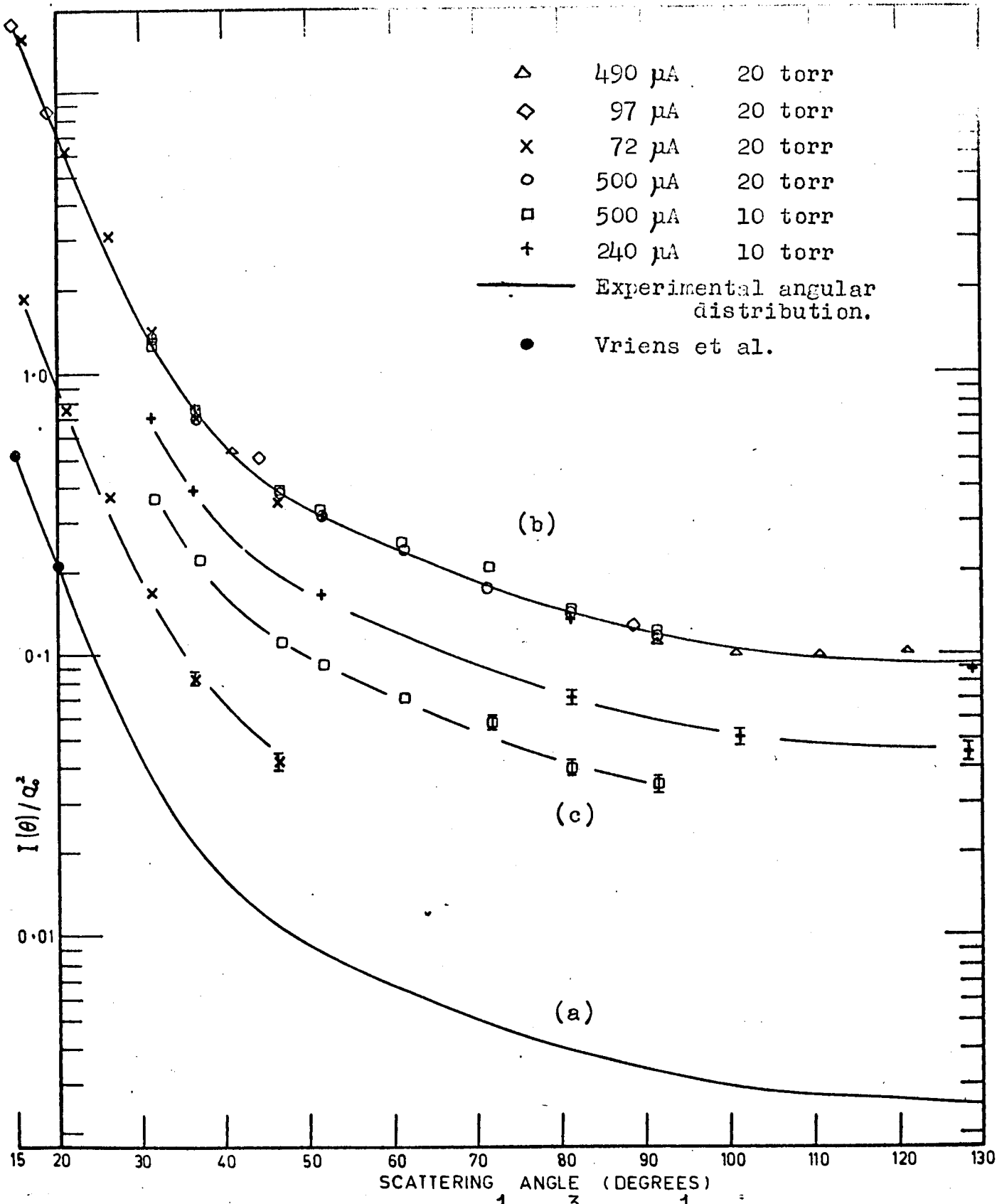

Figure 5.6 Excitation of the 2^1S, 2^3P and 2^1P state of helium by 100 eV electrons.

Curve (a) Experimental angular distribution normalized to the differential cross section of Vriens et al (1968a) at 15°

(b) Experimental angular distribution redrawn to show its associated data points. Electron gun currents and neutral beam source pressures for the separate experiments are given in the legend.

(c) Results of three separate experiments.

Unless shown otherwise standard deviation of data $\leqslant$ 3%.

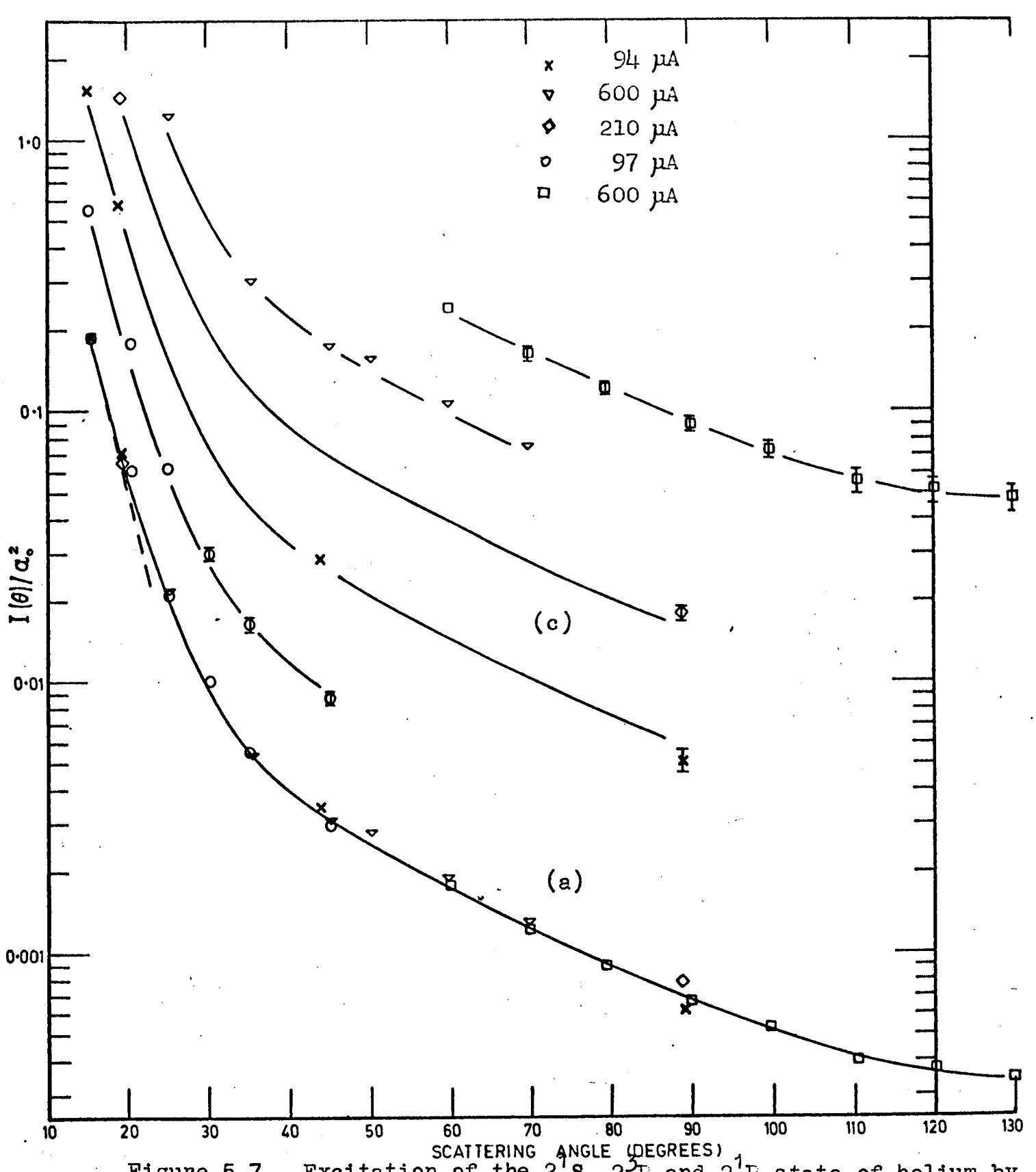

Figure 5.7 Excitation of the 2^1S, 2^3P and 2^1P state of helium by 200 eV electrons.

Curve (a) Experimental angular distribution normalized to the differential cross section of Vriens et al (1968a) at 15°. The associated data points are also shown on this curve.

(b) Experimental angular distribution redrawn to show its associated data points. Electron gun currents and neutral beam source pressures for the separate experiments are given in the legend.

(c) Results of five separate experiments.

Unless shown otherwise standard deviation of data $\leqslant$ 3%.

the latter source was demonstrated by observing (See Figure 5.8) that the angular distribution of 50 eV electrons elastically scattered by argon was the same for both no current and 300 amperes passing through the oven. Another source of stray magnetic fields was the 8 to 10 ampere cathode filament current. A number of measures were introduced to reduce the effect of this field. These included using a non-inductively wound filament, placing the 2 current supply leads (in the form of flat plates) within 0.03" of each other for most of their length within the scattering chamber, and arranging magnetic shielding around the electron gun.

An experimental test for the combined presence of many of the factors (including magnetic fields) which could contribute to the distortion of observed angular distributions, is to compare the shapes of angular distributions measured on both sides of zero scattering angle. This comparison was made at all of the energies studied and the angular distributions for both sides of 0^{o} were found to agree within experimental statistics. It should be noted however, that the presence of the same distortion on both sides of 0^{o} would not have been detected by this test.

5.2.8 Zero Angle Determination.

The most sensitive method of determining zero scattering angle, was considered to be the measurement of the angular distribution of 50 eV electrons elastically scattered from argon on both sides of the main electron beam, and to use the narrow minimum (occurring at approximately 70^{o}, see Figure 5.8), to determine zero scattering angle from the symmetry

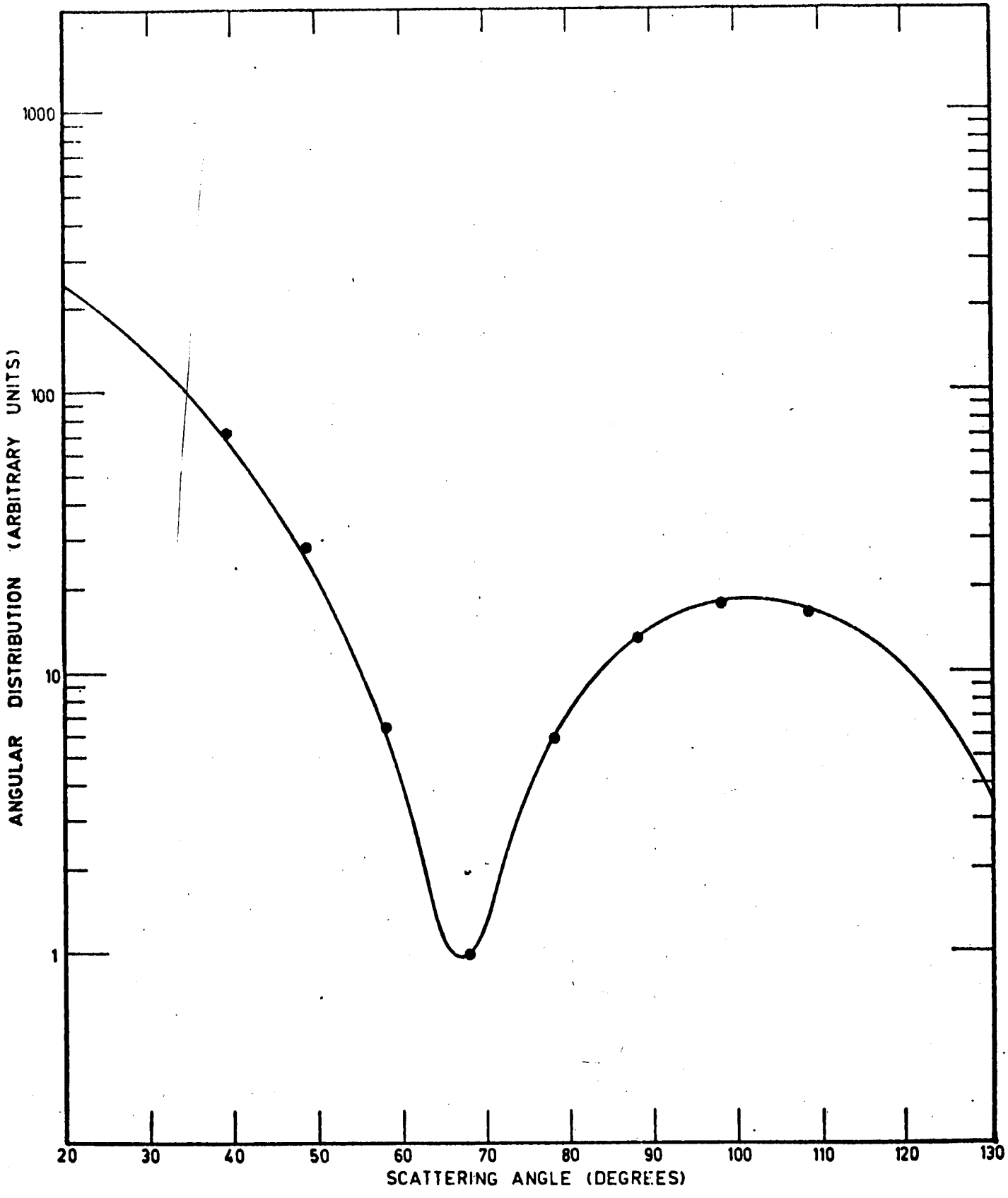

Figure 5.8 Angular distribution for elastic scattering of 50 eV electrons from argon.
Continuous surve is the experimental curve from Figure 5.9 for argon at room temperature.
Data points for eight angles using an argon beam whose source temperature is 2930° K.
Their standard deviation is less than 2%.

of the two angular distributions. The uncertainty in the determination of the scattering angles using this procedure is believed to be not greater than 1^{o}.

5.2.9 Multiple Scanning.

The need to perform multiple scanning was explained in Section 3.6.5. By using this technique, it is believed that the experimental results presented in this thesis are not subject to significant inaccuracies caused by small systematic drifts of time dependent parameters. The very long data accumulation times (for example 6 hours to measure inelastic scattering from atomic hydrogen at 8 angles) would also have averaged random drifts in experimental parameters.

5.2.10 Non Mono-energetic Electron Beam.

If the edge of the electron beam were to collide with electrodes of the electron gun, secondary electrons produced could result in a small fraction of the electron beam possessing a continuous energy distribution extending from zero up to the energy of the main beam. At large scattering angles, where the differential cross section for excitation of the 2s and 2 p states is small compared with elastic scattering, the observed inelastic beam signal would then include electrons which had been elastically scattered by the atomic hydrogen fraction of the neutral beam. Since measurement of the beam signal at energy losses between 3 and 7 eV (for which energy range there are no inelastic processes in either atomic or molecular hydrogen) did not reveal the presence of any beam signal, it was assumed that no significant low energy tail to the electron beam existed at the 10 eV energy loss corresponding to the 2s and 2p states

of atomic hydrogen. (Note that a further test would be to measure the beam signal at an energy loss of 10 eV using a neutral beam of helium.)

5.2.11 Mass Spectrometer.

It is believed that the ion collecting efficiency was essentially the same for both atomic and molecular hydrogen when operating the ion extraction field on the plateau as described in Section 3.5. While dependence of the ion signal on the square root of oven temperature was not necessary (see Section 2.2.4) to the experimental method used in this investigation, the fact that this square root relationship was observed to hold at room temperature source pressures below 0.5 m.m. for molecular hydrogen (for temperatures below that required to produce significant dissociation) supports the belief that the ion collecting efficiency was independent of the velocity of the particles of the neutral beam. Since it is considered that the maximum error of the mass analysis of the neutral beam is 10%, the error contributed to the atomic hydrogen measurements by non-ideal operation of the mass spectrometer would not have exceeded 3% of the atomic hydrogen results, because the molecular hydrogen correction to the observed beam data never exceeded 25% of the atomic hydrogen data.

5.3. Comparison with Earlier Results.

A further check on the performance of the apparatus was made by measuring angular distributions for elastic scattering of electrons from argon, helium and molecular hydrogen, and comparing the results with both those obtained by earlier experimentors and recent theoretical calculations. While

angular distributions for the inert gases and molecular hydrogen were measured repeatedly during the early 1930's (for which complete references are given by Webb, 1935a, 1935b) recent measurements have been restricted to those for helium by Vriens, Kuyatt, and Mielczarck (1968b), argon by Porteus (1963), and all of the inert gases by Mehr (1967). All of the experiments performed during the 1930's used the static gas technique and agreement between the various results was not always good. (See Section 2.1.1 for a discussion of possible sources of error.)

5.3.1 Elastic Scattering from Argon.

The curve obtained by drawing the best visual fit (See Section 5.1.1) to the results of the present investigation for elastic scattering of 50 eV and 100 eV electrons from argon are shown in Figures 5.9 and 5.10 respectively. The results of individual experiments performed on both sides (signified by the + and - signs) of the main electron beam and over a range of electron gun currents are included to demonstrate the good agreement between the separate measurements.

Experimental results of Mehr (1967), Webb (1935a) and Hughes and McMillen (1932a), have also been included in Figure 5.9 and 5.10 - their scaling factors being adjusted to obtain a best visual fit to the present results over all angles except the angular ranges near the minima observed at approximately 65^{o} and 130^{o}. The theoretical differential cross sections included in Figures 5.9 and 5.10 are those calculated by Coulthard (and reported by Mehr, 1967). The normalization of the results of Mehr to the calculations of Coulthard employed

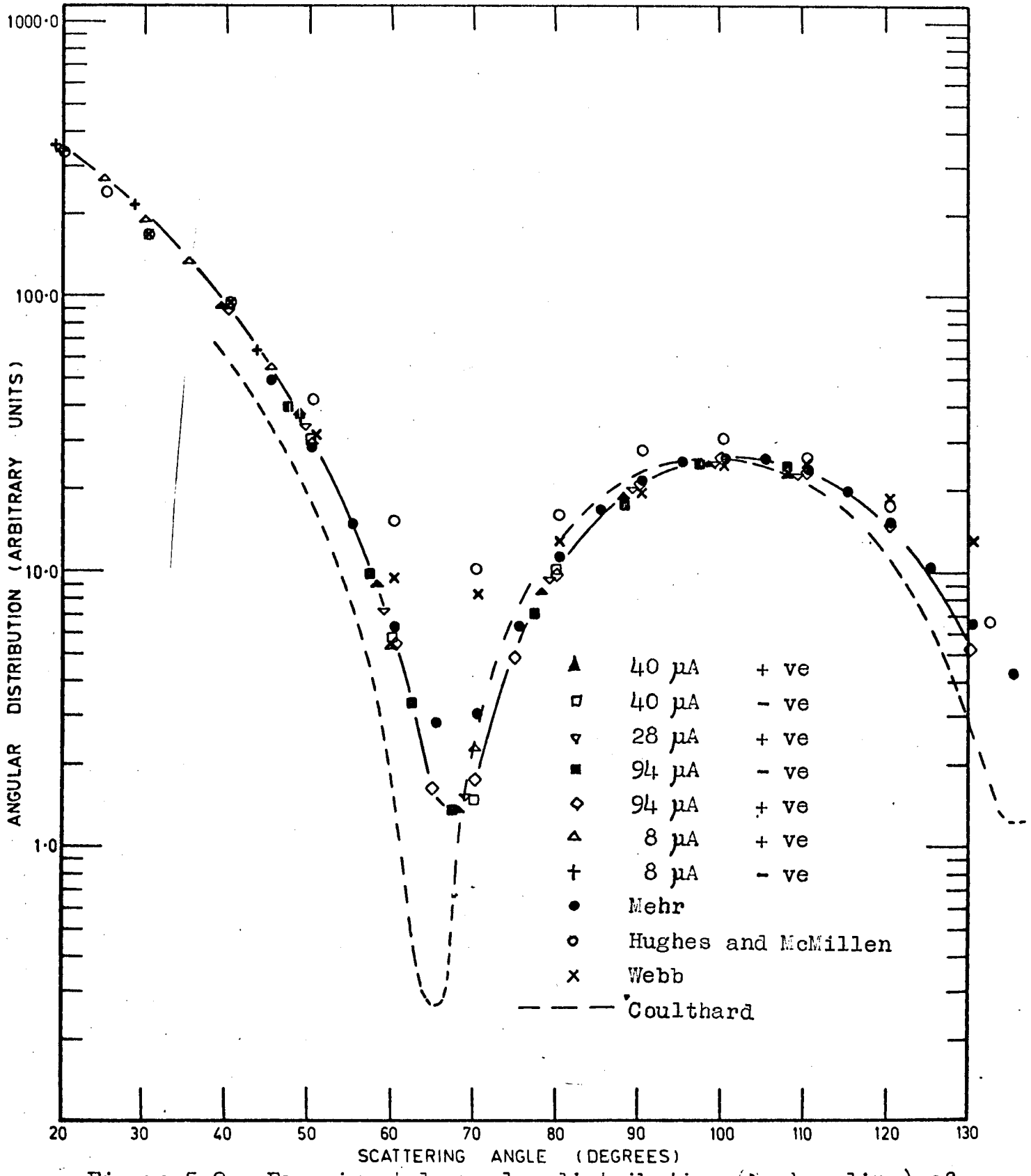

Figure 5.9 Experimental angular distribution (broken line) of 50 eV electrons elastically scattered from argon, showing data points for the present investigation and those of Mehr, and Hughes and Webb.

Standard deviation $\leqslant$ 1% except for $61^{\circ} < \theta < 72$ for which the standard deviation is typically 6%.

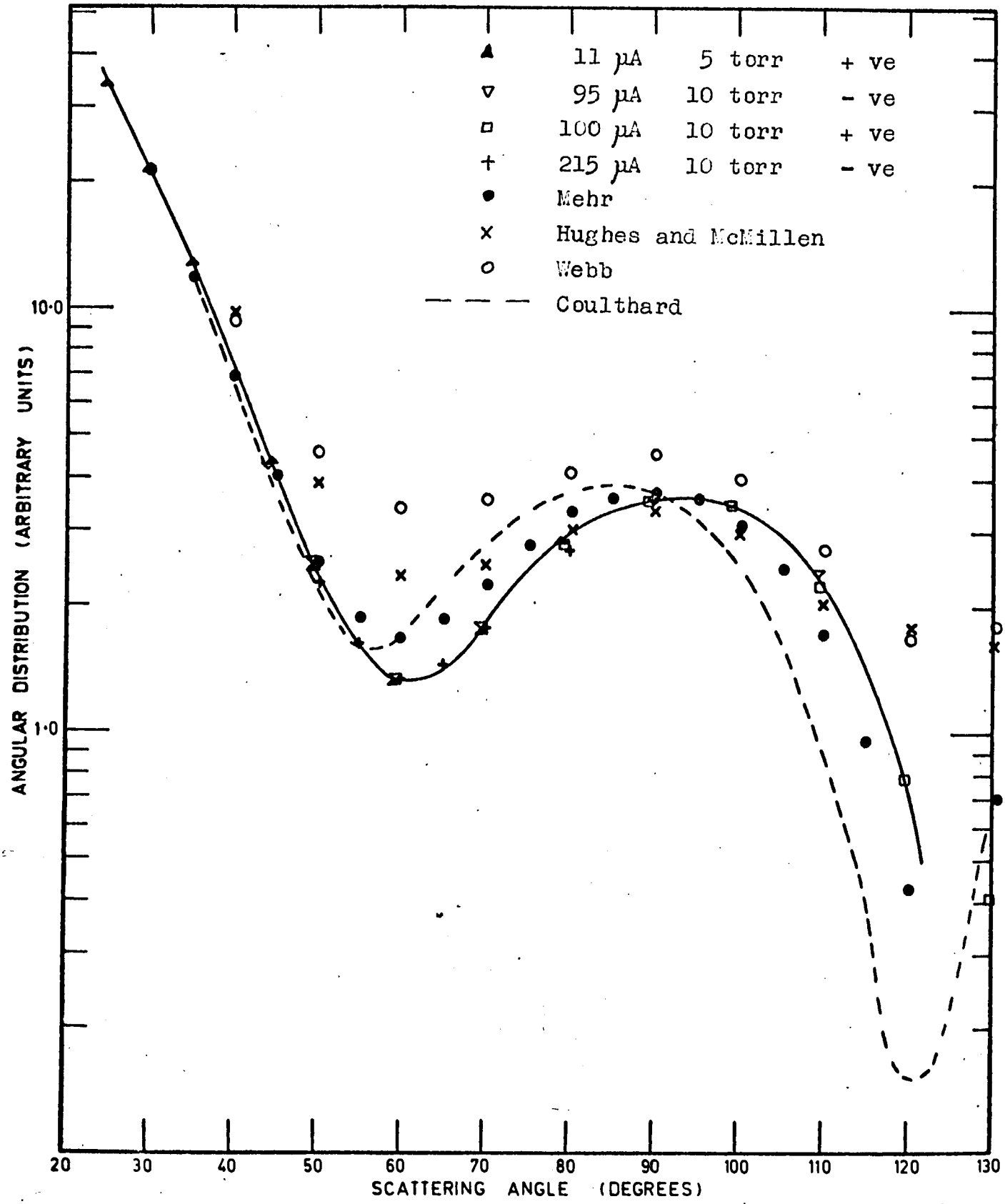

Figure 5.10. Experimentally angular distribution (broken line) of 100 eV electrons elastically scattered from argon, showing data points for the present investigation and those of Mehr, and Hughes, and Webb.

Standard deviation $\leqslant$ 3%.

in Figures 5.9 and 5.10 is identical to that used by Mehr (1967).

Mehr used the unmodulated beam technique (described in Section 2.1.2) to obtain his results. Agreement between the shape of the present results and those of Mehr over most of the angular range is excellent at 50 eV and fair at 100 eV. Theory and experiment have the same general shape at both 50 and 100 eV, although the agreement between experiment and theory at 100 eV is better for Mehr's results than the present measurements. The minimum occurring near 65^{o} in both the 50 and 100 eV angular distributions, is deeper in the present results than in the measurements of Mehr. This may be due to better angular resolution in the apparatus used to obtain the present results. In comparison with the present measurements, the minimum near 65^{o} in the results of Hughes and McMillen (1932a) and Webb (1935a) are shallow, despite the claim* by Hughes and McMillen of an angular resolution of 1^{o}.

The detection of electrons which had been scattered twice may have resulted in the distortion of both Hughes', and McMillen's and Webb's results.

5.3.2 Elastic Scattering from Helium.

Angular distributions for electrons elastically scattered from helium have been measured in the present investigation for incident electron energies of 25, 50 and 100 and 200 eV. In curves (a) of Figures 5.11 to 5.14 compare the present experimental angular distributions with the calculations of Khare and Moiseiwitsch (1965), and the laboratory measurements of Hughes, McMillen and Webb (1932). The scaling factor for the measurements of Hughes et al has been adjusted separately on

* Webb (1935) does not state the angular resolution in his apparatus.

each graph to obtain the best visual fit to the results of Khare and Moiseiwitsch. The relation of the data points to the experimental angular distribution is shown on curve (b) of Figures 5.11, 5.13 and 5.14. Data points for the single angular distribution measurement performed at 50 eV are shown on curve (a) of Figure 5.12.

Khare and Moiseiwitsch calculated the total scattering amplitude by summing the results of separate calculations of the direct and exchange scattering amplitudes. Phase shifts for the direct scattering amplitude were calculated by numerical integration of the distorted wave approximation equation (with exchange excluded). A potential that behaved as $-\alpha/r^4$ was included, to represent the polarization of the target atom by the Coulomb field of the incident electron. At 200 eV the exchange contribution to each partial wave was calculated using the first order exchange approximation (Bell and Moiseiwitsch, 1962) with direct scattering term omitted. For 25, 50 and 100 eV electron energies, zero and first order partial wave contributions to the exchange scattering amplitude were determined by subtracting the distorted wave contribution from the first order exchange approximation solution obtained using the phase shifts calculated by Morse and Allis (1933). Higher order partial waves were obtained using the method described for the 200 eV partial waves.

Visual fit of the present measurements at 25 and 50 eV (Figures 5.11 and 5.12 respectively) with the calculations of Khare and Moiseiwitsch, indicates excellent agreement between the shape of the two curves over the complete angular range

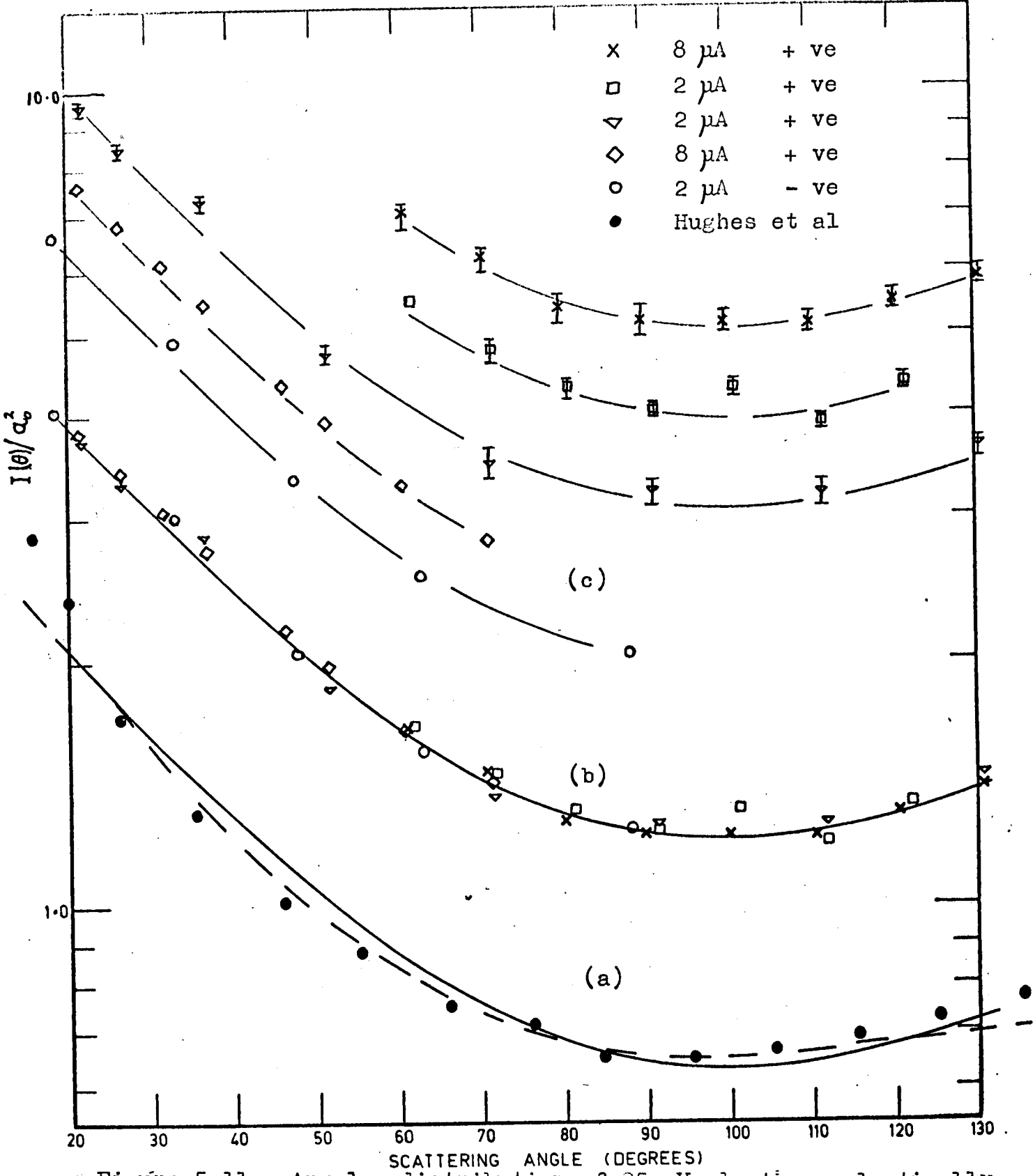

Figure 5.11 Angular distribution of 25 eV electrons elastically scattered from helium.
Curves (a) The results of the present investigation and the measurements of Hughes and McMillen have been adjusted for their best visual fit to the theoretical results of Khare and Moiseiwitsch.
Curve (b) Experimental angular distributions and associated data points.
Curve (c) Results of single experiments. Standard deviation $\leq 3\%$ unless shown otherwise.

———— Present experimental angular distribution.
— — — Khare and Moiseiwitsch.

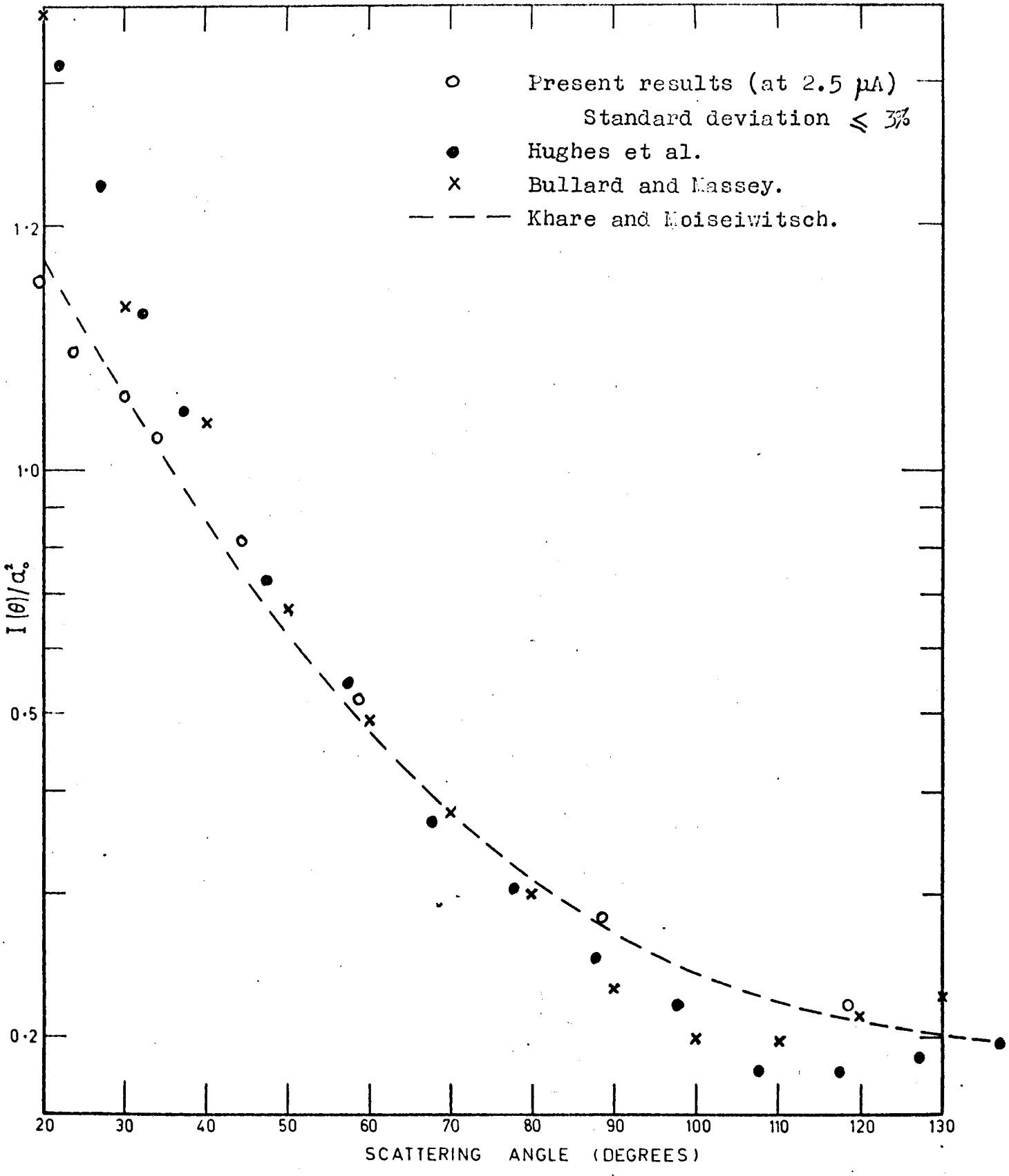

Figure 5.12 Angular distribution of 50 eV electrons elastically scattered from helium.
The three laboratory measurements of Bullard and Massey, Hughes et al, and the present investigation, have been adjusted visually for their best fit to the theoretical differential cross section of Khare and Moiseiwitsch.

investigated. The results of the individual experiments at 25 eV are drawn displaced from each other on Figure 5.11 (curves (c)). The results of Hughes et al also agree well with the shape of the present results at 25 and 50 eV, except for angles less than 40^{o} at the incident electron energy of 50 eV. The good agreement at 25 eV is believed to be particularly significant, because the influence of stray magnetic fields on the observed angular distributions is expected to be greatest at the lowest energy studied. The results of Bullard and Massey (1931b) at 50 eV, (shown on Figure 5.12) also agree well with the present results except for angles less than 40^{o}.

Vriens, Kuyatt and Mielczarck (1968b) have determined absolute elastic differential cross sections at 100 and 200 eV for scattering angles ranging from 5^{o} to 30^{o}. They used the results of an earlier experiment, (Vriens, Simpson and Mielczarck, 1968a), in which they obtained differential cross sections for excitation of the $2^{1}P$ state of helium by demonstrating the validity of the Born approximation (at 100 eV and higher energies), and normalised their experimental angular distributions using the known optical oscillator strength for the transition from the ground state to the $2^{1}P$ state. By measuring the ratio of elastic to $2^{1}P$ excitation at low angles, Vriens, Kuyatt and Mielczarck were able to normalize their elastic angular distributions to the $2^{1}P$ differential cross section. The apparatus used for all their experiments employed the static gas technique. Experimental errors of 2% have been claimed for both the 2^{1} P results (Vriens et al 1968a) and the ratios of the elastic to $2^{1}P$ differential cross sections (Vriens

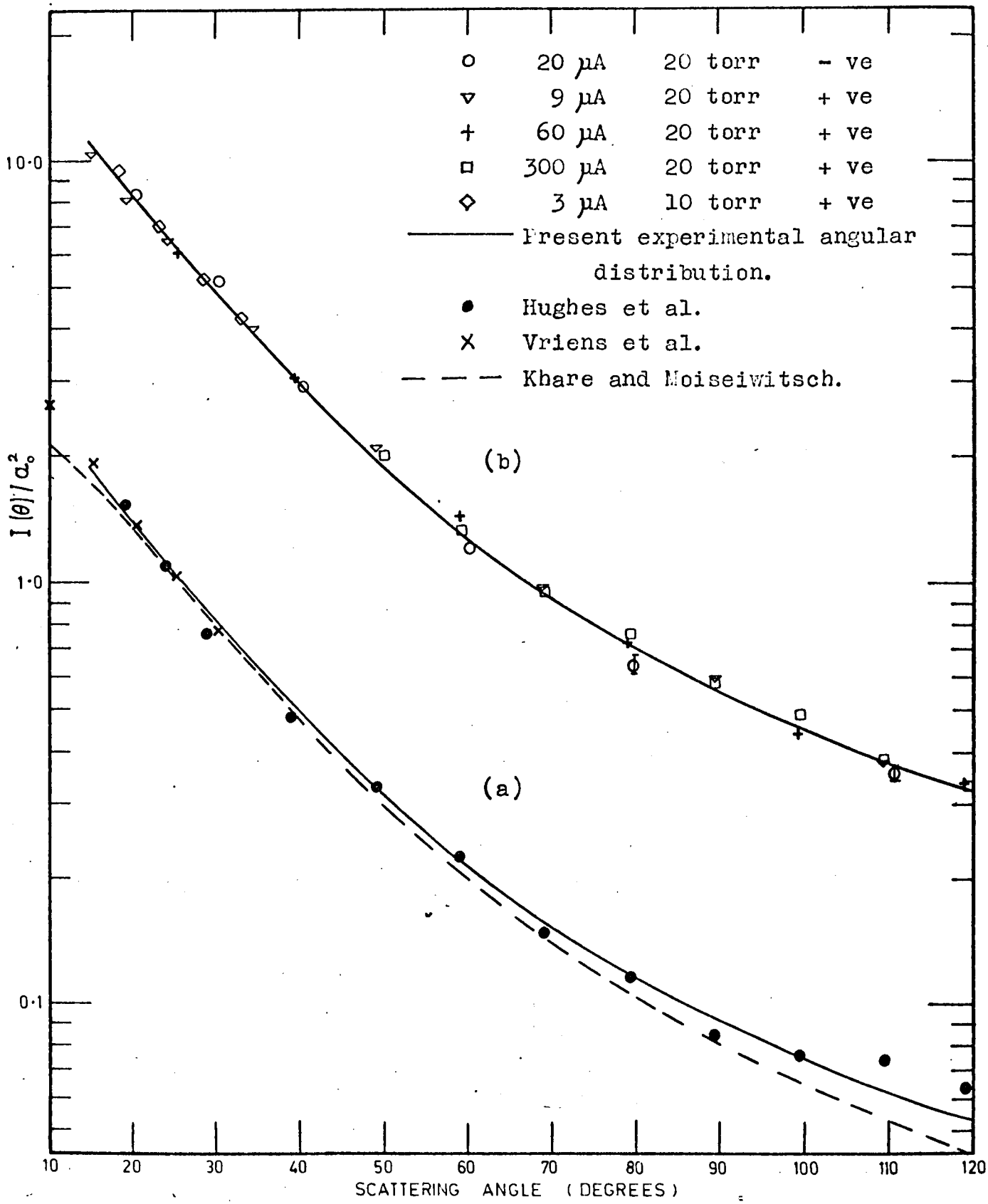

Figure 5.13 Angular distribution of 100 eV electrons elastically scattered from helium.
Curves (a) The results of the present investigation, and the measurements of Hughes et al, have been adjusted for their best visual fit to the experimental differential cross section of Vriens et al at 15°.
Curve (b) Individual data points are shown in relation to the experimental angular distribution.
The standard deviation $\leq$ 3% unless shown otherwise.

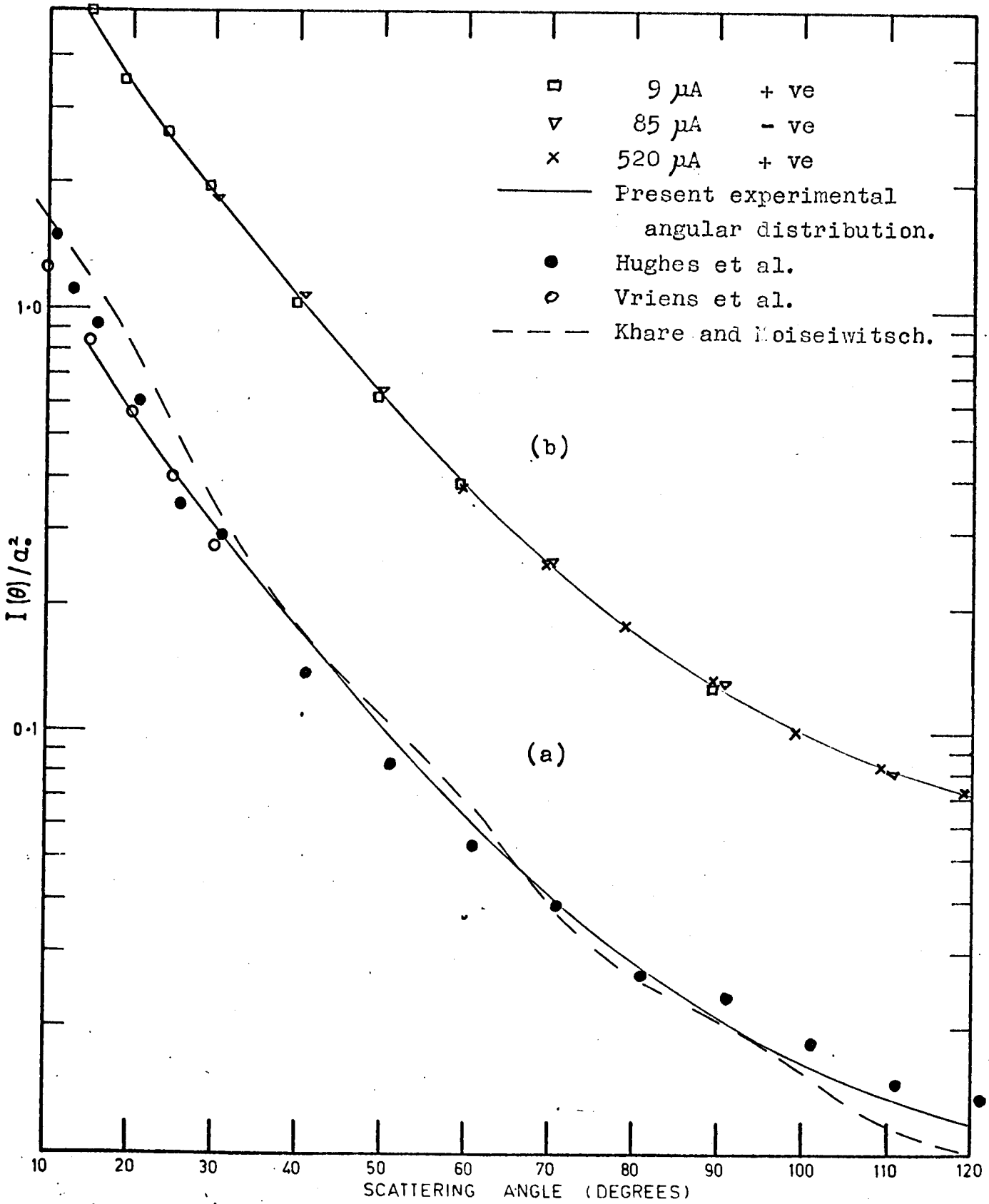

Figure 5.14 Angular distribution of 200 eV electrons elastically scattered from helium.
Curves (a) The results of the present investigation, and the measurements of Hughes et al, have been adjusted for their best visual fit to the experimental differential cross section of Vriens et al at 15°.
Curve (b) Individual data points are shown in relation to the experimental angular distribution.
The standard deviation of all points is $\leq$ 3%.

et al, 1968b), while systematic errors due to normalization of their 2^1P angular distributions (by means of the optical oscillator strength) may have resulted in the 2^1P differential cross section being 4% to 8% high at 100 eV and 1% at 200 eV (Vriens et al 1968a).

The present results, for 100 and 200 eV incident energy, have been normalized at 20^o to the elastic differential cross section data of Vriens et al, and are shown in Figures 5.13 and 5.14 respectively. Since the statistical accuracy of the present data was less than 2%, and good accuracy is claimed for the measurements to which they are normalized, there is good agreement with the calculations of Khare and Moiseiwitsch over the complete angular range studied in the present investigation for the data obtained at 100 eV, and angles greater than 30^o for the 200 eV results. The results of the present investigation are also in good agreement with the measurements of Hughes et al at both 100 and 200 eV.

5.3.3 Elastic Scattering from Molecular Hydrogen.

There is only poor agreement at large angles between the measurements of angular distributions for elastic scattering of electrons from molecular hydrogen by Hughes and McMillen (1932b), Webb (1935b) and the author, when all three results are adjusted for a good visual fit at small angles. This discrepancy is discussed in greater detail in Chapter 7, but it is noted here that Hughes and McMillen studied hydrogen with a different apparatus to that which they used for helium, and the shapes of the present angular distributions are in much better agreement with recent calculations by Khare and

Moiseiwitsch (1965) than are the results of Hughes and McMillen, and Webb.

5.4 Conclusions.

It is believed that the two procedures used in the present investigation, namely determining the area under the required peak (in the energy loss spectrum), and multiple scanning, have effectively prevented the introduction of errors by the variation of time dependent parameters. Possible sources of systematic error have been identified and experiments performed which may reveal their presence. Within the limits of statistical accuracy, no systematic errors were detected. Agreement between the present measurements and both published theoretical and experimental results has (in many cases) been very good.

Therefore it is believed that the total error contributed by all sources except random statistics (determined by beam and background counts) is less than 10%, with a maximum angular uncertainty of 1^{o}.

CHAPTER 6. THEORY OF LOW ENERGY ELECTRON SCATTERING.

In Chapter 1 it was explained that while the quantum mechanical principles in low-energy atomic physics are usually assumed to be fully understood, the technical difficulties involved in applying them in full to the collision of electrons with atoms have been insurmountable.

However, by using simplified descriptions of the collision system, approximate solutions can be found to the equations describing the interaction. A number of detailed reviews of the theoretical work on electron collisions with atoms have been published in the literature, among which are the articles by Moiseiwitsch and Smith (1968), Massey (1956), and Seaton (1962), and Peterkop and Veldre (1966). Presented in this chapter, is an outline of the mathematical approximations (and their formalism) referred to in the discussion of atomic and molecular hydrogen. Unless stated otherwise, the Section 6.1, dealing with atomic hydrogen, follows the review article by Moiseiwitsch and Smith (1968), while the discussion of molecular hydrogen is based on the paper by Khare and Moiseiwitsch (1965).

6.1 Atomic Hydrogen.

6.1.1 Introduction.

The Schrodinger equation for a system composed of a hydrogen atom and an incident electron is

$$\left[-\frac{\hbar^2}{2m}\left(\nabla_1^2 + \nabla_2^2\right) - \frac{e^2}{r_1} - \frac{e^2}{r_2} + \frac{e^2}{r_{12}} - E \right] \Psi(\underline{r}_1, \underline{r}_2) = 0, \qquad (6.1)$$

where $\underline{r}_1$, $\underline{r}_2$ are the position vectors of electrons 1, 2 referred to the proton as origin, r_{12} is the interelectron distance, E is

the total energy of the system and $\Psi(\underline{r}_1,\underline{r}_2)$ is the total wave function for the two electrons.

Let

$$\Psi(\underline{r}_1,\underline{r}_2) = \sum_p F_p(\underline{r}_2)\ \psi_p(\underline{r}_1) \qquad (6.2)$$

where $\sum$ denotes a summation over the discrete and an integration over the continuum states, and ψ_p are the set of orthogonal and normalized hydrogen atom wave functions satisfying the equation

$$\left(-\frac{\hbar^2}{2m}\nabla^2 - \frac{e^2}{r} - E_p\right)\psi_p(\underline{r}) = 0\ , \qquad (6.3)$$

where the E_p are the associated eigenenergies.

Substituting (6.2) into (6.1), multiplying by $\psi_n^*(\underline{r}_1)$, and integrating with respect to $\underline{r}_1$ one obtains

$$(\nabla_2^2 + k_n^2)\,F_n(\underline{r}_2) = \frac{2m}{\hbar^2}\iint \psi_n^*(\underline{r}_1)\,V(\underline{r}_1,\underline{r}_2)\,\Psi(\underline{r}_1,\underline{r}_2)\,d\underline{r}_1 \qquad (6.4)$$

where

$$V(\underline{r}_1,\underline{r}_2) = \frac{e^2}{r_{12}} - \frac{e^2}{r_2} \qquad (6.5)$$

in the interaction energy between electron 2 and a hydrogen atom composed of electron 1 and the proton, and the wave number k_n is given by

$$k_n^2 = \frac{2m}{\hbar^2}(E - E_n)\ . \qquad (6.6)$$

If $\underline{k}_1$ is the wave vector of the electron 2 incident on a hydrogen atom in the ground state, then the asymptotic form required for the function $F_n(\underline{r})$ at large distance r is

$$F_n(\underline{r}) \sim e^{i\underline{k}_1\cdot\underline{r}}\delta_{n1} + \frac{e^{ik_n r}}{r} f_n(\theta,\phi)\ , \qquad (6.7)$$

where $f_n(\theta,\phi)$ is the scattering amplitude corresponding to excitation of the nth state of the hydrogen atom and θ , ϕ are the polar angles of $\underline{r}$ referred to the direction of incidence as polar axis.

The plane wave $e^{i\underline{k}_1\cdot\underline{r}}$ represents a density of electrons of one per unit volume, and therefore a flow of $k_1 \hbar/m$ electrons across unit area per unit time.

The second part of (6.7) is an outgoing spherical wave which represents the scattered electron at large distances r from the atom.

Equation (6.4) may be solved using the Green's function for a free particle to yield

$$F_n(\underline{r}) = e^{i\underline{k}_1\cdot\underline{r}}\delta_{n1} - \frac{2m}{\hbar^2}\iint \frac{e^{ik_n|\underline{r}-\underline{r}_2|}}{4\,|\underline{r}-\underline{r}_2|}\,\psi_n^*(\underline{r}_1)$$

$$\times\ V(\underline{r}_1,\underline{r}_2)\ \Psi(\underline{r}_1,\underline{r}_2)\,d\underline{r}_1\,d\underline{r}_2 \quad . \qquad (6.8)$$

By comparing the asymptotic form taken by (6.8) with (6.7), the expression obtained for the scattering amplitude is

$$f_n(\theta,\phi) = -\frac{m}{2\pi\hbar^2}\iint e^{-i\underline{k}_n\cdot\underline{r}_2}\,\psi_n^*(\underline{r}_1)$$

$$\times\ V(\underline{r}_1,\underline{r}_2)\,\Psi(\underline{r}_1,\underline{r}_2)\ d\underline{r}_1\,d\underline{r}_2 \quad . \qquad (6.9)$$

If one incident electron crosses unit area (perpendicular to the beam) each second, then the number of electrons deflected per second into the solid angle $d\Omega$ about the angle θ after exciting the nth state of atomic hydrogen is

$$I_n(\theta)\,d\Omega = \frac{k_n}{k_1}\left|\,f_n(\theta,\phi)\,\right|^2 d\Omega \quad . \qquad (6.10)$$

The total cross section has the form

$$Q_n = \frac{k_n}{k_1}\iint \left| f_n(\theta,\phi)\right|^2 \sin\theta \, d\theta \, d\phi \qquad (6.11)$$

6.1.2 First Born Approximation.

At sufficiently high impact energies, the interaction potential $V(\underline{r}_1,\underline{r}_2)$ may be treated as a small perturbation, and the solution of (6.9) to first order in $V(\underline{r}_1,\underline{r}_2)$ is found by substituting

$$\Psi(\underline{r}_1,\underline{r}_2) \sim e^{i\underline{k}_1\cdot\underline{r}_2}\,\psi_1(\underline{r}_1) \qquad (6.12)$$

into the right hand side of (6.9). This yields the first Born approximation to the scattering amplitude

$$f_n(\theta,\phi) = \frac{m}{2\pi\hbar^2}\int e^{i\underline{K}\cdot\underline{r}_2}\, V_{n1}(\underline{r}_2)\, d\underline{r}_2 \qquad (6.13)$$

where

$$\underline{K} = \underline{k}_1 - \underline{k}_n \qquad (6.14)$$

is the momentum change of the incident electron and

$$V_{n1}(\underline{r}_2) = \int \psi_n^*(\underline{r}_1)\, V(\underline{r}_1,\underline{r}_2)\, \psi_1(\underline{r}_1)\, d\underline{r}_1 \qquad (6.15)$$

Evaluating (6.13) for the particular case of elastic scattering (Corinaldesi and Trainor, 1952), and excitation of the 2s and 2p states (Moiseiwitsch and Smith, 1968) of atomic hydrogen, one obtains for the first Born approximation differential cross sections for these states:

$$I_{1s}(\theta) = \frac{4\,a_o^2\,(K^2+8)^2}{(K^2+4)^4}\,, \qquad (6.16)$$

$$I_{2p}(\theta) = \frac{288\,k_n\,a_o^2}{k_1\,K^2\,(K^2\,a_o^2+\frac{9}{4})^6}\,, \qquad (6.17)$$

and

$$I_{2p}(\theta) = \frac{288\, k_n\, a_o^2}{k_1\, K^2\, (K^2 a_o^2 + \frac{9}{4})^6} \quad . \qquad (6.18)$$

From equations (6.16) to (6.18) it can be seen that at sufficiently large angles, the differential cross sections for elastic, $1s \rightarrow 2s$, and $1s \rightarrow 2p$ excitation, decay like K^{-4}, K^{-12} and K^{-14} respectively.

If an expansion of the total wave function is made in terms of the angular momentum eigenstates of the incoming electron, the total excitation cross section Q_n may be expressed as a sum over partial cross sections Q_n corresponding to the orbital angular momentum quantum number ℓ of the incoming electron. That is

$$Q_n = \sum_{\ell = o} Q_n^{\ell} \quad . \qquad (6.19)$$

Calculations of the Q_n^{ℓ} for 2s and 2p excitation from the ground state using the first Born approximation reveals that for a given impact energy, many more partial waves make a contribution to the total $1s \rightarrow 2p$ excitation cross section than to the $1s \rightarrow 2s$ cross section.

This contrasting behaviour of the differential and total cross sections arises from the different asymptotic form of the interaction potentials at large distances r:- $V_{2s,1s}$ decreasing exponentially with increasing r, while $V_{2p,1s}$ falls off more slowly with an r^{-2} dependence for large r.

6.1.3 Second Born Approximation.

One limitation of the first Born approximation is that it neglects coupling to all states other than the initial and final states of the transition. By treating the first

Born approximation as the first stage of an iterative solution of (6.8), the scattering amplitude correct to the second order in V can be shown to have the form

$$f_n(\theta,\phi) = f_n^{(1)}(\theta,\phi) + f_n^{(2)}(\theta,\phi) , \quad (6.20)$$

where $f_n^{(1)}$ is the first Born approximation to the scattering amplitude given by (6.13) and $f_n^{(2)}$ is given by the formula

$$f_n^{(2)}(\theta,\phi) = \frac{m^2}{\pi\hbar^4} \sum_p \iint e^{i(\underline{k}_1\cdot\underline{r}_2' - \underline{k}_n\cdot\underline{r}_2)} \frac{e^{ik_p|\underline{r}_2 - \underline{r}_2'|}}{4\pi|\underline{r}_2 - \underline{r}_2'|} \times V_{np}(\underline{r}_2)\, V_{p1}(\underline{r}_2')\, d\underline{r}_2\, d\underline{r}_2' . \quad (6.21)$$

The second Born approximation should be an improvement on the first Born approximation because it is allowing for some distortion of the incident electron wave function. Furthermore it is evident from (6.21) that the second Born approximation includes transitions to the final state through all possible intermediate states.

To evaluate (6.21) completely would involve great computational difficulty. However, since about two-thirds of the polarizability of a hydrogen atom arises from the 2p state (Moiseiwitsch, 1962), a good approximation to $f^{(2)}$ can be obtained by assuming that the terms corresponding to the 1s, 2s and 2p intermediate states provide a major contribution to $f^{(2)}$, and the terms corresponding to all other intermediate states can be neglected. The effect of the 1s and 2s states is often termed distortion of the atom while the effect of the 2p state is called polarization of the atom.

Kingston, Moiseiwitsch and Skinner (1960) have shown that the differential cross section correct to third order

in the interaction energy is

$$I_n(\theta) = \left| f_n^{(1)} \right|^2 (1 + 2\alpha) \qquad (6.22)$$

where

$$\alpha = \frac{\mathcal{R} f_n^{(2)}}{f_n^{(1)}} \quad . \qquad (6.23)$$

6.1.4 Impulse Approximation.

Calculations of the differential cross section for electrons exciting the 2s and 2p states of atomic hydrogen performed by Akerib and Borowitz (1961) using the impulse approximation have not been considered in this thesis because a number of errors in their paper make the results they obtained unreliable (Coleman and McDowell, 1965).

6.1.5 Exchange Scattering.

If non-symmetrized wave functions are used, the boundary conditions for $\Psi(\underline{r}_1, \underline{r}_2)$ are

$$\Psi(\underline{r}_1, \underline{r}_2) \sim e^{i\underline{k}_1 \cdot \underline{r}_2} + \sum_n \frac{e^{ik_n r_2}}{r_2} f_n(\theta, \phi)\, \psi_n(\underline{r}_1) \text{ as } r_2 \to \infty \qquad (6.24)$$

and

$$\sim \sum_n \frac{e^{ik_n r_1}}{r_1} g_n(\theta, \phi)\, \psi_n(\underline{r}_2) \text{ as } r_1 \to \infty, \qquad (6.25)$$

where f_n and g_n are referred to as the direct and exchange scattering amplitudes for electrons exciting the nth state of atomic hydrogen.

Indistinguishability of the electrons may be taken into account by expressing the total wave function describing the system in the two symmetrized forms

$$\Psi^{\pm}(\underline{r}_1, \underline{r}_2) = \Psi(\underline{r}_1, \underline{r}_2) \pm \Psi(\underline{r}_2, \underline{r}_1) \quad , \qquad (6.26)$$

where $\Psi(\underline{r}_1,\underline{r}_2)$ is given by (6.2) and the positively and negatively symmetrized functions Ψ^+ and Ψ^- are associated with singlet and triplet scattering respectively. By substituting (6.26) into the Schrodinger equation (6.1), multiplying throughout by $\psi_n^*(\underline{r}_1)$ and integrating with respect to $\underline{r}_1$, the equation for $F_n^{\pm}$ becomes

$$\left(\nabla_2^2 + k_n^2 \right) F_n^{\pm}(\underline{r}_2) = \frac{2m}{\hbar^2} \sum_p R_{np}^{\pm}(\underline{r}_2) \quad , \tag{6.27}$$

where

$$R_{np}^{\pm}(\underline{r}_2) = F_p^{\pm}(\underline{r}_2) \int \psi_n^*(\underline{r}_1) V_2(\underline{r}_1,\underline{r}_2) \psi_p(\underline{r}_1)\, d\underline{r}_1 \pm \psi_p(\underline{r}_2) \int \psi_n^*(\underline{r}_1) \left[V_1(\underline{r}_1,\underline{r}_2) - \frac{\hbar^2}{2m} (\nabla_1^2 + k_p^2) \right] F_p^{\pm}(\underline{r}_1)\, d\underline{r}_1 \, , \tag{6.28}$$

with

$$V_1(\underline{r}_1,\underline{r}_2) = \frac{e^2}{r_{12}} - \frac{e^2}{r_1} \quad , \tag{6.29}$$

and

$$V_2(\underline{r}_1,\underline{r}_2) = \frac{e^2}{r_{12}} - \frac{e^2}{r_2} \quad , \tag{6.30}$$

being the interaction energy with electron 1 and electron 2 incident on the atom respectively.

Equation (6.27) may be solved using the Green's function for a free particle, and the scattering amplitudes $f_n^{\pm}$ are found to be

$$f_n^{\pm}(0,\phi) = \frac{m}{2\pi\hbar^2} \sum_p \int e^{-i\underline{k}_n \cdot \underline{r}_2} R_{np}^{\pm}(\underline{r}_2)\, d\underline{r}_2 . \tag{6.31}$$

The differential cross section for excitation of the nth state of atomic hydrogen is then given by (Mott and

Massey, 1965b)

$$I_n(\theta) = \frac{k_n}{k_1}\left[\tfrac{1}{4}\left|f_n^+(\theta,\phi)\right|^2 + \tfrac{3}{4}\left|f_n^-(\theta,\phi)\right|^2\right], \quad (6.32)$$

where $\frac{1}{4}$ and $\frac{3}{4}$ are the spin statistical weighting factors for the singlet and triplet states respectively.

Note that the direct f_n and exchange g_n scattering amplitudes are related to f_n^+ and f_n^- by

$$f_n^+ = f_n + g_n \quad (6.33)$$

and

$$f_n^- = f_n - g_n \quad (6.34)$$

6.1.6 Born - Oppenheimer Approximation.

By setting

$$F_1^{\pm}(\underline{r}) = e^{i\underline{k}\cdot\underline{r}}$$

$$F_p^{\pm}(\underline{r}) = 0 \quad (p \neq 1) \quad (6.35)$$

in formula (6.28) for $R_{np}^{\pm}$ and substituting the resulting expression in (6.27) one obtains the Born - Oppenheimer approximation to the scattering amplitude, which is given by

$$f_n^{\pm}(\theta,\phi) = \frac{m}{2\pi\hbar^2}\iint e^{i(\underline{k}_1 - \underline{k}_n)\cdot\underline{r}_2}\,\psi_n^*(\underline{r}_1)\,V_2(\underline{r}_1,\underline{r}_2)\,\psi_1(\underline{r}_1)\,d\underline{r}_1 d\underline{r}_2$$

$$\mp \frac{m}{2\pi\hbar^2}\iint e^{i(\underline{k}_1\cdot\underline{r}_1 - \underline{k}_n\cdot\underline{r}_2)}\,\psi_n^*(\underline{r}_1)\,V_1(\underline{r}_1,\underline{r}_2)\,\psi_1(\underline{r}_2)\,d\underline{r}_1 d\underline{r}_2, \quad (6.36)$$

where the first term is the first Born scattering amplitude f_n given by (6.13) and the second term is the exchange scattering amplitude g_n. Analytical expressions for the $f_n^{\pm}$ given by (6.36) have been obtained by Corinaldesi and Trainor (1952) for the $1s \rightarrow 2s$, $1s \rightarrow 2p0$ and $1s \rightarrow 2p\pm1$ excitation of atomic hydrogen.

Bell (1965) has pointed out a discrepancy in the analysis of Corinaldesi and Trainor, and has shown that the correct procedure leads to a non-vanishing expression for the exchange scattering amplitude for the $m = \pm 1$ levels. However, there is a misprint in equation (3) of Bell's paper, the correct expression being given by Mott and Massey (1965c).

6.1.7 Symmetric Approximation of Borowitz.

The usual method of treating the scattering of electrons in the Born approximation is to use the interaction of the incoming electron with both the bound electron and proton (in the atom) as the perturbation. Borowitz (1956) calls this the method of "asymmetric perturbation".

An alternative procedure is to take the interaction of the two electrons with each other as the perturbation. Borowitz (1956) refers to this as the "symmetric perturbation" procedure, and has used it to derive approximate formulae for the direct and exchange scattering amplitudes for excitation of the 2s and 2p states of atomic hydrogen at large values of the momentum transfer.

6.1.8 First Order Exchange Approximation.

The expression for the scattering amplitude in the Born - Oppenheimer approximation (6.36) suffers from the defect that the addition of a constant potential to the interaction energy V_2 between the colliding particles produces a non-vanishing change in the scattering amplitude, due to the lack of orthogonality between the initial and final state wave functions (Schiff, 1955).

Bell and Moiseiwitsch (1963) have derived an approximation, called the first order exchange approximation, which is exact to the first order in the interaction potential, and remains unaltered if a constant is added to V_2.

6.1.9 Distorted Wave Approximation.

A two state approximation involving just the initial (ground) state of the hydrogen atom and the final state n, in which full allowance is made for the distortion of the incident and scattered electron waves, may be derived from (6.27) by ignoring all other states in the summation, and assuming the back coupling of the final state n to the initial state 1 is sufficiently weak to be set equal to zero. Then the scattering amplitude in this approximation (referred to as the distorted wave approximation with exchange) can be expressed as

$$f_n^{\pm}(\theta,\phi) = \frac{m}{2\pi\hbar^2}\int \mathcal{F}_n^{\pm}(\underline{r}_2)\left[V_{n1}(\underline{r}_2)\mathcal{F}_1^{\pm}(\underline{r}_2) \pm \int K_{n1}(\underline{r}_1,\underline{r}_2)\mathcal{F}_1^{\pm}(\underline{r}_1)\,d\underline{r}_1\right] d\underline{r}_2 \quad , \quad (6.37)$$

where

$$K_{n1}(\underline{r}_1,\underline{r}_2) = \psi_1(\underline{r}_2)\,\psi_n^*(\underline{r}_1)\left(\frac{e^2}{r_{12}} + E_1 + E_n - E\right), \quad (6.38)$$

E_1 and E_n are the energies of the ground and nth state of atomic hydrogen respectively, and $\mathcal{F}_1^{+-}$ and $\mathcal{F}_n^{\pm}$ are the solutions of the equation,

$$\left[\nabla_2^2 + k_p^2 - \frac{2m}{\hbar} V_{pp}(\underline{r}_2)\right]\mathcal{F}_p^{\pm}(\underline{r}_2) \mp \frac{2m}{\hbar}\int K_{pp}(\underline{r}_1,\underline{r}_2)\,\mathcal{F}_p^{\pm}(\underline{r}_1)\,d\underline{r}_1 = 0 \quad (6.39)$$

which have the asymptotic form

$$\mathcal{F}_p^{\pm}(\underline{r}) \sim e^{(-1)^{\delta_{pn}} \underline{k}_p \cdot \underline{r}} + \frac{e^{ik_1 r}}{r} f_p^{\pm}(\theta, \phi) \qquad (6.40)$$

for p = 1 and p = n respectively.

The distorted wave approximation without exchange is obtained by setting K_{11}, K_{n1} and K_{nn} equal to zero in (6.37) and (6.39).

6.1.10 Partial Wave Expansion.

Let the atomic hydrogen electron have the principle quantum number n and orbital angular momentum quantum number ℓ_1, the free electron have wave number k_n and orbital angular momentum quantum number ℓ_2, and a denote the set of quantum numbers $n\ell_1\ell_2$. Also suppose L and M_L are the quantum numbers of the total orbital angular momentum of incident and bound electrons, and S and M_s the total spin angular momentum numbers. Since the total orbital and spin angular momenta are conserved separately throughout the collision, their quantum numbers remain unaltered. By expanding the wave function (6.26) in terms of angular momentum eigenfunctions, the set of coupled differential equations for the radial functions $F_a^{LS}(r)$ (representing the unbound electron) are obtained:

$$\left[\frac{d^2}{dr^2} + k_n^2 + \frac{\ell_2(\ell_2+1)}{r^2} \right] F_a^{LS}(r)$$

$$= \frac{-2m}{\hbar^2} \sum_{a'} \left[V^{L}_{aa'}(r) - W^{LS}_{aa'}(r) \right] F^{LS}_{a'}(r) = 0, \qquad (6.41)$$

where $V^{L}_{aa'}(r)$ and $W^{LS}_{aa'}(r)$ are the potential and exchange interaction terms (for which explicit expressions are given by Percival and Seaton, 1957) while a and a' denote initial and

final states of the atom. The asymptotic behaviour of $F_a^{LS}(r)$ is chosen to have the form at large r of

$$F_a^{LS}(r) \sim \frac{1}{k_n^{\frac{1}{2}}} \left[\sin\left(k_n r - \tfrac{1}{2}\ell_2\pi \right) \delta_{aa'} + \cos\left(k_n r - \tfrac{1}{2}\ell_2\pi\right) R_{aa'} \right] , \qquad (6.42)$$

or alternatively

$$F_a^{LS}(r) \sim \frac{1}{k_n^{\frac{1}{2}}} \left[e^{-i(k_n r - \frac{1}{2}\ell_2\pi)} \delta_{aa'} - e^{i(k_n r - \frac{1}{2}\ell_2\pi)} S_{aa'} \right], \qquad (6.43)$$

where $R_{aa'}$ and $S_{aa'}$ are the elements of the reactance matrix $\underline{R}$ and the scattering matrix $\underline{S}$, respectively. The scattering matrix $\underline{S}$ is both symmetrical and unitary, and is related to the $\underline{R}$ matrix by the formula

$$\underline{S} = \left[\underline{1} + i\,\underline{R}\right]\left[\underline{1} - i\,\underline{R}\right]^{-1} . \qquad (6.44)$$

The unitary property of the scattering matrix may be shown to imply the conservation of particles during the interaction (Seaton 1962).

The differential cross section may be conveniently expressed in terms of the $\underline{T}$ matrix, which is defined by the formula

$$\underline{T} = \underline{1} - \underline{S} = -2i\,\underline{R}\left[\underline{1} - i\,\underline{R}\right]^{-1} . \qquad (6.45)$$

If $I_{n'\ell'_i}(\theta,\phi)$ represents the differential cross section for electrons exciting the $n'\ell'$ state of atomic hydrogen from the $n\ell_1$ state, then it may be shown that (Love and Thomas, 1958)

$$I_{n'\ell'_1}(\theta) = \frac{(2S+1)}{4\pi(2\ell_1+1)k_n^2} \sum_{L_c=0}^{\infty} B^S_{L_c}(n'_1\ell'_1, n_1\ell_1)\, P_{L_c}(\cos\theta) \qquad (6.46)$$

where the expansion coefficients $B^{S}_{L_c}$ are a function of the transition matrix elements (the explicit form being given by Scott, 1965).

6.1.11 Unitarized Born Approximation.

By setting $\underline{R} = \underline{R}_B$ in (6.45), where the elements of $\underline{R}_B$ are calculated in the Born approximation, an approximate solution of the Schrodinger equation is obtained which satisfies the unitary condition, and makes some allowance for the coupling of intermediate states with both the initial and final states. (This approximation is known by the titles unitarized Born approximation or Born II approximation.)

6.1.12 Close Coupling Approximation.

Since the inclusion of all possible states in the expansion of the wave function for the system leads to an infinite number of the equations (6.41), solutions can only be found if a finite number of the states are retained. The finite set of coupled integro - differential equations resulting are known as the close-coupling approximation, the order of the approximation depending on the number of atomic states retained in the expansion of the total wave function.

6.2 Molecular Hydrogen.

Assuming that the total wave function for a molecule can be expressed as the product of electronic, vibrational and rotational wave functions, (a good approximation according to Herzeberg, 1950b), the Schrodinger equation for the electrons of a hydrogen molecule and on incident electron moving in the field of fixed nuclei is given by

$$\left[-\frac{\hbar^2}{2m}\left(\nabla_1^2 + \nabla_2^2 + \nabla_3^2\right) + V_m + V(\underline{r}_1;\underline{r}_2,\underline{r}_3) - E \right]\Psi = 0 \qquad (6.47)$$

where $$V(\underline{r}_1;\underline{r}_2,\underline{r}_3) = \frac{e^2}{r_{12}} + \frac{e^2}{r_{13}} - \frac{e^2}{r_{A1}} - \frac{e^2}{r_{B1}} \qquad (6.48)$$

is the interaction potential between incident electron 1 and the hydrogen molecule (containing electrons 2 and 3), r_{A1}, r_{B1} are the distances of the incident electron from the two nuclei A and B respectively, V_m is the interaction potential for an isolated molecule, and E is the total electronic energy of the system. If r_A and r_B are the distances of any one of the electrons from the nuclei A and B respectively, then each of the two electrons within the molecule may be represented approximately by an LCAO (Slater, 1963) molecular orbital u(r) of the form

$$N\ (v(r_A) + v(r_B)) \qquad (6.49)$$

where $$v(r) = e^{-\mathcal{Z}r}\ , \qquad (6.50)$$

and N is a normalizing factor. The wave function for the undistorted molecule may then be expressed in the separated form

$$\Psi_o(\underline{r}_2,\underline{r}_3) = u(\underline{r}_2)\, u(\underline{r}_3) \qquad (6.51)$$

By employing a similar procedure to that used to solve the Schrodinger equation for electron scattering from atoms, Khare and Moiseiwitsch (1965) show that the first Born approximation to the elastic scattering amplitude $f(\theta)$ for electrons incident upon hydrogen molecules may be expressed by the equation

$$f(\theta) = -\frac{m}{2\pi\hbar^2}\iiint e^{i\underline{K}.\underline{r}_1} \left|\Psi_o(\underline{r}_2,\underline{r}_3)\right|^2 V(\underline{r}_1;\underline{r}_2,\underline{r}_3)\, d\underline{r}_1\, d\underline{r}_2\, d\underline{r}_3 \,. \qquad (6.52)$$

By substituting (6.48) and (6.51) into (6.52), and noting the form of u (r), (from equations 6.49 and 6.50) one obtains

$$f(\theta) = \frac{m}{2\pi\hbar^2 K^2} \cos(\underline{K}.\underline{R}/2) \left[1 - \frac{32\pi N^2 Z}{(K^2 + 4Z^2)^2} \right]$$

$$- \frac{8N^2}{K^2} \int e^{i\underline{K}.\underline{r}} e^{-Z(r_A + r_B)} d\underline{r} \qquad (6.53)$$

where $\underline{r}$ is referred to the mid point of AB.

A series expansion for $f(\theta)$ given by (6.53) can be obtained using spherical functions, and the expression obtained evaluated numerically. After averaging over all angles of orientation of the molecule, an expression (equation 58 in the paper by Kare and Moiseiwitsch) can be obtained for the differential cross section $\bar{I}(K)$.

In particular Khare and Moiseiwitsch draw attention to the presence of a $(1 + \frac{\sin Kr}{Kr})$ factor in $\bar{I}(K)$ which appears also in the expression derived for the differential cross section $\bar{I}_s$ obtained by regarding the molecule as consisting of two hydrogenic atoms that are sufficiently far apart to be independent of each other, but which both contribute to the phase of the wave function for the scattered electrons. The hydrogenic atoms differ from normal hydrogen atom by possessing an unquantized nuclear charge Z = 1.193. Since this separated atom approximation $\bar{I}_s$ for elastic scattering (without the inclusion of exchange) never differs from the exact expression $\bar{I}$ by more than 4%, the direct scattering amplitude is taken to be the separated atom limiting case, namely

$$f_d(\theta) \sim f_s(K) \cos(\underline{K}.\underline{R}/2) \tag{6.54}$$

$$\text{where } f_s(\theta) = \frac{4(K^2 + 8Z^2)}{(K^2 + 4Z^2)^2} \quad . \tag{6.55}$$

Allowance is made for exchange by using the exchange part of the first order exchange approximation (see Section 6.1.8).

Again Khare and Moiseiwitsch show that the separated hydrogenic atom approximation may be expected to yield a good approximation for the scattering amplitude. An expression for the complete scattering amplitude is then obtained by summing the separated hydrogenic atom approximations for the direct and exchange scattering amplitudes, and used to obtain the differential cross section for elastic scattering of electrons from molecular hydrogen.

CHAPTER 7.

ELECTRON SCATTERING FROM MOLECULAR HYDROGEN.

Introduction.

In Section 1.3.2 attention was drawn to the discrepancy between the measurements of a number of experimenters in the early 1930's, and recent calculations by Khare and Moiseiwitsch (1956), for the angular distributions of electrons elastically scattered from molecular hydrogen at both small and large angles. This chapter reports the measurement of these angular distributions with the present apparatus for incident electron energies of 30, 50, 100 and 200 eV over the angular range extending from 20^{o} to 130^{o}. Preliminary results are also given for the angular distributions of electrons exciting the $b\left(^{3}\Sigma_{u}^{+}\right)$ state of molecular hydrogen.

7.1 Elastic Scattering.

7.1.1 Results.

Curve (b) of Figure 7.1 shows the experimental angular distribution obtained for elastic scattering of 30 eV electrons from molecular hydrogen and the associated data points. The experimental angular distribution has been redrawn below curve (b), and compared with the laboratory measurements reported by Hughes and McMillen (1932b) and Webb (1935b). The results obtained by these experimentors have been adjusted for their best visual fit to the present results over the angular range extending from 20^{o} to 100^{o} (curves (a) of Figure 7.1). While there is general agreement for the shape of the angular distribution between 20^{o} and 100^{o}, both the results of Hughes and McMillen, and Webb rise steeply with increasing angles at

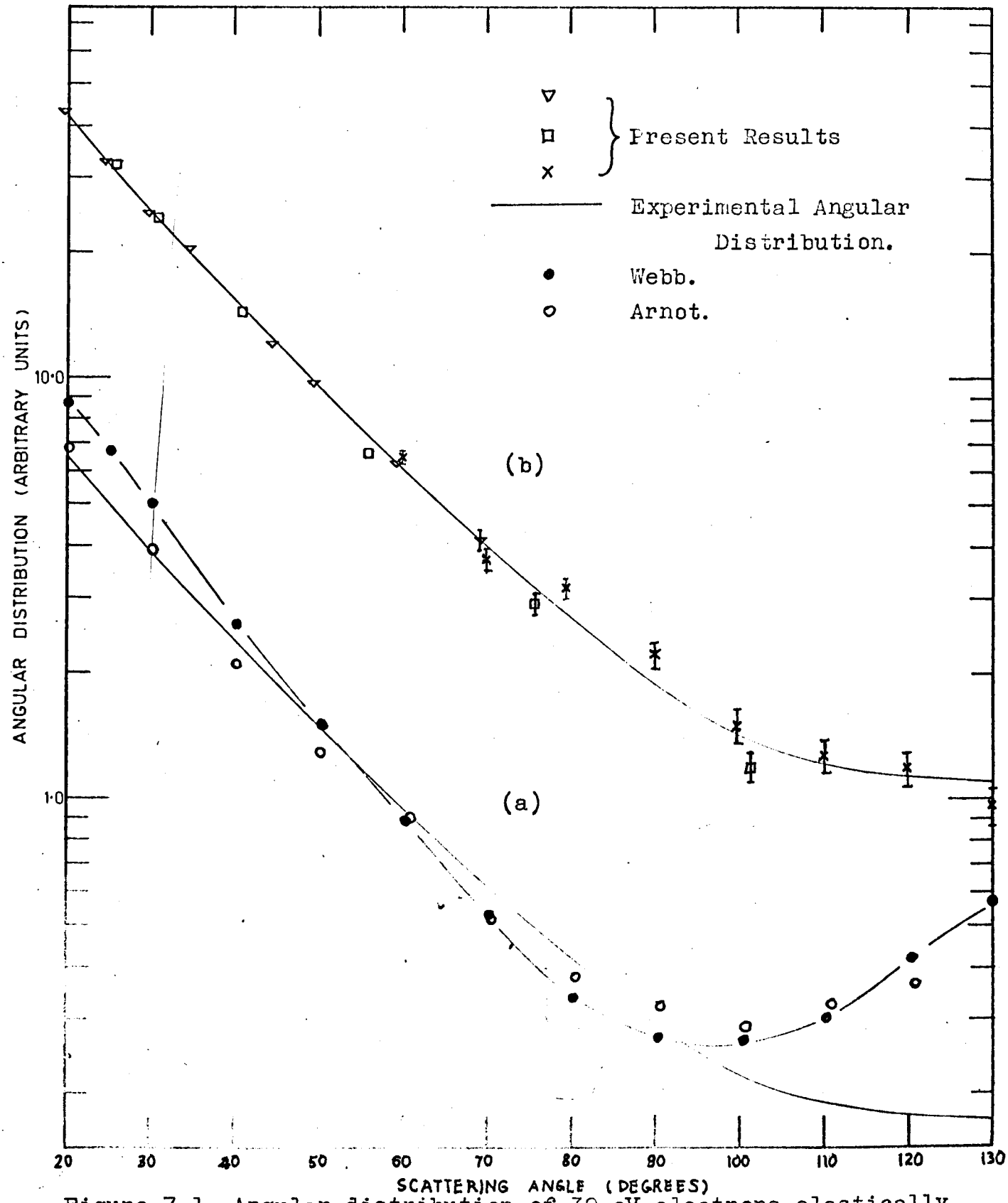

Figure 7.1 Angular distribution of 30 eV electrons elastically scattered from molecular hydrogen.
Curve (a) The results of Webb, and Arnot are adjusted for their best visual fit to the present angular distribution over the angular range 20 to 100°.
Curve (b) Present experimental angular distribution and the associated data points. The standard deviation of each point is $\leq$ 3% unless shown otherwise.

angles greater than 100^{o}, whereas the results of the present investigation decrease slowly out to 130^{o} (the largest angle at which measurements were performed).

Various results for elastic scattering of 50, 100 and 200 eV electrons from molecular hydrogen are given on Figures 7.2, 7.3 and 7.4 respectively. As in Figure 7.1, the comparison between previously reported and present results is shown by the curves (a), while the experimental angular distribution obtained during the present investigation is displaced to curve (b) so that its relation to the associated data points may be shown. All three laboratory measurements have been separately normalized to the differential cross section calculations of Khare and Moiseiwitsch at each energy. The range of angles over which the visual adjustment has been made has been restricted in each case to that for which there is best agreement between the theoretical and experimental results. For the present investigation this angular range extends from 20^{o} to 100^{o}, while for the results of previous experiments, it is from 20^{o} to 80^{o} at 50 eV, 20^{o} to 70^{o} at 100 eV, and 20^{o} to 50^{o} at 200 eV.

The results of the present investigation agree very well with the shape of the theoretical differential cross section over the complete angular range studied at 100 and 200 eV. However, the experimental angular distribution at 50 eV clearly rises more rapidly than the theoretical results for scattering angles less than 40^{o}. This difference may also exist at 100 eV for angles less than 30, as may be seen by examining Figure 7.3.

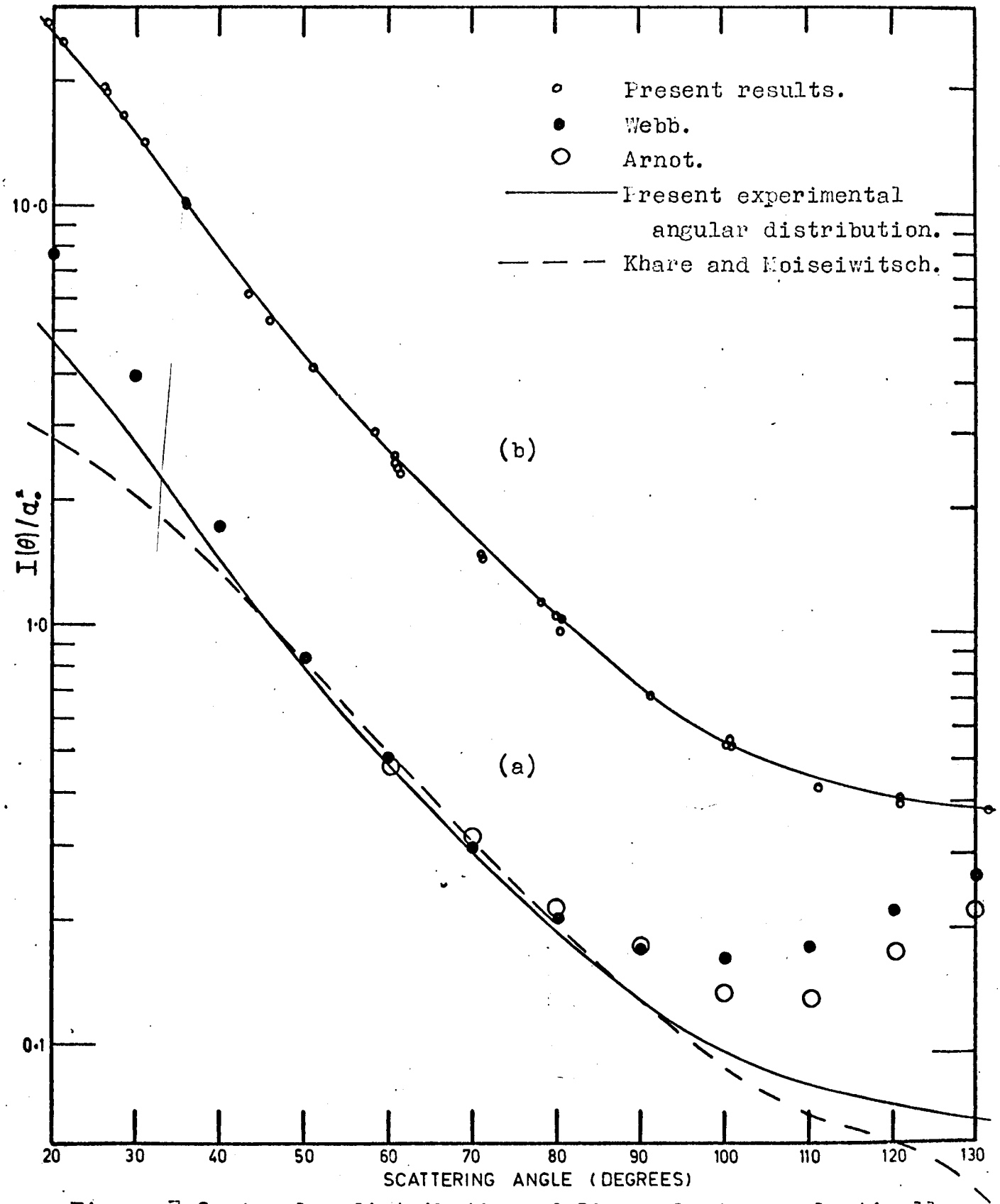

Figure 7.2 Angular distribution of 50 ev electrons elastically scattered from molecular hydrogen.
Curve (a) The present experimental angular distribution, and the measurements of Webb, and Arnot have been adjusted for their best visual fit to the theoretical differential cross section of Khare and Moiseiwitsch over the angular range from 20^{0} to 80^{0}.
Curve (b) Present experimental angular distribution and the associated data points. The standard deviation of each point is $\leq 3\%$.

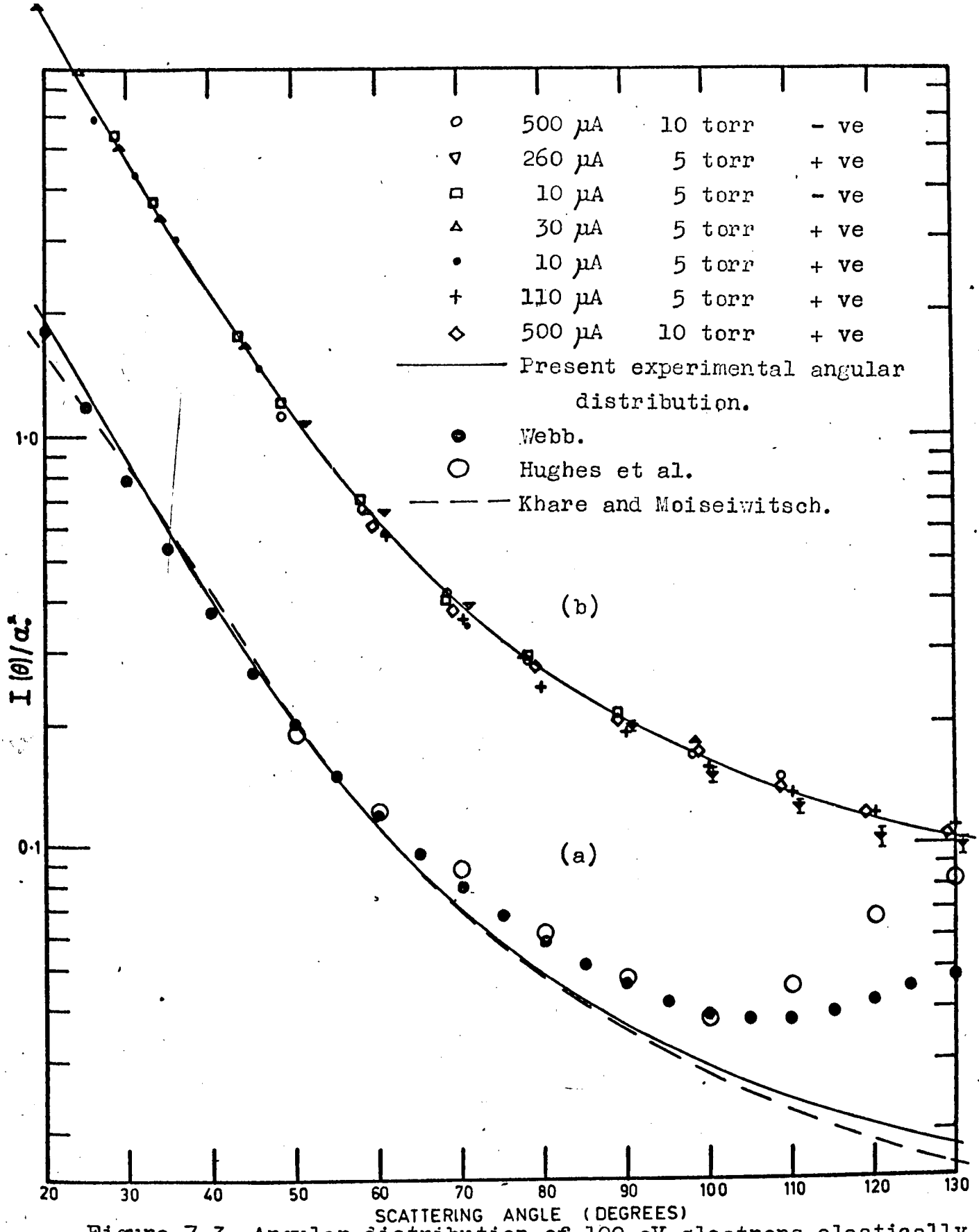

Figure 7.3 Angular distribution of 100 eV electrons elastically scattered from molecular hydrogen.

Curve (a) The results of Webb, and Arnot are adjusted for their best visual fit to the present angular distribution over the angular range 20^{0} to 70^{0}.

Curve (b) Present experimental angular distribution and the associated data points. The standard deviation of each point is $\leqslant$ 3% unless shown otherwise.

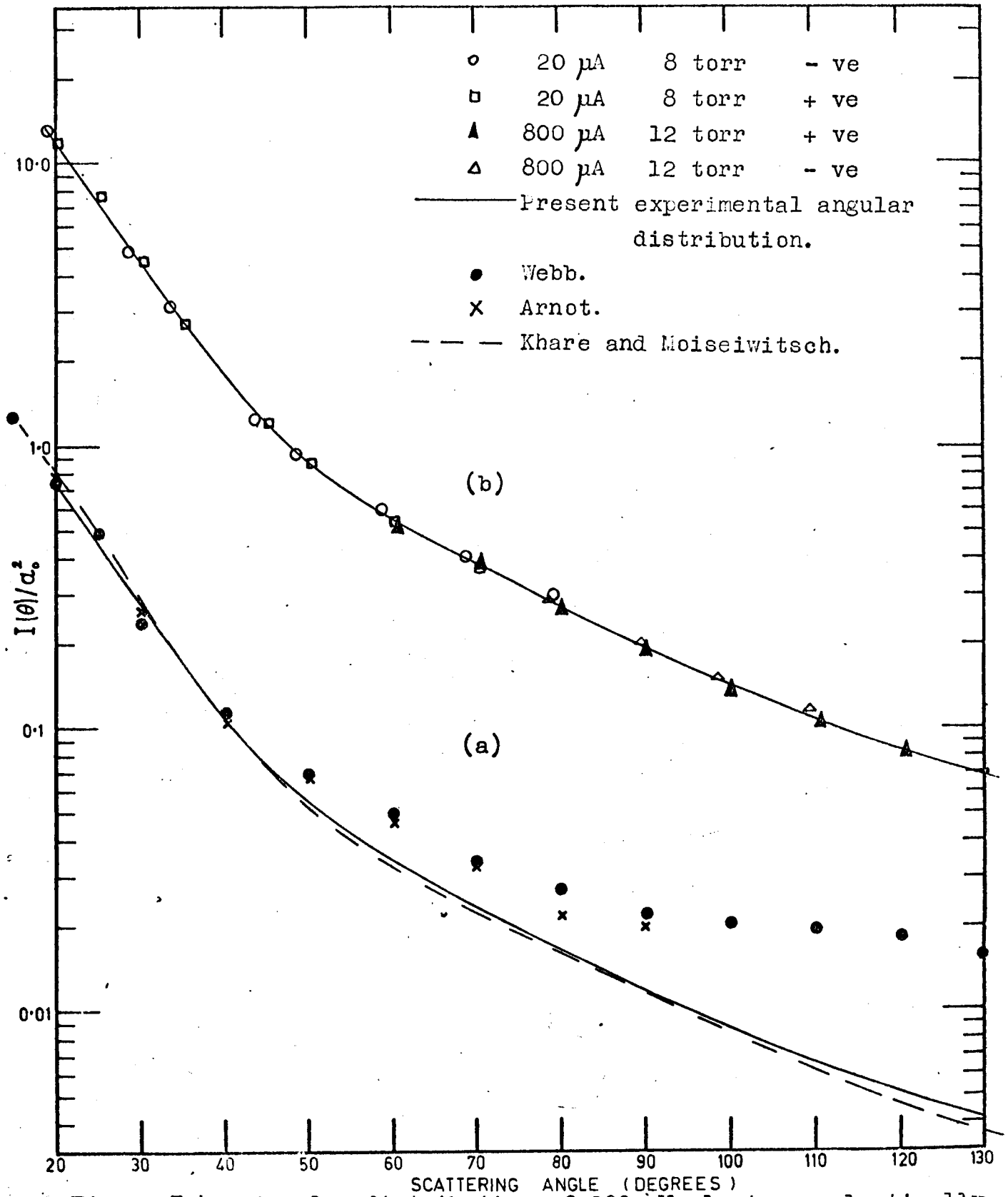

Figure 7.4 Angular distribution of 200 eV electrons elastically scattered from molecular hydrogen.

Curve (a) The results of Webb, and Hughes are adjusted for their best visual fit to the present angular distribution over the angular range 20^{0} to 50^{0}.

Curve (b) Present experimental angular distribution and the associated data points. The standard deviation of each point is $\leq$ 3%.

At 50 eV, the experimental angular distribution also decreases more slowly than the theoretical curve for angles greater than 100°.

There is fair agreement between the shapes of the angular distribution measurements of Webb and those of the present investigation except at large scattering angles, where the results of the two different investigations diverge with increasing angle. A similar conclusion can be made between the present results and those of Hughes and McMillen, although it is significant that the results of the earlier experimentors also diverge from each other at large angles for incident electron energies of 50 and 100 eV. In particular at 100 eV and scattering angle of 130°, the difference between the results of the earlier experimentors is similar to that between the result of Webb and those of the present investigation. Since both the earlier experiments were performed using the static gas technique (see Section 2.1.1), this suggests that inadequate allowance may have been made for the background signal. Another possible explanation for the discrepancy is that impurities, whose differential cross section increases at large scattering angles, may have been present in the hydrogen supply used in earlier experiments. Among the gases which have been observed to have this property are nitrogen, carbon monoxide and methane (Arnot, 1931, and Mohr and Nicoll, 1932).

7.1.2 Discussion.

The calculation (see Section 6.2) performed by Khare and Moiseiwitsch to determine the differential cross section for elastic scattering from molecular hydrogen used the first order exchange approximation (see Section 6.1.8). These

authors also showed that to a good approximation, elastic scattering from the hydrogen molecule may be considered as arising from the interference of the electron waves scattered from two separated hydrogenic atoms whose nuclear charge is unquantized. If exchange is neglected, the differential cross section does not rise as steeply at small angles as is observed experimentally. (See Figures 6 and 7 of Khare and Moiseiwitsch, 1965.) However, with the inclusion of exchange, excellent agreement between the shapes of the experimental and theoretical angular distributions is obtained at 100 and 200 eV. At 50 eV, the theoretical differential cross section, even with exchange effects included, does not rise as rapidly as the laboratory angular distribution. This may be due to the general inadequacy of the first Born approximation at lower energies, or neglect of the polarization of the hydrogen molecule by the incident electron, or both of these limitations. Polarization of the hydrogen molecule was not allowed for in the theoretical calculation because the dipole polarizability of molecular hydrogen is sufficiently large to ensure that use of the adiabatic approximation would necessarily produce considerable overestimation of the contribution from polarization.

7.2 Inelastic Scattering.

It was pointed out in Section 1.3.3, that while excitation of the $b\left(^3\Sigma_u^+\right)$ state of molecular hydrogen had been observed in the energy loss spectrum of electrons scattered in the forward direction at low energies, no measurements had been reported at larger angles. The energy loss spectrum for electrons scattered from molecular hydrogen through 20^o and 60^o

are shown on Figures 7.5 and 7.6 respectively, for energy losses ranging from 6.7 eV to 13.2 eV (Channels 0 and 45 respectively). The dashed line on each curve was obtained by averaging visually the scatter of the data points. The prominent energy loss peak in both diagrams corresponds to electrons exciting a number of the lower vibrational levels of the B and C states of molecular hydrogen. Clearly evident also in the spectrum of electrons scattered through 60^{o} (Figure 7.6), are electrons which have suffered energy losses down to approximately 8 volts. At a scattering angle of 20^{o}, however, the number of electrons which have given up energy from approximately 8 to 11 eV is very small compared to the number exciting the B and C states.

By applying the Frank - Condon principle (Herzberg 1950b) to the lower level potential energy curves for molecular hydrogen (Figure 7.7), an estimate can be obtained for the range of energy losses expected for electrons exciting the $b\left(^{3}\Sigma_{u}^{+}\right)$ state. According to the Frank - Condon principle, the most probable transitions in diatomic molecules are those which leave the positions and momenta of the nuclei unchanged. Such transitions are often referred to as vertical transitions and may be represented on the potential energy diagram as vertical lines. The two extreme transitions which can occur between the lowest vibrational level of the ground state $H_2\left(^{1}\Sigma_{g}^{+}\right)$ and the $b\left(^{3}\Sigma_{u}^{+}\right)$ state of molecular hydrogen have been shown on Figure 7.7 by the two vertical lines. Since the repulsive $b\left(^{3}\Sigma_{u}^{+}\right)$ state has no discrete eigenstates, electrons exciting this state could be expected to possess a continuous energy distribution extending over the approximate energy range from

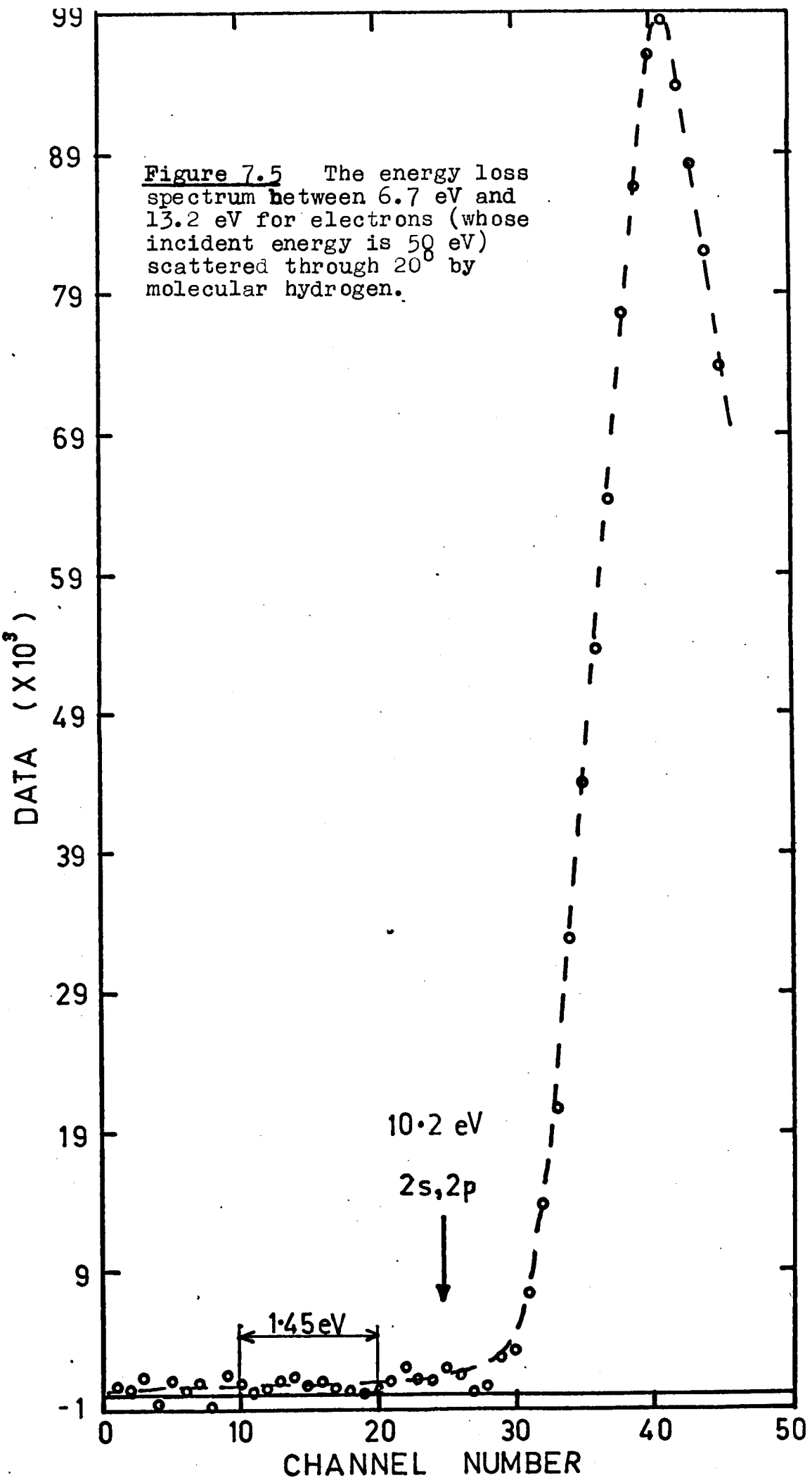

Figure 7.5 The energy loss spectrum between 6.7 eV and 13.2 eV for electrons (whose incident energy is 50 eV) scattered through 20° by molecular hydrogen.

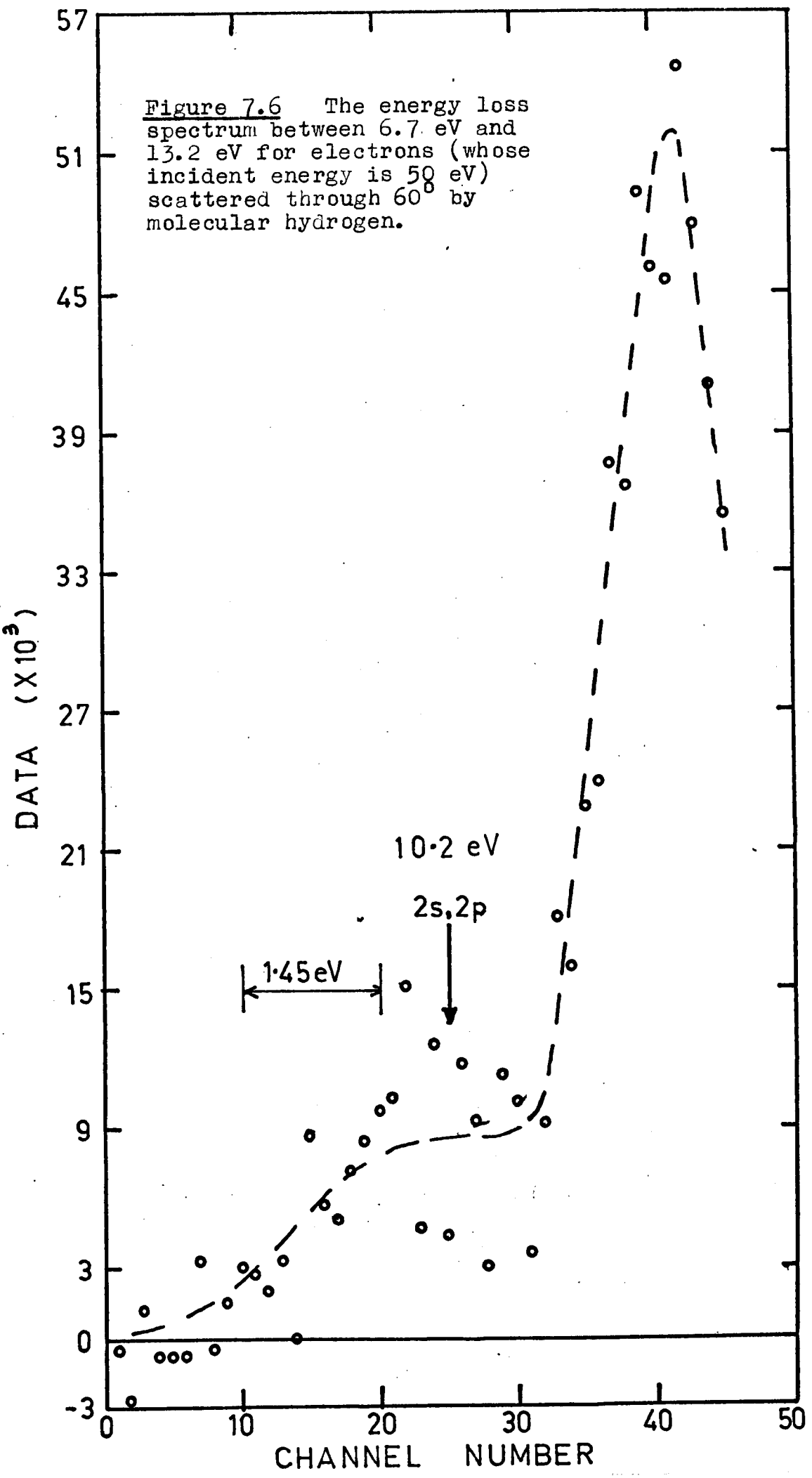

Figure 7.6 The energy loss spectrum between 6.7 eV and 13.2 eV for electrons (whose incident energy is 50 eV) scattered through 60° by molecular hydrogen.

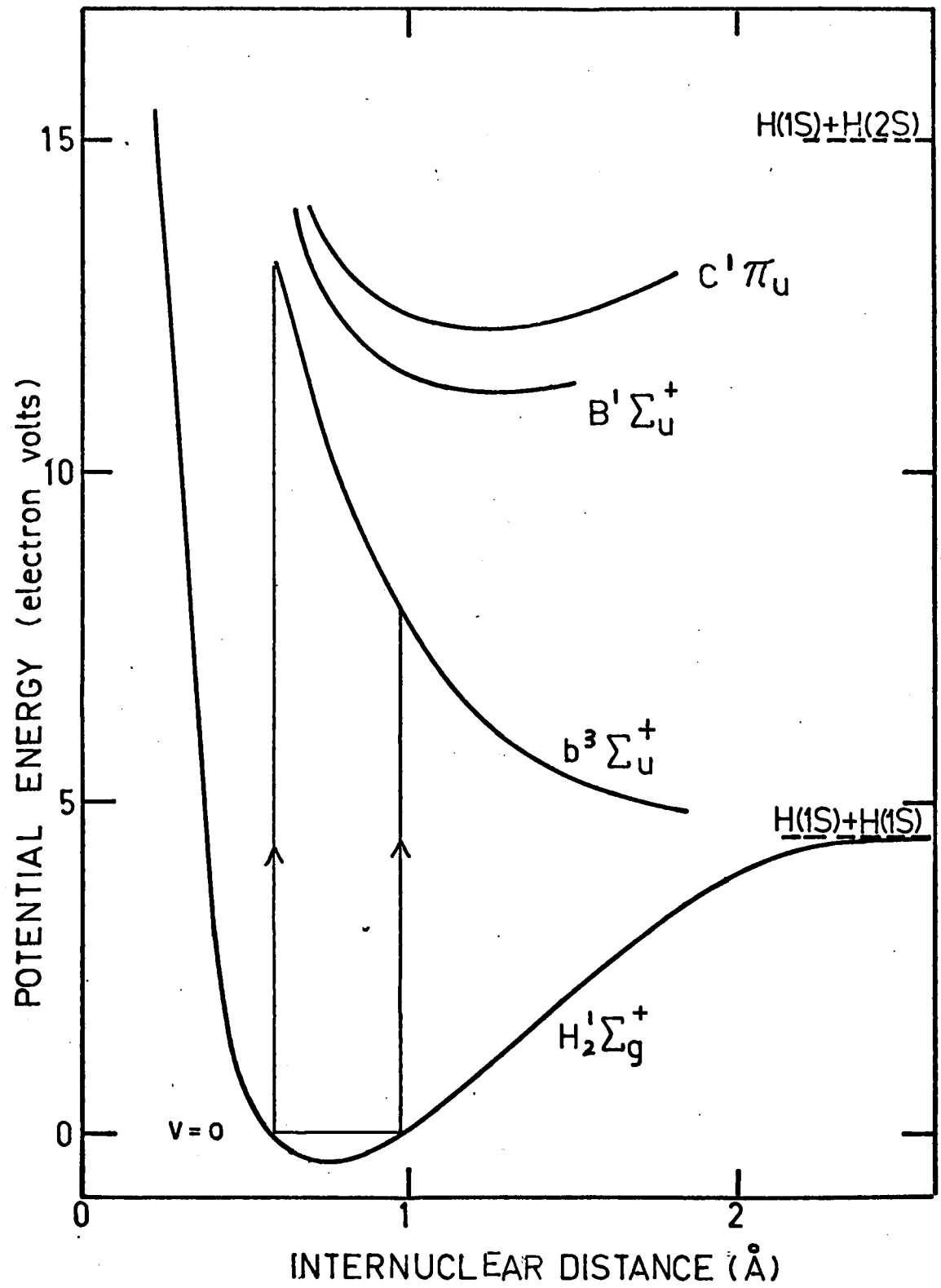

Figure 7.7 Potential energy curves for H_2 showing 2 possible vertical transitions from the ground state to the b $\left(^3\Sigma_u^+\right)$ state.

8 eV to 13 eV. Electrons suffering the higher energy losses would also be indistinguishable from those exciting the B and C states above approximately 11.5 eV. This conclusion is consistent with the observed energy loss spectrum (see Figure 7.6).

Preliminary information on the angular distribution of electrons exciting the $b\left(^3\Sigma_u^+\right)$ state of molecular hydrogen has been obtained by summing the experimental data for the 9 channels (a range of 1.3 eV) centred around the channel corresponding to a principle energy loss of 10.2 eV at a number of angles. Results obtained are shown on Figure 7.8 for incident electron energies of 50, 100 and 200 eV. The random error of the data points for the results at 200 eV is particularly large, and where incomplete error bars are shown, the statistical error contribution was so large that the sum of the 9 channels yielded a negative result. The results obtained at 50 and 100 eV suggest that the angular distribution decreases only slowly with increasing angle between 20^o and 70^o, while at large angles, it decreases more rapidly. At 200 eV, the angular distribution observed decreases rapidly with increasing angle from 20^o to 80^o.

From an examination of the energy spectrum at each angle and energy studied, the general conclusion was made that the ratio of the number electrons scattered (at each angle) which had excited the $b\left(^3\Sigma_u^+\right)$ state and the sum of the number of electrons exciting the B and C states, reached a maximum at angles near 60^o, and became very small at 20^o.

Figure 7.8 Angular distribution of electrons (losing from 9.6 to 10.9 eV of energy) exciting molecular hydrogen to the $b\left(^3\Sigma_u^+\right)$ state.

The angular scale extends from 20^o to 130^o on each graph.

Graph (a) Incident electron energy of 50 eV.

" (b) Incident electron energy of 100 eV.

" (c) Incident electron energy of 200 eV.

I represents two standard deviations.

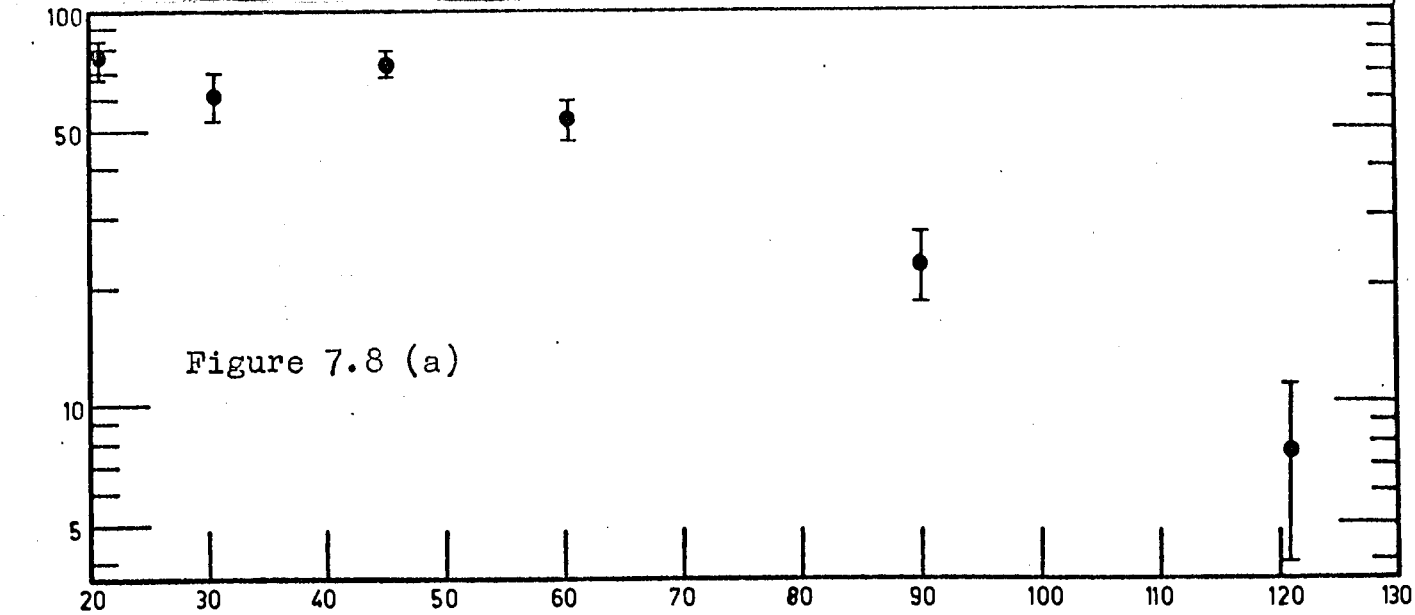

Figure 7.8 (a)

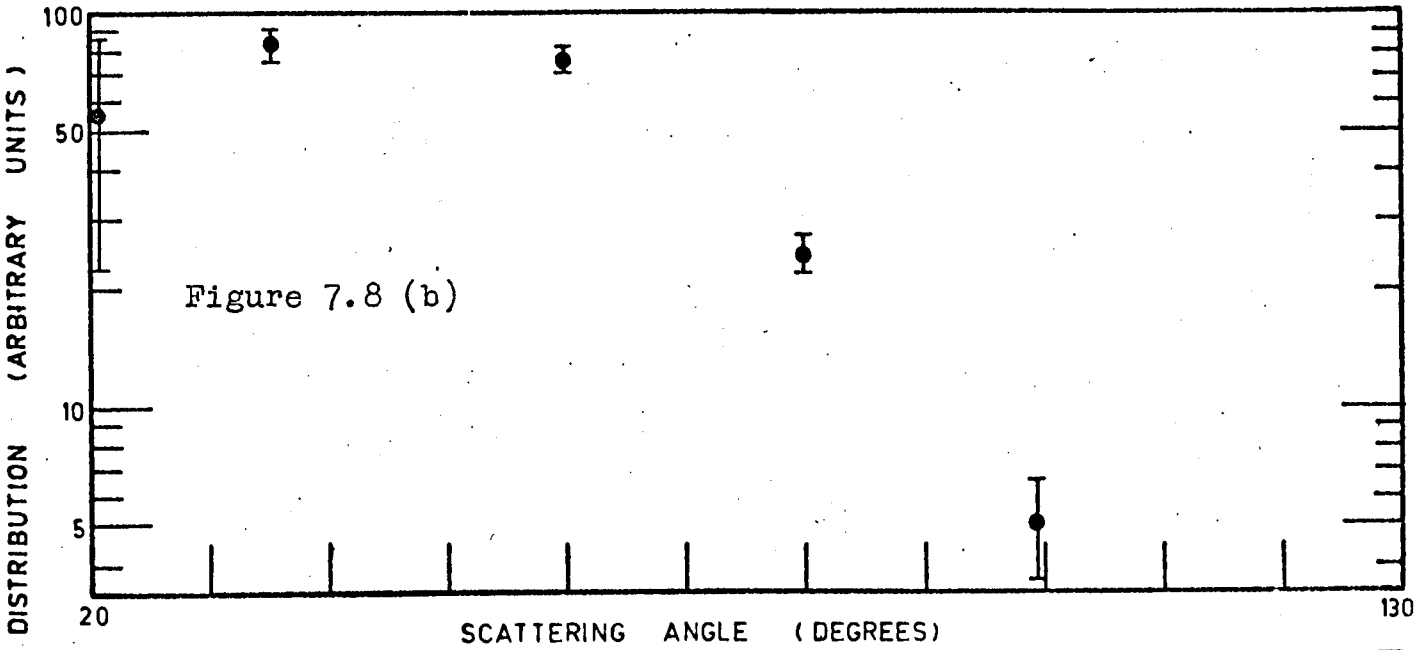

Figure 7.8 (b)

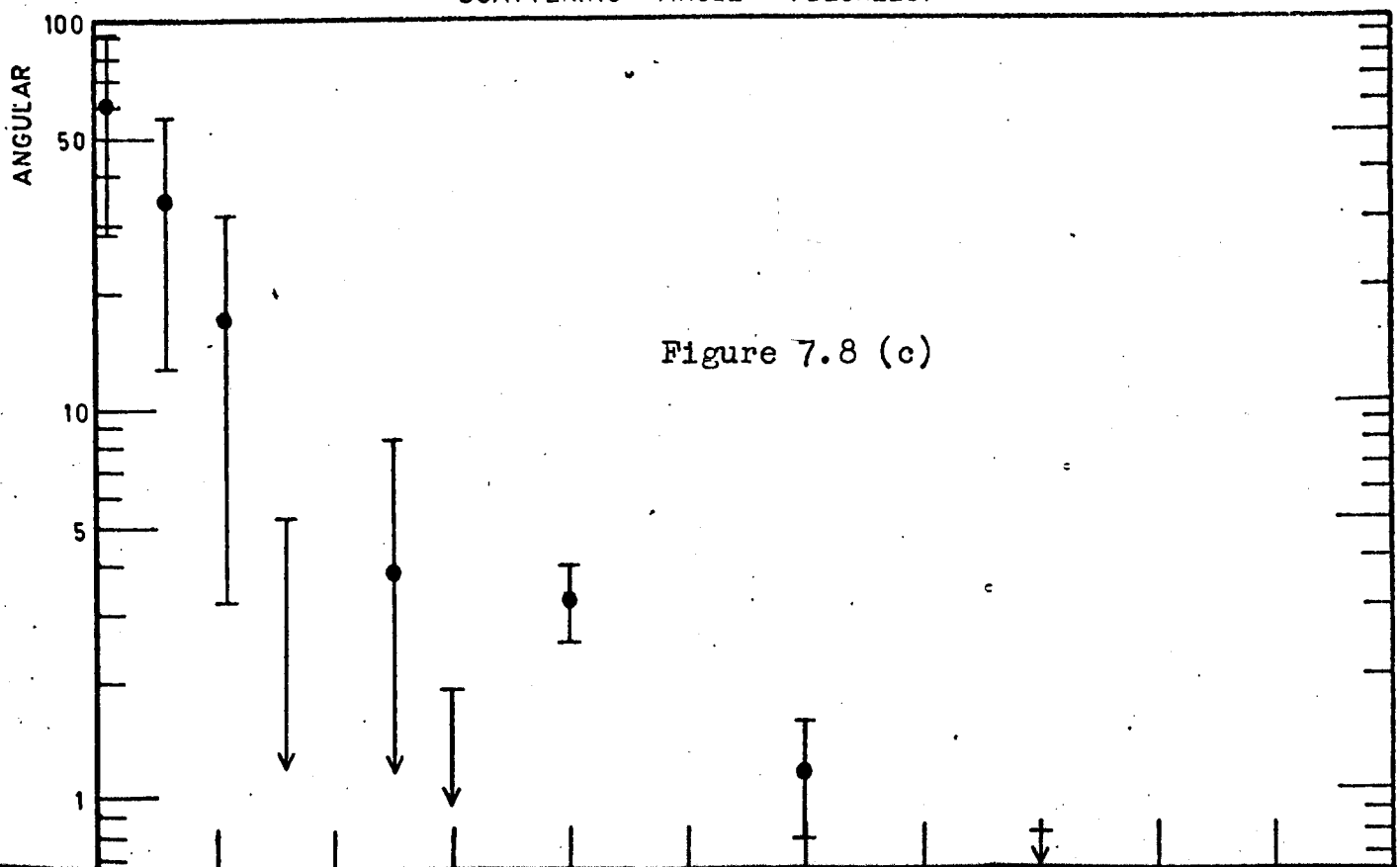

Figure 7.8 (c)

CHAPTER 8.

INELASTIC ELECTRON SCATTERING FROM ATOMIC HYDROGEN

This chapter describes the results of the present investigation into the angular distribution of electrons which have excited the combined 2s and 2p states of atomic hydrogen at 50, 100 and 200 eV. Graphs of the experimental angular distributions are given in this Chapter and numerical values are tabulated in Appendix D. Comparison is also made in this chapter between these results and approximate solutions of the Schrodinger equation for the collision.

8.1 Incident Electron Energy of 50 eV.

8.1.1 Results.

The experimental angular distribution for the combined excitation of the 2s and 2p states of atomic hydrogen obtained at 50 eV is shown in Figure 8.1 by curve (a), together with the associated data points. The individual experiments whose results have been combined to obtain curve (a) are redrawn separately displaced from one another (curves (b)). The angular distribution is observed to decrease rapidly (and almost exponentially) with increasing angle for scattering angles from 18^{o} to 45^{o}, while for angles greater than 45^{o}, the rate of decrease is much less than at smaller angles.

The experimental angular distribution at 50 eV has been reproduced on Figure 8.2, together with the results of calculations (based on the close coupling approximation) by Scott (1965) for electrons whose incident energy is 54 eV. The present angular distribution has been arbitrarily normalized to the close coupling results at 20^{o}. There is good agreement

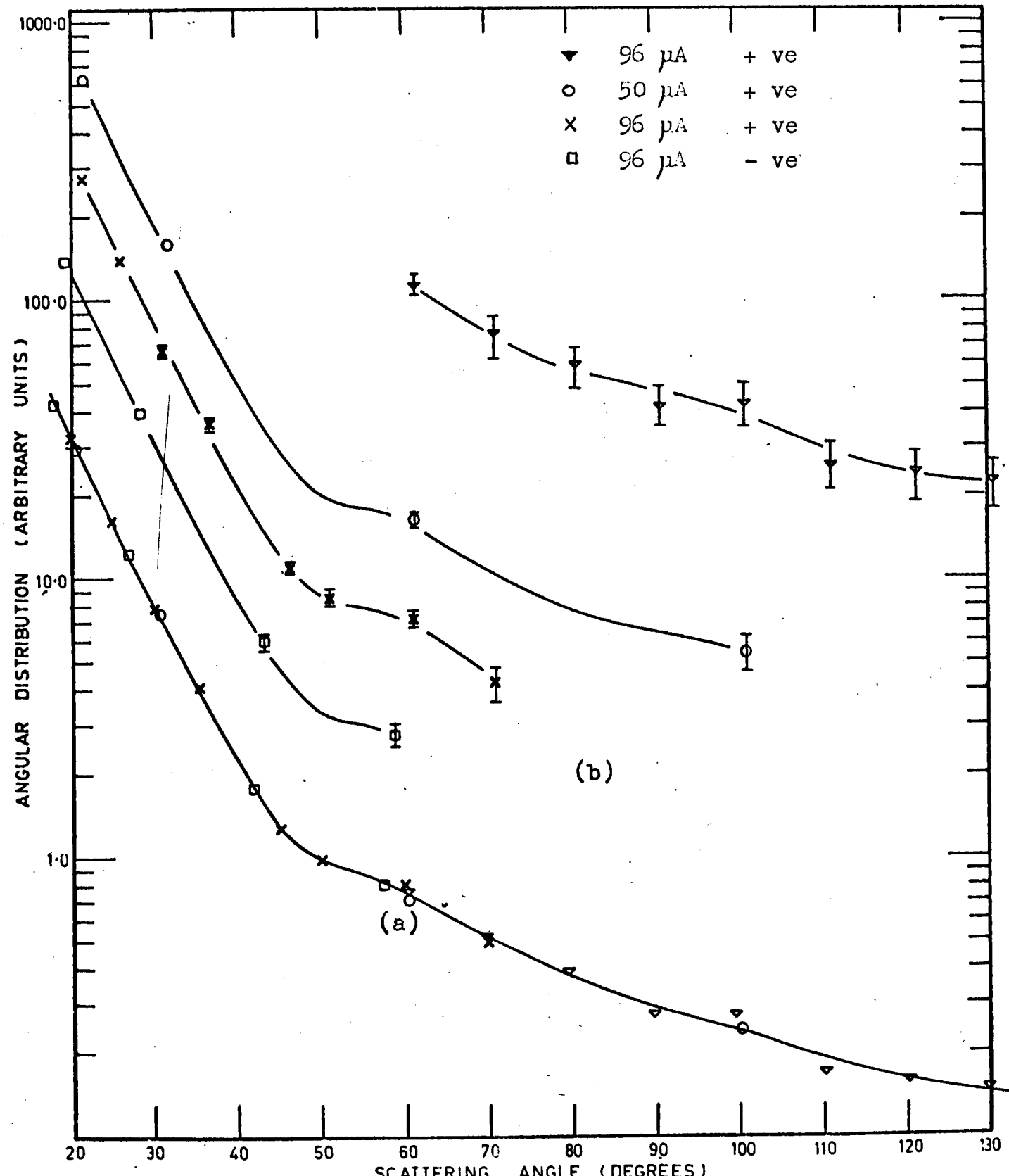

Figure 8.1 Angular distribution of electrons (of 50 eV incident energy) exciting the combined 2s and 2p states of atomic hydrogen.
Curve (a) Experimental angular distribution and associated data points. (———)
Curves (b) Results of individual experiments. The standard deviation $\leq$ 3% unless shown otherwise.

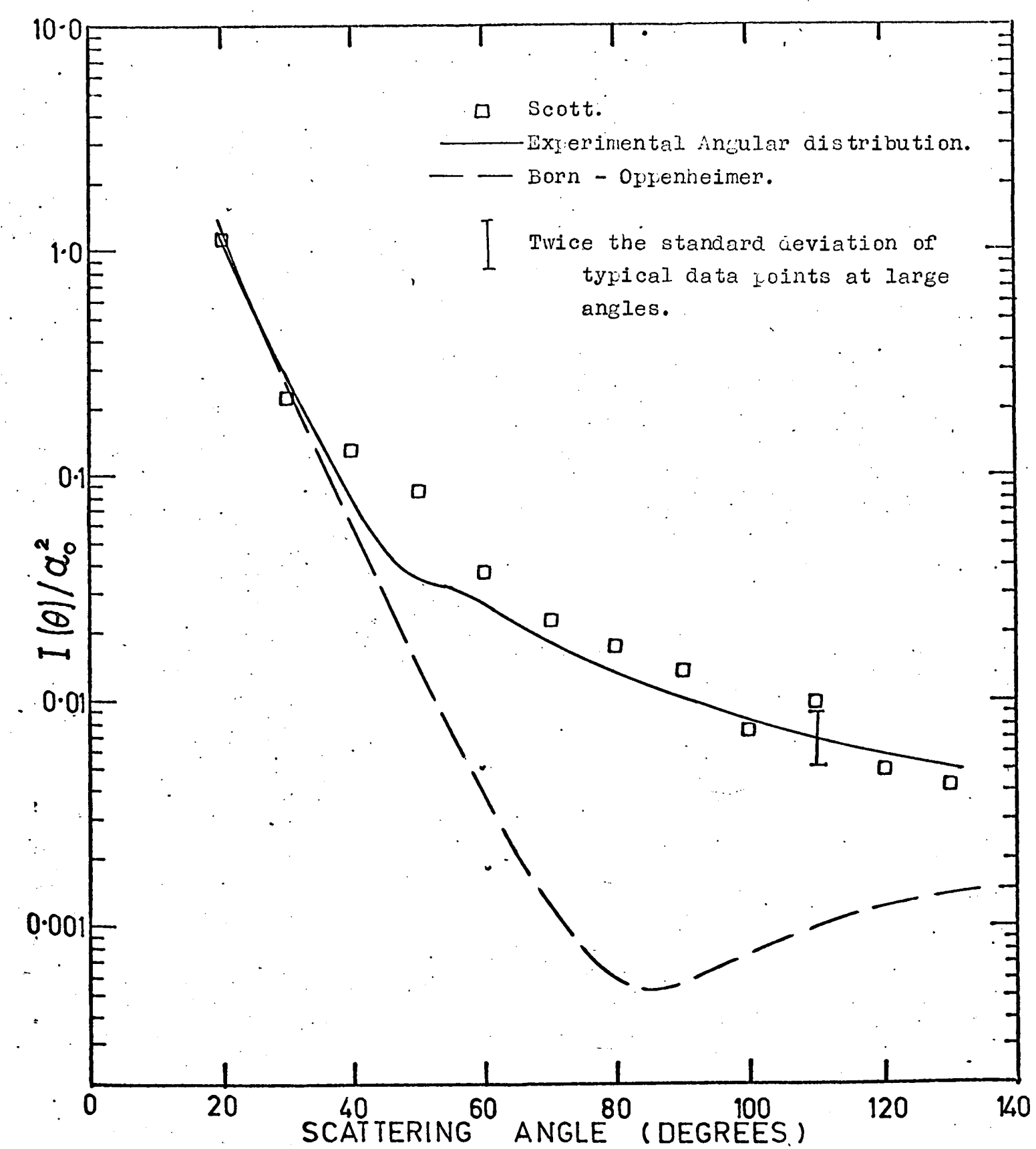

Figure 8.2 The experimental angular distribution of electrons (of 50 eV incident energy) exciting the combined 2s and 2p state of atomic hydrogen normalized at 20^{0} to the differential cross section of Scott (based on the close coupling approximation) for an incident energy of 54 eV.

Shown also is the Born - Oppenheimer approximation for 54 eV incident electrons.

between the shape of the experimental and theoretical results over most of the angular range except near 45^{o}, where the theoretical result decreases less rapidly than the laboratory measurement.

It is interesting to compare this good general agreement obtained for inelastic scattering from atomic hydrogen with the situation for elastic scattering from the same gas at 50 eV. Teubner (1967) observed that if the experimental angular distributions were normalized at 60^{o} to the 54 eV differential cross section for elastic scattering based on the close coupling approximation (calculated also by Scott, 1965), then experiment agreed with theory for angles greater than 60^{o}, but for smaller angles it increased more rapidly than the theoretical result. Attention may also be drawn to the situation for the total cross sections for excitation of the 2s and 2p states of atomic hydrogen (which was discussed earlier in Section 1.2). While not being as good as could be hoped for, the agreement between total cross section measurements and results of close coupling calculations for excitation of the 2s and 2p states is probably within a factor of two.

Comparison of the shape of the Born - Oppenheimer differential cross section (Figure 8.2) at 54 eV with that of the experimental angular distribution, indicates there is good agreement over the angular range extending from 20^{o} to 45^{o}, but quite a considerable difference over the angular range from 45^{o} to 120^{o}. At larger angles the two curves again appear to approach one another.

8.1.2 Discussion.

The calculations performed by Scott (1965) made use of the reactance matrix elements (see Section 6.1.10) computed by Burke, Schey and Smith (1963), in the five state 1s - 2s - 2p close coupling approximation. Although there is considerable controversy over the accuracy of such calculations in the close coupling approximation (because of the limited number of states included, Burke, 1963), they are probably the best results available at the moment (Scott, 1965). The expression used by Scott to derive the differential cross sections I_{2s} and I_{2p} for excitation of the 2s and 2p states respectively is given by equation (6.46). The summation over L_c in (6.46) however, was terminated at $L_c = 26$, because only incident and scattered orbital angular momentum quantum numbers ℓ up to 13 were used by Scott to determine the coefficients $B^S_{L_c}$ of (6.46).

The discrepancy between theory and experiment observed around 45^o, may be due to a number of limitations of Scott's method. One of these limitations has been mentioned previously, namely the exclusion of all states other than 1s, 2s and 2p in the close coupling calculation of the $\underline{R}$ matrix elements by Burke et al. Also, since the $\underline{R}$ matrix elements were only available up to $\ell = 7$, it was necessary to use Born approximation calculations for partial waves $8 \leqslant \ell \leqslant 13$. (Compare this procedure with that of the unitarized Born approximation, Section 6.1.11.) Although this method used the plane wave representation of the partial waves, it still retained the unitary property of the $\underline{R}$ matrix and included some allowance

for coupling of the intermediate states to the initial and final states. Furthermore the convergence of the series of $P_{L_c}(\cos\theta)$ cannot be established by examining the coefficients $B^{S}_{L_c}$, because the cut off in ℓ at $\ell = 13$ prevented the inclusion of all possible ℓ values in the calculation of $B^{S}_{L_c}$ for L_c values greater than 13. This is particularly important for the larger L_c values. For example, if $L_c = \ell_1 + \ell_2$[#], then at $L_c = 26$ only $\ell_1 = 13$ and $\ell_2 = 13$ could be included even though there were substantial contributions from $\ell_1 = 14$, $\ell_2 = 12$ and other combinations of ℓ_1 and ℓ_2.

The results of the calculations of Scott for I_{2s} and I_{2p} are shown on Figure 8.3, together with their sum $(I_{2s} + I_{2p})$. At small scattering angles I_{2s} is small compared with I_{2p}. However, at large angles the relative magnitude of the two differential cross sections fluctuates rapidly because of fine structure in the 2p differential cross section. The results of the present investigation have not possessed sufficient statistical accuracy to establish whether or not there is any fine structure in the sum of I_{2s} and I_{2p}. Since the coupling between the ground states and p states extends out to greater distances than is the case between s states (see Section 6.1.2), the fine structure in I_{2p} at large angles may reduce to that of I_{2s} with the inclusion of ℓ values greater than 13 in the calculation of the $B^{S}_{L_c}$.

A comparison of I_{2s} and I_{2p} at 54 eV calculated in the Born - Oppenheimer approximations are given in Figure 8.4, together with their sum. Particularly significant is the change in relative importance of 2s and 2p excitation between small and

---

#ℓ_1, ℓ_2 are free electron orbital angular momentum quantum numbers.

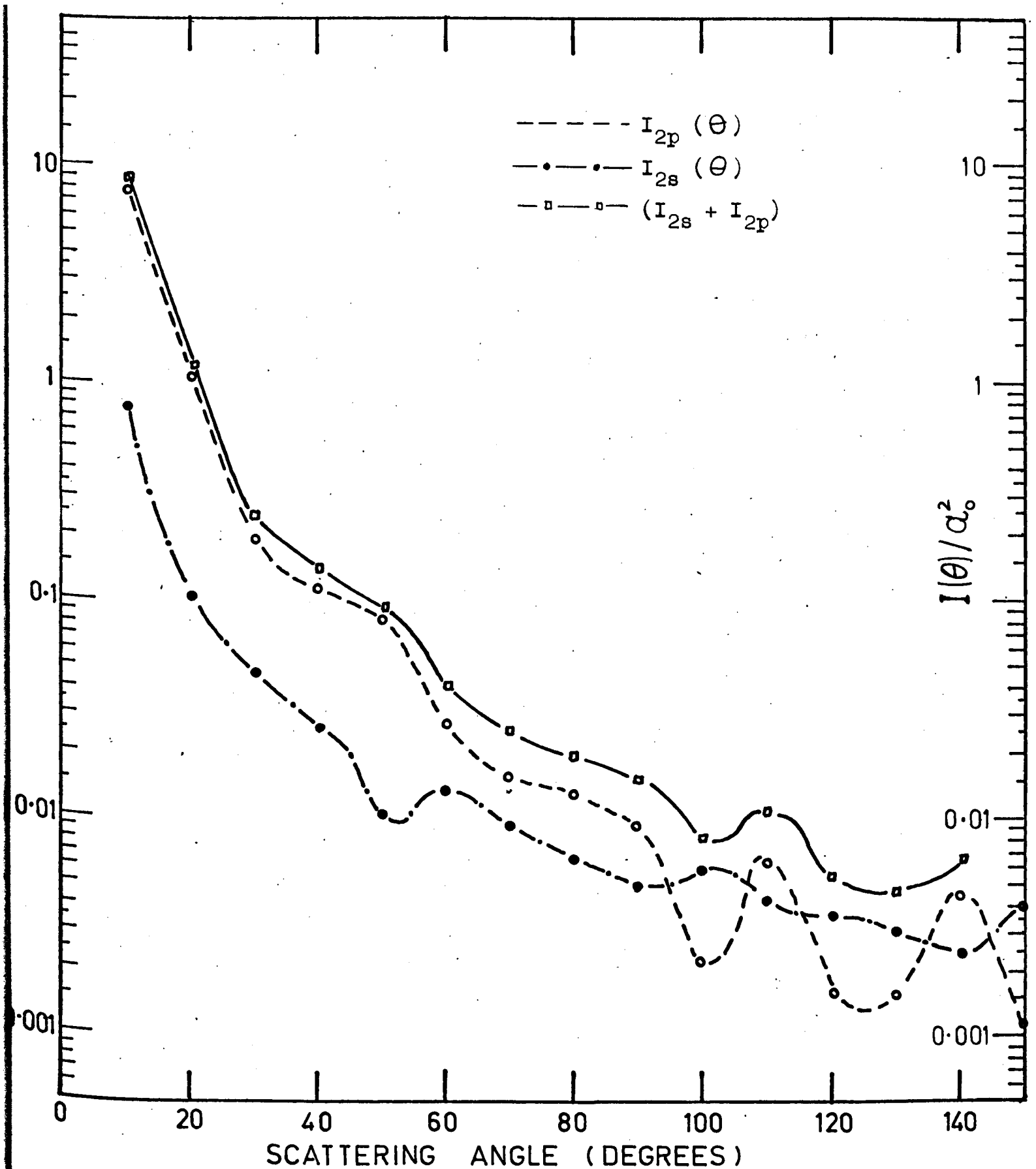

Figure 8.3 Differential cross sections of electrons exciting the 2s and 2p states of atomic hydrogen and the sum of these cross sections for incident electron energy of 54 eV calculated by Scott (based on close coupling approximations).

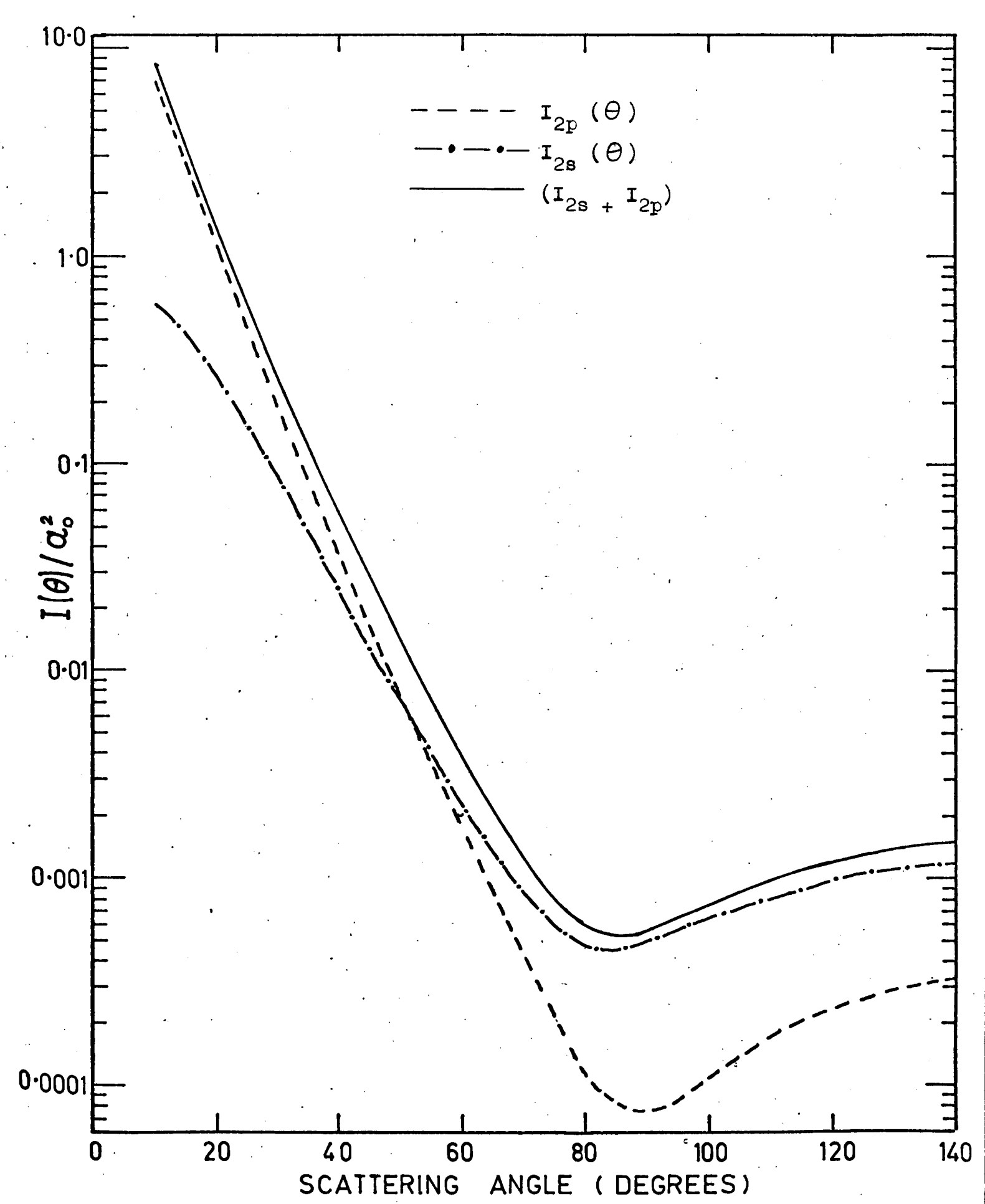

Figure 8.4 Differential cross sections of electrons exciting the 2s and 2p states of atomic hydrogen and the sum of these cross sections for incident electron energy of 54 eV calculated in the Born - Oppenheimer approximation.

large scattering angles.

If it is assumed (from the good agreement between the shapes of the experimental angular distributions and $(I_{2s} + I_{2p})$ calculated by Scott), that the close coupling approximation estimates both I_{2s} and I_{2p} with fair accuracy at 54 eV, then the comparison of close coupling and Born - Oppenheimer approximation values for I_{2s} (Figure 8.5) and I_{2p} (Figure 8.6) respectively, suggests that at large angles, the Born - Oppenheimer approximation underestimates the 2p excitation process by a greater amount than it does the 2s excitation process For both 2s and 2p excitation, it can be seen from Figures 8.5 and 8.6 respectively, that the addition of exchange to the first Born approximation results in the differential cross sections rising for angles greater than 90^{o}.

Shown also on Figure 8.5 is the differential cross section for excitation of the 2s state at 54 eV, calculated in the second Born approximation (including only terms to the third order in the interaction potential) by Kingston, Moiseiwitsch and Skinner (1960). Even though this calculation has included both distortion and polarization of the target atom due to the 1s, 2s and 2p intermediate states, the differential cross section obtained is in no better agreement with the close coupling I_{2s} than is the first Born approximation result. Scott (1968) has also derived I_{2s} at 54 eV using the unitary Born approximation. While the results of this calculation agree with those of the close coupling approximation for small scattering angles, the unitary Born approximation yields values for I_{2s} which are approximately a factor of 5 smaller than the

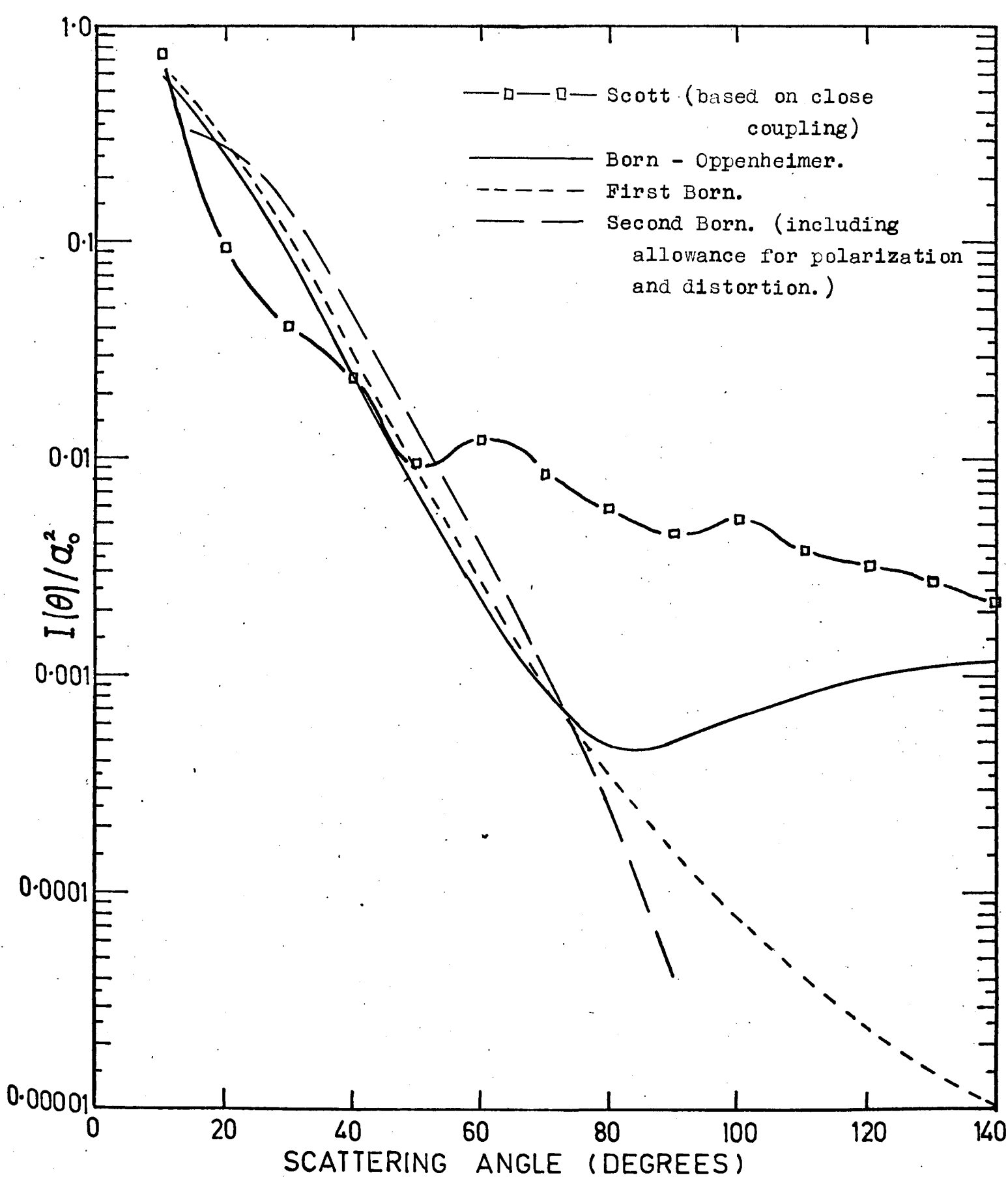

Figure 8.5 Differential cross section of electrons exciting the 2s state of atomic hydrogen in a number of approximations for an incident electron energy of 54 eV.

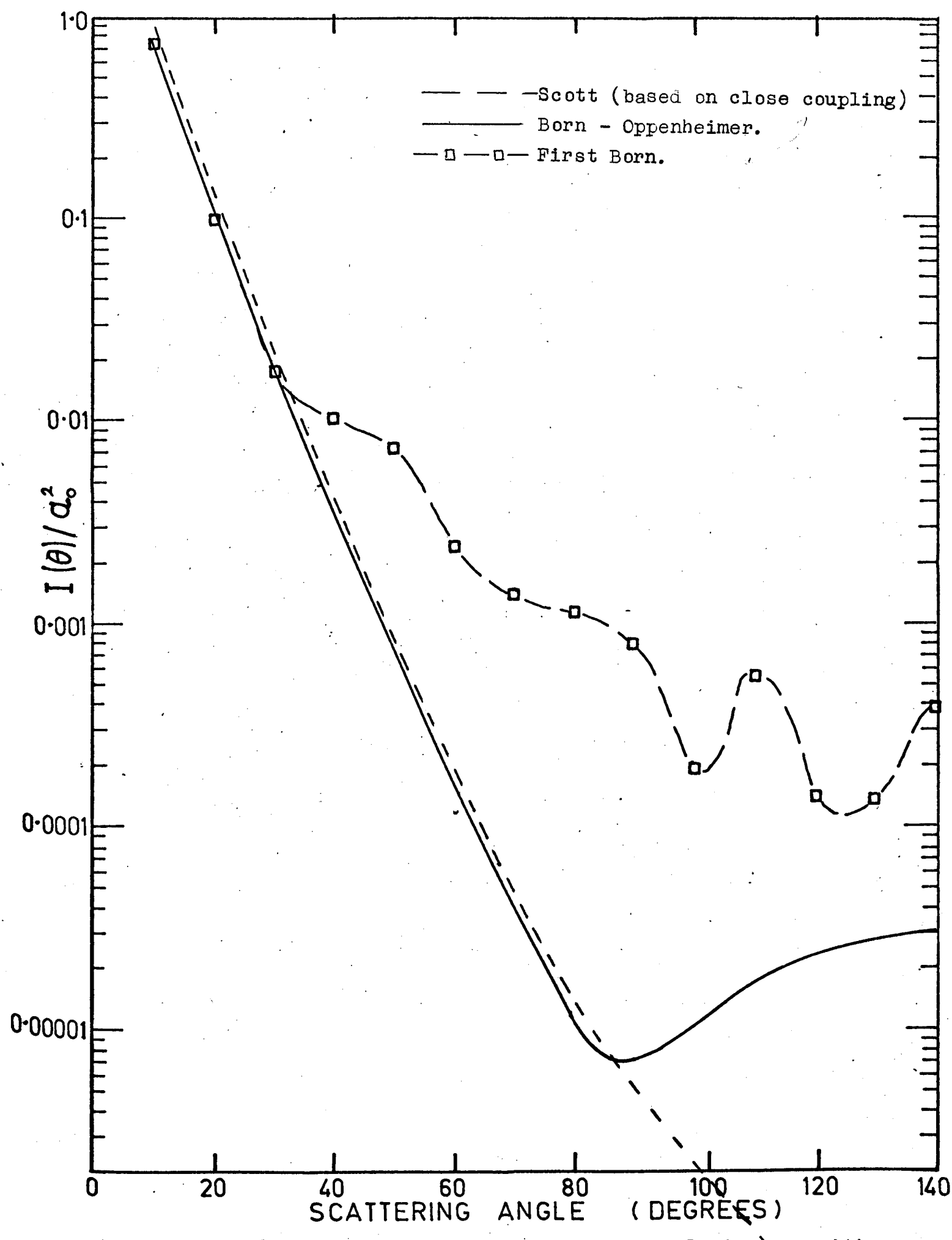

Figure 8.6 Differential cross section of electrons exciting the 2p state of atomic hydrogen in a number of approximations for an incident electron energy of 54 eV.

close coupling approximation results at large angles. Better agreement at large angles could possibly be obtained (if the inclusion of exchange were to have the same effect on the unitary Born approximation as it has on the first Born approximation) by using the Born - Oppenheimer approximation to calculate the $\underline{R}$ matrix elements.

8.2 Incident Electron Energies of 100 and 200 eV.

8.2.1 Results.

The results of the present investigation into the angular distribution of electrons exciting the combined 2s, 2p states of atomic hydrogen at 100 and 200 eV are shown on Figures 8.7 and 8.8 respectively. Data points associated with the 100 eV experimental angular distribution are included in Figure 8.7.

The data points on Figure 8.8 are the results of the single experiment performed at 200 eV. The present results have been arbitrarily normalized to the Born - Oppenheimer differential cross section at each energy. (No close coupling calculations for I (θ) have been performed at energies greater than 54 eV.) It is found that the shape of the differential cross section obtained using the Born - Oppenheimer approximation does not agree with the results of the present investigation at either 100 or 200 eV (see Figures 8.7 and 8.8) over the complete angular range studied.

8.2.2 Discussion.

There is some similarity between the shape of the present results for inelastic scattering and the differential cross section for elastic scattering at large angles, particularly

Figure 8.7 Angular distribution of electrons (of 100 eV incident energy) exciting the combined 2s and 2p states of atomic hydrogen, normalized to the Born - Oppenheimer differential cross section at 25^{o}. Data points associated with the experimental angular distribution are also shown. Their standard deviation $\leqslant$ 3% unless shown otherwise. The shape of the angular distribution for electrons elastically scattered from atomic hydrogen is also shown.

□ 260 μA

o 275 μA

× 95 μA

———— Experimental angular distribution.

—— —— – Born - Oppenheimer differential cross section. $(I_{2s} + I_{2p})$

— — — — Born - Oppenheimer elastic angular distribution.

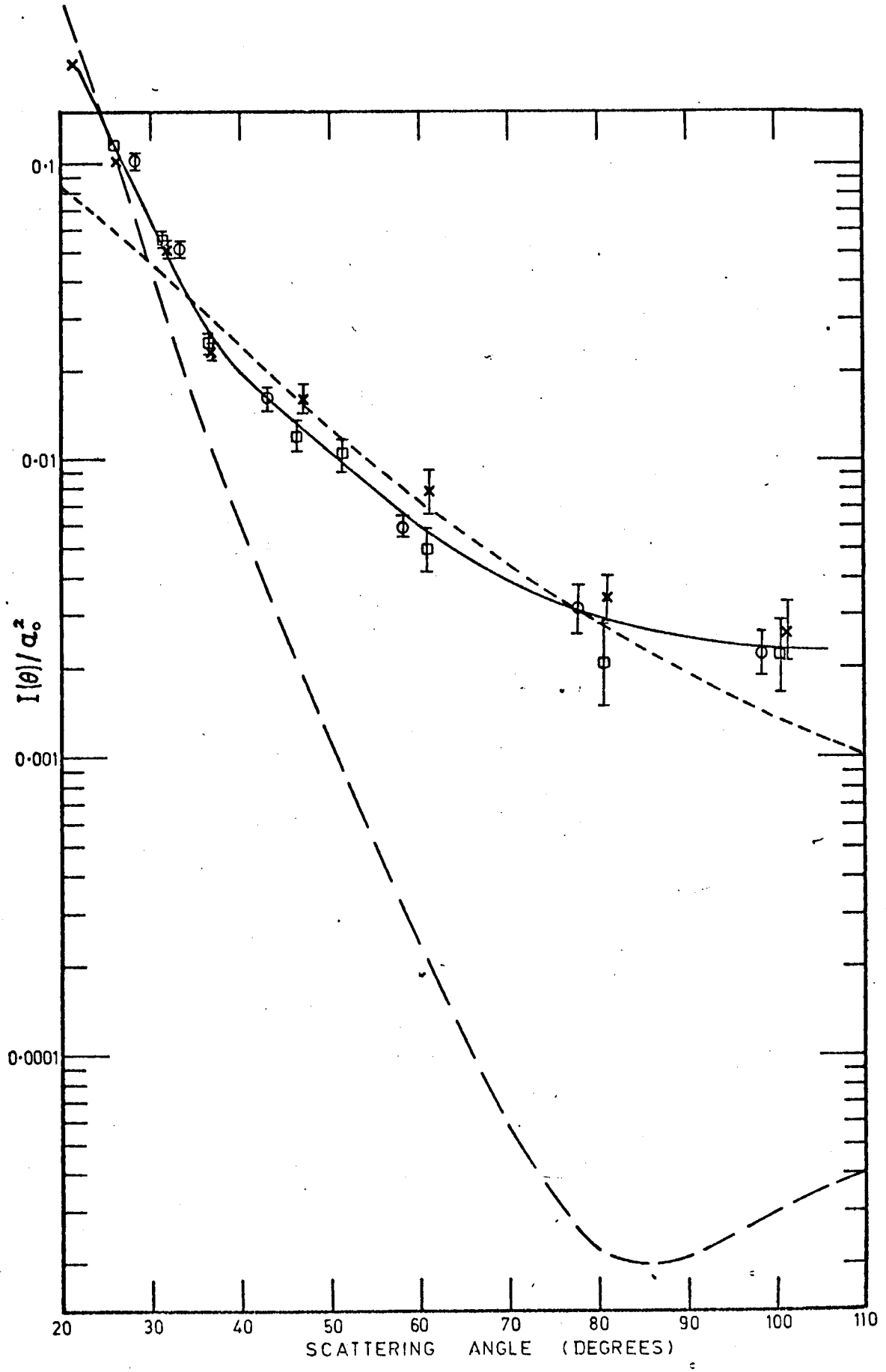
0·1
0·01
0·001
0·0001
I(θ)/a₀²
20
30
40
50
60
70
80
90
100
110
SCATTERING ANGLE (DEGREES)

Figure 8.8 Angular distribution of electrons (of 200 eV incident energy) exciting the combined 2s and 2p states of atomic hydrogen, normalized to the Born - Oppenheimer differential cross section at 25^{o}. Data points associated with the experimental angular distribution are also shown. Their standard deviation $\leq$ 3% unless shown otherwise. The shape of the angular distribution for electrons elastically scattered from atomic hydrogen is also shown.

Also included in the experimental result expected using the Born - Oppenheimer approximation to obtain a worst case calculation for the detection of electrons which have been scattered by two different hydrogen atoms.

a. • Data points. (Standard deviation is 3% at 21^{o}.)

b. — — — Born - Oppenheimer differential cross sections I_{2s} and I_{2p}).

c. — — — — — Born - Oppenheimer elastic angular distribution.

d. —•——•— Predicted experimental result (in the Born - Oppenheimer approximation) allowing for double scattering processes.

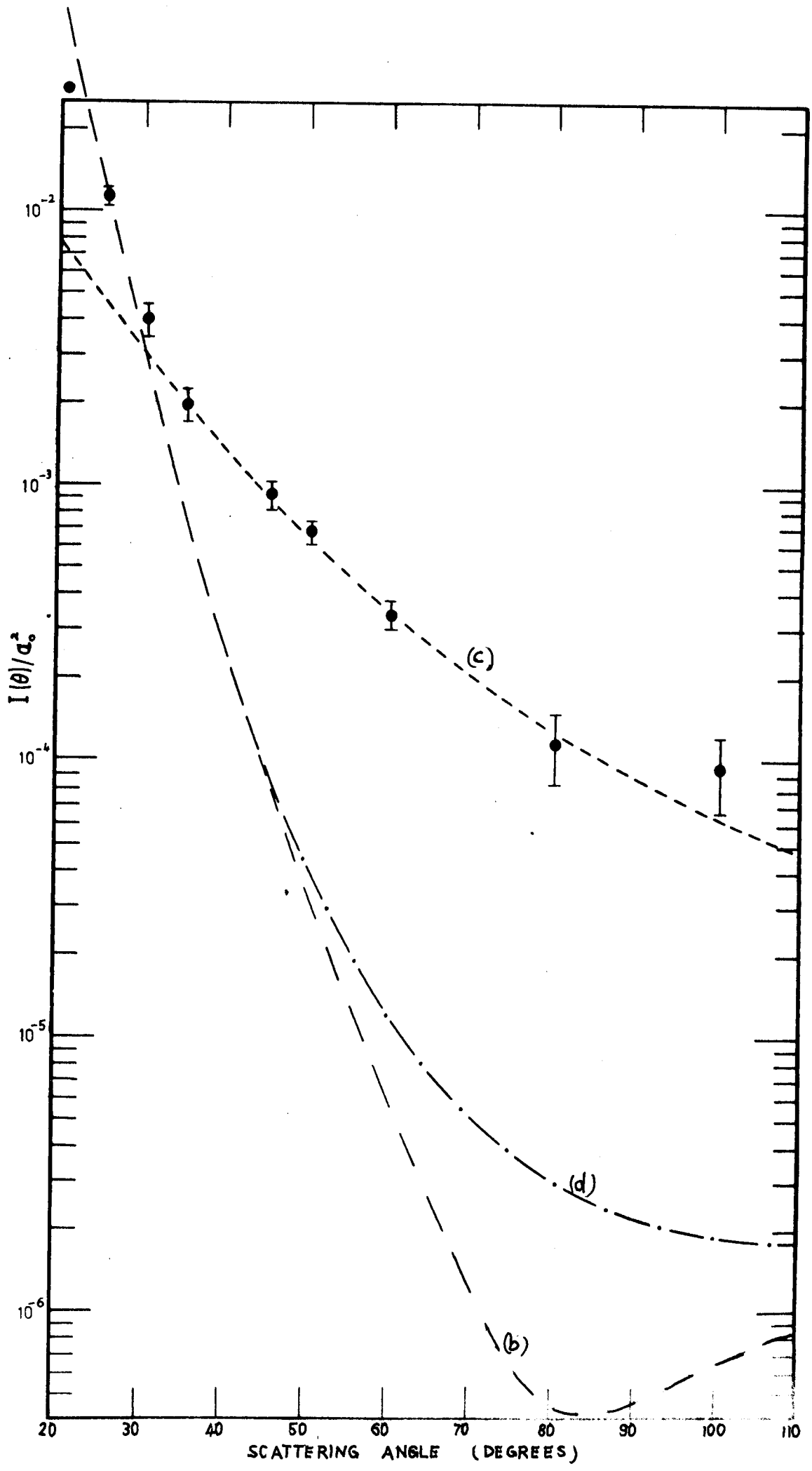
10^{-2}
10^{-3}
10^{-4}
10^{-5}
10^{-6}
$I(\theta)/a_o^2$
(c)
(d)
(b)
20
30
40
50
60
70
80
90
100
110
SCATTERING ANGLE (DEGREES)

at the incident electron energy of 200 eV. This similarity can be seen by examining Figure 8.7 and 8.8, on which Born - Oppenheimer approximation calculations of the differential cross section for elastic scattering have been entered (after renormalizing the elastic scattering calculations to bring them close to the experimental results at large angles). The Born - Oppenheimer approximation for the elastic differential cross section may be used to make this comparison at high energies, since its values lie within a few percent of the first Born approximation results at 200 eV for scattering angles greater than 30^{o}, and the shape of the later result has been shown (Teubner, 1967) to be close to the experimental elastic angular distribution.

The double scattering process discussed in Section 2.1.1 could be expected to produce an inelastic angular distribution for a particular excitation process which would resemble the shape of the elastic differential cross sections, if three quantities were sufficiently large. These are: the number density (present throughout the scattering chamber) of the gas studied, the ratio of the differential cross sections for small and large angle inelastic scattering, and the differential cross section for elastic scattering at large angles.

Let us consider first the results obtained at 200 eV. Then a worst case calculation (see Appendix C) suggests that if the differential cross section for excitation of the 2s and 2p states derived using the Born - Oppenheimer

approximation were correct at 200 eV, then five* times as many electrons suffering the double scattering process would be detected at an angle of 80^{o}, as those observed which had been scattered once only (inelastically). The distorted differential cross section one would expect to observe over the angular range from 20^{o} to 110^{o}, for the worst case conditions considered in Appendix C, has been included on Figure 8.8 (curve (d)). In view of the large discrepancy between the shapes of the distorted differential cross section, and the observed angular distribution, it is believed that double scattering processes have not contributed any significant signal at large angles**, and that the shape of the differential cross section for excitation of the combined 2s and 2p states of atomic hydrogen does resemble that of the elastic differential cross section.

---

* This calculation should not suffer any significant error due to inaccuracies in the Born - Oppenheimer approximation results for inelastic scattering in the forward direction, since this approximation yields correct total cross sections for excitation of the 2s and 2p states at 200 eV (Moiseiwitsch and Smith, 1968c). It may also be noted that the optically allowed transition dominates the inelastic scattering at small angles.

** This could be experimentally verified by measuring the angular distributions for a range of background atomic hydrogen number densities. However this test was not performed during the present investigation because it was not until the apparatus had ceased to be operational that the similarity between elastic and inelastic angular distributions was realized.

Since the ratios of the combined 2s, 2p differential cross sections for small angle and large angle scattering are much less at 100 eV than 200 eV, double scattering process would not have distorted the experimental angular distribution at 100 eV.

While it is believed that the contribution to the scattering at large angles by electrons which collided with two different atoms may be neglected, there is the further possibility that the double collision processes previously discussed might be experienced by an electron while in the field of a single atom. Now the basic assumption on which the Born approximation is derived is that there is only a very weak interaction between an incident electron and an atom, so that the possibility of a transition occurring in the atom during an impact is very small and the chance of two such transitions may be neglected. If, however, the incident electron is moving slow enough, the chance of a transition may be so high that the possibility of two transitions occurring during the collision cannot be ignored. Massey and Mohr (1933) have discussed qualitatively, the general effect such processes would have on the angular distributions, by allowing for the distortion of the wave functions of the incident and scattered electrons by the field of the atom in its ground state and excited state respectively. Owing to the long range of the field for coupling between the ground state and excited state for optically allowed transitions, the incident electron at large distances from the atom may cause a transition in the atom and lose energy in the process without appreciable deviation from its course. During the remainder

of its path in the atomic field, these electrons may be elastically scattered by the field of the excited atom. If the energy loss is small compared with the incident energy, the angular distribution of electrons elastically scattered (after being inelastically scattered in the forward direction) will resemble the angular distribution of electrons which have been elastically scattered only. Furthermore at sufficiently high energy, these two scattering processes will result in angular distributions that are almost indistinguishable from the second double process in which electrons are first elastically scattered and then inelastically scattered in the forward direction. Since the first Born approximation differential cross section for elastic scattering is considerably larger than that for inelastic scattering at large angles (for example in the case of atomic hydrogen it has been shown in Section 6.1.2, that the differential cross sections decrease as K^{-4} for elastic, and K^{-12} and K^{-14} for 2s and 2p excitation respectively), the number of electrons scattered through large angles which have made only the single (inelastic) collision with the atom are insignificant compared with those making double collisions if the incident electron energy is not excessively high.

Calculations performed by Massey and Mohr (1934) using the distorted wave approximation* have shown that at

* A description of the improvement to be expected by using the distorted wave approximation which supplements that already given, is that small changes in the phase shifts reduces the very high cancellation (predicted by the first Born approximation) between the partial waves at large angles.

energies considerably above threshold the angular distribution is dominated by the distortion terms, and have verified the similarity between the elastic and inelastic angular distributions at large angles, for the scattering of electrons from neon and argon. It could therefore be expected, that calculations of the differential cross sections for excitation of the 2s and 2p states of atomic hydrogen which allowed for the distortion of the wave function for the unbound electron (for example distorted wave and second Born approximations), would predict angular distributions which were similar to the general shape observed experimentally.

9.1 Conclusions.

The results of the present investigation into the angular distribution of electrons elastically scattered from helium are in general agreement with both the results of earlier experimentors (see Section 5.3.2) and the shape of the theoretical differential cross section based on the distorted wave approximation (together with a polarization potential) and the first order exchange approximation over the energy range from 25 to 200 eV. The present measurements, when normalized to known experimental differential cross sections at 100 and 200 eV, agree well with the theoretical results over the complete angular range investigated (15^{o} to 120^{o}).

For elastic scattering from molecular hydrogen, the wide discrepancy at large scattering angles between the results of previous experiments and the shape of the theoretical differential cross section (based on the first order exchange approximation), have not been observed. Rather, the results of the present investigation have been in very good agreement with the shape of the theoretical result over the complete angular range investigated at incident electron energies of 100 and 200 eV. However the laboratory measurement still rises more rapidly than the theoretical result for angles less than 40^{o}, and lies above the calculated result for large scattering angles at 50 eV. The discrepancy at small angles may possibly be attributed to no allowance being made for the polarizability of the hydrogen molecule.

Good agreement has been obtained over most of the angular range studied, between the shapes of the experimental

angular distribution (measured at 50 eV) and the differential cross section for 54 eV electrons exciting the combined 2s and 2p states of atomic hydrogen, the calculation of which was based on the close coupling approximation (and supplemented by first Born approximation values for the higher angular momentum states). The experimental result was found to decrease more rapidly than the theoretical curve over a narrow angular range near 45^{o}. The statistical accuracy of the present measurements was insufficient to establish whether the fine structure in the theoretical results for excitation of the 2p state actually exists, or whether this structure is due to inadequacies in the particular calculation performed.

At energies greater than 54 eV, no differential cross section calculations based on the close coupling approximation are currently available for inelastic scattering from atomic hydrogen. Comparison of the present results for excitation of the combined 2s and 2p states of atomic hydrogen with the shape of the differential cross section given by the Born - Oppenheimer approximation reveals the complete inadequacy of this approximation at large scattering angles at 100 and 200 eV - the discrepancy being much greater at 200 eV than at the lower energy. It is suggested that distortion of the incident and scattered electron wave functions dominates the true scattering at large angles, and that this conclusion is supported by the similarity (particularly at 200 eV), between the observed inelastic angular distribution and the shape of the differential cross section for elastic electron scattering from atomic hydrogen.

9.2 Suggestions for further Experimental Studies.

The results of the present investigation have yielded angular distributions only. The accuracy of various theoretical approximations used to study atomic collisions could be checked further, if these measurements were placed on an absolute basis. Such differential cross sections at energies of 100 eV and above could be obtained using the present apparatus, by making use of the known experimental differential cross sections for excitation of the 2^1P state of helium. This may be done by determining the ratio (at a particular angle) of the differential cross sections for excitation of the combined 2s and 2p states of atomic hydrogen and the 2^1P state of helium. The experiment suggested would use a neutral beam consisting of a mixture of helium and highly dissociated molecular hydrogen. The composition of the neutral beam would be determined by mass analysis, and good statistical accuracy could be obtained by scanning repeatedly over the two relevant portions of the energy loss spectrum.

Using a similar procedure, the known angular distributions for elastic electron scattering from molecular and atomic hydrogen, could then be normalized to the experimental combined 2s and 2p differential cross sections. Alternatively, experiments using a neutral beam consisting of molecular hydrogen and helium could be used to normalize the elastic molecular hydrogen angular distributions.

The study of atomic hydrogen may be extended further by separately measuring the angular distributions of electrons exciting the metastable 2s state and the 2p state,

using coincidence detection of the scattered electron and Lyman alpha photon (emitted by the decay of the excited atom) to determine the state produced.

Fused glass capillary arrays are available (Johnson, Stair and Pritchard, 1966) which enable neutral beams of stable gases to be produced whose number density is orders of magnitude larger than that obtained by the slit source used in the present investigation. Replacement of the present slit source by such an array would enable the angular distribution of electrons exciting the $b\left({}^3\Sigma_u^+\right)$ state of molecular hydrogen to be investigated with far greater statistical accuracy than was possible (in a reasonable period of time) during the present investigation.

NORMALIZATION OF ATOMIC HYDROGEN ANGULAR DISTRIBUTIONS

The technique as used by Vriens (1967a) involves measuring the angular dependence of the scattered intensity for a number of transitions and determining the intensity ratio between different inelastic events at a given incident energy and at one or more angles. When the absolute value of one of these inelastic events is known, the measured ratios can be used to normalize the remaining angular distributions. It is intended in subsequent experiments to apply this principle to a beam consisting of a mixture of helium and atomic hydrogen, and normal the combined 2s, 2p excitation of hydrogen to the known 2^1P excitation of helium (Vriens, 1967a). The ratio of elastic to combined 2s, 2p excitation of hydrogen then enables the elastic angular distributions to be normalized.

The facility is therefore incorporated in the A.C.U. to permit two separate energy ranges to be scanned through sequentially so that different scattering events can be included in the automated system without it being necessary to accumulate data from the intermediate energy range.

Similarly two widely spaced inelastic events can be studied in the same gas (as in the case of some of the inert gases), and also the ratio of the elastic to one of the inelastic transitions can be determined by repeatedly scanning over the two energy intervals.

The logic required to include two energy ranges in the automatic scanning sequence is provided by the DOUBLE RANGE CONTROL section of the MASTER CONTROL UNIT.

If individual particles are observed by a system which has a dead time t_d then the number of particles observed n_o during a particular time T is given by

$$n_o = \frac{n_i}{1 + \dot{n}_i t_d} \tag{B.1}$$

where n_i is the number of particles incident during time T and $\dot{n}_i$ is their time rate of arrival.

Consider a modulated beam system in which a single scaler determines the beam signal by adding the beam and background signals during the half cycle for which the neutral beam ison, and subtracting the background during the second half of each cycle. Let N' and 2 M' be the number of beam and background particles respectively incident on a detector during the total time T. Then the observed beam N'_o in time T is given (by using equation B.1)

$$N'_o = \frac{N' + M'}{1 + \frac{N' + M'}{T} 2 t_d} - \frac{M'}{1 + \frac{M'}{T} 2 t_d} \tag{B.2}$$

Let

$$t' = \frac{2 t_d}{T} \tag{B.3}$$

Then substituting equation (B.3) into equation (B.2) and rearranging yields

$$N' = \frac{N'_o (1 + M' t')^2}{1 - (1 + M' t') N'_o t'} \tag{B.4}$$

Let S'_o be the observed total signal for the time T, when the scaler is operated in add mode at all times.

Then

$$S'_o = \frac{N' + M'}{1 + (N' + M')\,t'} + \frac{M'}{1 + M'\,t'} \qquad (B.5)$$

Subtracting equation (B.2) from equation (B.5) yields

$$D'_o = \frac{2\,M'}{1 + M'\,t'} \qquad (B.6)$$

where

$$D'_o = S'_o - N'_o \qquad (B.7)$$

Solving equation (B.6) for the true background count $2M'$ in time T gives

$$2\,M' = \frac{2\,D'_o}{2 - D'_o\,t'} \qquad (B.8)$$

and therefore

$$1 + M'\,t' = \frac{2}{2 - D'_o\,t'} \qquad (B.9)$$

Substituting equation (B.9) in (B.4) and simplifying (noting equation B.7) yields for the corrected beam signal,

$$N' = \frac{4\,N'_o}{(2 - S'_o\,t')^2 - (N'_o\,t')^2} \qquad (B.10)$$

Note - if the beam count rate is small enough,

$$(N'_o\,t')^2 \ll (2 - S'_o\,t')^2$$

Therefore equation (B.10) can be simplified (noting B.3) to yield

$$N' = \frac{N'_o}{\left(1 - \frac{S'_o}{T}\,t_d\right)^2} \qquad (B.11)$$

It is interesting to compare equation (B.11) with the relationship obtained by rearranging equation (B.1) for n_i, namely

$$n_i = \frac{n_o}{1 - \dot{n}_i t_d} \qquad (B.12)$$

It is evident that the dependence of N' (as given by equation B.11) at high total count rates is significantly different from n_i (as given by equation B.12).

In the present equipment the time during which the signal may be scaled is limited to a window interval t_w. Let the modulating frequency be f. Then t' in all the previous expressions becomes

$$\frac{2 t_d}{T f t_w} \qquad (B.13)$$

which is written as t in the following expressions.

Since the time T_{beam} required to produce statistically good observed beam signals N_o is usually much greater than the time T_{total} necessary to obtain satisfactory total observed counts S_o, the expression for S'_o in equations (B.7), (B.10) and (B.11) becomes

$$S'_o = \frac{T_{beam}}{T_{total}} S_o \qquad (B.14)$$

If N_o is the observed beam signal, then the corrected beam signal N_e (from equation B.10) is given by

$$N_e = \frac{4 N_o}{\left(2 - \frac{T_{beam}}{T_{total}} S_o t\right)^2 - (N_o t)^2} \qquad (B.15)$$

and the corrected total background signal $2\,M_e$ (from equation B.8) is

$$2\,M_e = \frac{2\,D_o}{2 - D_o\,t} \qquad (B.16)$$

where

$$D_o = \frac{T_{beam}}{T_{total}}\,S_o - N_o \qquad (B.17)$$

DOUBLE SCATTERING CONTRIBUTION TO INELASTIC SCATTERING.

Consider the particular experiment in which the angular distribution of electrons exciting the combined 2s and 2p states of atomic hydrogen is measured. A double scattering process has been described in Sections 2.1.1 and 5.2.4 (c) that may result in the detection of scattered electrons, which are indistinguishable from electrons making single inelastic collisions. In this process, electrons are elastically scattered through a large angle by atoms in the neutral beam, and inelastically scattered in the forward direction by the atomic hydrogen fraction of the background gas. An approximate formula is derived in this Appendix for the ratio of the number electrons detected at a particular angle that have made double collisions to those making a single collision in which atomic hydrogen is excited to either the 2s or 2p state.

Let L be the path length of electrons which travel from the cathode, through the interaction region, to the entrance aperture of an electron spectrometer. Let n_{beam} and n_{back} be the number densities of atomic hydrogen in the neutral beam and background gas respectively. If $I_{el}(\theta)$ and $I_{in}(\theta)$ are the differential cross sections for elastic and inelastic (combined 2s and 2p) scattering as a function of the angle θ, and $n_{back} L I_{in} \ll 1$, then the probability $P_{back}(\theta)$ of an electron being inelastically scattered by the atomic hydrogen fraction of the background gas in the forward direction (along the defined path) through an angle less than θ_o is given by

$$P_{back}(\theta_o) = 2\pi \int_0^{\theta_o} n_{back} L I_{in}(\theta') \sin\theta' \, d\theta' \qquad (C.1)$$

Since the angle through which electrons may be inelastically scattered and still pass through the interaction region decreases with increasing distance from the interaction region, θ_o is taken to be half the angle subtended by the neutral beam at a point mid-way between the cathode and neutral beam. If b is the average path length of electrons while crossing the neutral beam, then the probability $P_D(\theta)$ of electrons being both inelastically scattered by the background gas and elastically scattered into a narrow range of angles $\Delta\theta$ about the angle θ by the neutral beam, is given by

$$P_D(\theta) = 2\pi n_{beam} b P_{back}(\theta_o) I_{el}(\theta) \sin\theta \Delta\theta \quad (C.2)$$

Let $P_s(\theta)$ be the probability of an electron being scattered once only (inelastically) by atoms in the neutral beam, then

$$P_s(\theta) = 2\pi n_{beam} b I_{in}(\theta) \sin\theta \Delta\theta \quad (C.3)$$

Substituting equating equation (C.1) into (C.2) and dividing by equation (C.3) yields an approximate formula for the ratio of double to single scattering probabilities which is given by

$$\frac{P_D(\theta)}{P_s(\theta)} = 2\pi n_{back} L \int_o^{\theta_o} I_{in}(\theta') \sin(\theta') d\theta' \frac{I_{el}(\theta)}{I_{in}(\theta)} \quad (C.4)$$

Examples: Two examples are shown in Table C.1 of the ratio of $P_D(\theta) / P_s(\theta)$ at an angle of 80^o for the combined excitation of atomic hydrogen to the 2s and 2p states.

In each example the background atomic hydrogen pressure was observed (using the mass spectrometer) to be about $\frac{1}{4}$ of the background molecular hydrogen pressure. (approximately 10^{-6} m.m.)

Numerical values for the differential cross section at 54 eV are the results of the close coupling calculations of Scott (1965, 1968), and at 200 eV are based on the Born - Oppenheimer approximation (see Chapter 8).

Table C.1

Energy (eV)	$I_{in}(80)$ (a_o^2)	$I_{el}(80)$ (a_o^2)	$\int_0^{5^\circ} I_{in}(\theta) \sin\theta \, d\theta$ (a_o^2)	$\frac{P_D(80)}{P_s(80)}$
54	1.8×10^{-2}	9×10^{-2}	3.3	5×10^{-4}
200	5×10^{-7}	6×10^{-3}	10	5

n_{back} = 10^{10} atoms per cm^3 at room temperature.

L = 20 cms

θ_o = 5°

Since the calculation performed here should provide an approximate upper limit for the ratio of double to single scattering at the angle 80°, it is clear from Table C.1 that there was no significant double scattering at 54 eV. However, if the Born - Oppenheimer approximation is valid at 200 eV, double scattering could possibly have been responsible at large angles for much of the observed beam signal at that energy.

This subject is discussed further in Chapter 8.

ANGULAR DISTRIBUTIONS OF ELECTRONS EXCITING THE COMBINED 2s AND 2p STATES OF ATOMIC HYDROGEN.

For convenience of tabulation, the numerical results at 50 and 100 eV, have been taken directly from the experimental angular distributions (Figures 8.1 and 8.7 respectively), and the statistical errors* quoted represent the standard deviation of typical data points obtained at or near the angles specified. The individual data points (see Figure 8.8) and their standard deviations are given for the results at 200 eV. The maximum systematic error is believed to be less than 10% (see Section 5.4).

ANGLE	50 eV			100 eV		
20^0	6400	±	2%	2500	±	3%
25^0	3050	±	2%	1300	±	3%
30^0	1550	±	3%	600	±	8%
35^0	800	±	6%	300	±	10%
40^0	425	±	6%	190	±	10%
45^0	250	±	8%	140	±	10%
50^0	190	±	9%	100	±	10%
55^0	170	±	12%	74	±	15%
60^0	150	±	14%	55	±	17%
70^0	100	±	18%	36	±	25%
80^0	72	±	20%	28	±	25%
90^0	56	±	20%	24	±	20%
100^0	48	±	20%	22	±	20%
110^0	38	±	25%			
120^0	32	±	25%			
130^0	29	±	25%			

ANGLE	200 eV		
21°	2100	±	3%
25.5°	840	±	10%
30.5°	300	±	15%
35.5°	150	±	18%
45.5°	68	±	13%
50.2°	50	±	12%
60°	25	±	16%
80°	8.5	±	30%
100°	7	±	35%

* The statistical errors of these measurements could be determined more accurately by using the method of least squares to combine the data from the individual experiments to produce a single angular distribution.

BIBLIOGRAPHY

AKERIB, R., and BOROWITZ, S., 1961, Phys. Rev. 122, 1177.

ALTSHULER, S., 1963, J. Geophys. Res. 68, 4707.

ARNOT, F.L., 1931, Proc. Roy. Soc. (London) A133, 615.

ARRECHI, F.T., GATTI, E., and SONA, A., 1966, Rev. Sci. Instr. 37, 942.

BATES, D.R., FUNDAMINSKY, A., LEECH, J.W., and MASSEY, H.S.W., 1950, Phil. Trans. Roy. Soc. (London) A243, 93.

BELL, K.L., and MOISEIWITSCH, B.L., 1963, Proc. Roy. Soc. (London) A276, 346.

BOWEN, H.C., CHENEVIX-TRENCH, T., DRACKLEY, S.D., FAUST, R.C., and SAUNDERS, R.A., 1967, J. Sci. Instrum. 44, 343.

BOYD, R.L.F., and GREEN, G.W., 1958, Proc. Phys. Soc. (London) 71, 351.

BRIGLIA, D.D., and RAPP, D., 1965, J. Chem. Phys. 42, 3201.

BULLARD, E.C., and MASSEY, H.S.W., 1931a, Proc. Roy. Soc. (London) A130, 579.

BULLARD, E.C., and MASSEY, H.S.W., 1931b, Proc. Roy. Soc. (London) A133, 637.

BURKE, P.G., 1963, Proc. Phys. Soc. (London) 82, 443.

BURKE, P.G., ORMONDE, S., and WHITAKER, W., 1967, Proc. Phys. Soc., 92, 319.

BURKE, P.G., SCHEY, H.M., and SMITH, K., 1963, Phys. Rev. 129, 1258.

BURKE, P.G., and SEATON, M.J., 1961, Proc. Phys. Soc. (London) 77, 199.

BURKE, P.G., and SMITH, K., 1962, Revs. Modern Phys. 34, 458.

CARTWRIGHT, D.C., and KUPPERMANN, A., 1967, Phys. Rev. 163, 86.

CHAMBERLAIN, G.E., SIMPSON, J.A., MIELCZAREK, S.R., and KUYATT, C.E., 1967, J. Chem. Phys. 47, 4266.

CHAMBERLAIN, G.E., SMITH, S.J., and HEDDLE, D.W.O., 1964, Phys. Rev. Letters 12, 647.

COLEMAN, J.P. and McDOWELL, M.R.C., 1965, in Abstracts of "The Fourth International Conference on the Physics of Electronic and Atomic Collisions (Quebec, 2-6 August, 1965) (Science Bookcrafters, Inc., Hastings-on-Hudson, New York), P.23.

CORRIGAN, S.J.B., 1965, J. Chem. Phys. 43, 4381.

CROTHERS, D., 1967, Proc. Phys. Soc. (London) 91, 855.

CROTHERS, D., and McCARROLL, R., 1965, Proc. Phys. Soc. (London) 86, 753.

DANCE, D.F., HARRISON, M.F.A., and SMITH, A.C.H., 1966, Proc. Roy. Soc. A290, 74.

FITE, W.L., 1962, in "Atomic and Molecular Processes", D.R. BATES, Ed. (Academic Press Inc., New York), p.421.

FITE, W.L., and BRACKMAN, R.T., 1958a, Phys. Rev. 112, 1141.

FITE, W.L., and BRACKMAN, R.T., 1958b, Phys. Rev. 112, 1151.

FITE, W.L., GERJUOY, E., 1965, Science, 150, 516.

FITE, W.L., STEBBINGS, R.F., and BRACKMAN, R.T., 1959, Phys. Rev. 116, 356.

FROST, R.D., PURL, O.T., and JOHNSON, H.R., 1962, Proc. I.R.E. 50, 1800.

GILBODY, H.B., STEBBINGS, R.F., and FITE, W.F., 1961, Phys. Rev. 121, 794.

GOLDEN, D.E., and BANDEL, H.W., 1965, Phys. Rev. Letters 14, 1010.

HADDAD, G.N., 1967, Thesis, University of Adelaide, Section 4.4.7 and Appendix C.

HARROWER, G.A., 1955, Rev. Sci. Inst. 26, 850.

HASS, G.A., 1967, in "Methods of Experimental Physics", HUGHES, V.W., and SCHULTZ, H.L., Eds. (Academic Press Inc.), (New York), Vol. 4A, p.1.

HEDDLE, D.W.O., and KEESING, R.G.W., 1967a, Proc. Roy. Soc.A299, 212.

HEDDLE, D.W.O., and KEESING, R.G.W., 1967b, Proc.Phys. Soc. 91, 510.

HEIDEMAN, H.G.M., KUYATT, C.E., and CHAMBERLAIN, G.E., 1966, J. Chem. Phys. 44, 440.

HEITLER, W., and LONDON, F., 1927, Zeits, f. Phys. 44, 455.

HERZBERG, G., 1950a, "Molecular Spectra and Molecular Structure, Diatomic Molecules." (D. Van Nostrand Co. Inc., Princeton, New Jersey) p. 149.

HERZBERG, G., 1950b, "Molecular Spectra and Molecular Structure, Diatomic Molecules." (D. Van Nostrand Co. Inc., Princeton, New Jersey) p. 199.

HILS, D., KLEINPOPPEN, H., and KOSCHMEIDER, H., 1966, Proc. Phys. Soc. (London) 89, 35.

HUGHES, A.L., and McMILLEN, J.H., 1932a, Phys. Rev. 39, 585.

HUGHES, A.L., and McMILLEN, J.H., 1932b, Phys. Rev. 41, 39.

HUGHES, A.L., McMILLEN, J.H., and WEBB, G.M., 1932, Phys. Rev. 41, 154.

JOHNSON, J.C., STAIR, A.T., and PRITCHARD, J.L., 1966, J. Appl. Phys. 37, 1551.

JONES, H., and WIDDINGTON, R., 1928, Phil, Mag. 6, 889.

KHARE, S.P., 1966, Phys. Rev. 149, 33.

KHARE, S.P., and MOISEIWITSCH, B.L., 1965, Proc. Phys. Soc. (London) 85, 821.

KHASHABA, S., and MASSEY, H.S.W., 1958, Proc. Phys. Soc. (London) 71, 574.

KINGSTON, A.E., MOISEIWITSCH, B.L., and SKINNER, B.G., 1960, Proc. Roy. Soc. (London) A258, 245.

KINGSTON, A.E., and SKINNER, B.G., 1961, Proc. Phys. Soc. 77, 724.

KUPPERMANN, A., and RAFF, L.M., 1963, Disc. Faraday Soc., No. 35, p. 30.

KUYATT, C.E., and SIMPSON, J.A., 1967, Rev. Sci. Instr. 38, 103.

LAMB, W.E., and RETHERFORD, R.C., 1950, Phys. Rev. 79, 549.

LAMB, W.E., and RETHERFORD, R.C., 1951, Phys. Rev. 81, 222.

LEVENTHAL, M., ROBISCOE, R.T., and LEA, K.R., 1967, Phys. Rev. 158, 49.

LEW, H., 1967a, Methods of Experimental Physics, HUGHES, V.W., and SCHULTZ, H.L., Eds. (Academic Press Inc., New York, 1967), Vol. 4A, 178.

LEW, H., 1967b, Methods of Experimental Physics, HUGHES, V.W., and SCHULTZ, H.L., Eds. (Academic Press Inc., New York, 1967), Vol. 4A, 160.

LICHTEN, W., and SCHULTZ, S., 1959, Phys. Rev. 116, 1132.

MARRIOTT, R., 1958, Proc. Phys. Soc. (London) 72, 121.

MARTON, L., and SIMPSON, J.A., 1958, Rev. Sci. Instr. 29, 567.

MASSEY, H.S.W., 1930, Proc. Roy Soc. (London) A.129, 616.

MASSEY, H.S.W., 1956, in "Handbuch der Physik", S. FLUGGE, Ed. (Springer - Verlog, Berlin) Vol.36/II, P.307.

MASSEY, H.S.W., 1956a, in "Handbuch der Physik, S. FLUGGE, Ed. (Springer - Verlog, Berlin) Vol. 36/2,p.396-408.

MASSEY, H.S.W., 1964, in Atomic Collision Processes, M.R.C. McDOWELL, Ed. (North-Holland Publ. Co., Amsterdam, P.3. (Proceedings of the Third International Conference on the Physics of Electronic and Atomic Collisions (London, 22-26 July, 1963).

MASSEY, H.S.W., and BURHOP, E.H.S., 1952a, "Electronic and Ionic Impact Phenomena" (Oxford Clarendon Press).

MASSEY, H.S.W., and BURHOP, E.H.S., 1952b, "Electronic and Ionic Impact Phenomena" (Oxford Clarendon Press)p.84.

MASSEY, H.S.W., and MOHR, C.B.O., 1932a, Proc. Roy. Soc. (London) A135, 258.

MASSEY, H.S.W., and MOHR, C.B.O., 1932b, Proc. Roy. Soc. (London) A136, 289.

MASSEY, H.S.W., and MOHR, C.B.O., 1933, Proc. Roy. Soc. (London) A140, 613.

MASSEY, H.S.W, and MOHR, C.B.O., 1934, Proc. Roy. Soc. A.146,880.

McDANIEL, E.W., 1964, "Collision Phenomena in Ionized Gases", (John Wiley, New York).

McGOWAN, J.W., and FINEMAN, M.A., 1965, Abstracts of Papers, IVth International Conference on the Physics of Electronic and Atomic Collisions, Quebec, 1965 (Science Bookcrafters, Inc., New York, 1965),p.429.

MEHR, J., 1967, Z. Physik, 198, 345.

MILLER, K.J., and KRAUSS, M., 1967, J. Chem. Phys. 47, 3754.

MOHR, C.B.O., and NICOLL, F.H., 1932, Proc. Roy. Soc. (London) A.138, 469.

MOISEIWITSCH, B.L., 1962a, in "Atomic and Molecular Processes", D.R. BATES, Ed. (Academic Press Inc., New York, 1962), p. 300.

MOISEIWITSCH, B.L., 1962b, in "Atomic and Molecular Processes", D.R. BATES, Ed. (Academic Press Inc., New York, 1962), p. 304.

MOISEIWITSCH, B.L., and PERRIN, R., 1965, Proc. Phys. Soc.(London) 85, 51.

MOISEIWITSCH, B.L., and SMITH, S.J., 1968a, Rev. Mod. Phys.40, 238

MOISEIWITSCH, B.L., and SMITH, S.J., 1968b, Rev. Mod. Phys.40,286.

MOISEIWITSCH, B.L., and SMITH, S.J., 1968c, Rev. Mod. Phys.40,238. Tables 12, 13 and Figures 12, 13.

MOISEIWITSCH, B.L., and SMITH, S.J., 1968d, Rev. Mod.Phys.40, 278.

MORSE, P.M., and ALLIS, W.P., 1933, Phys. Rev. 44, 269.

MOTT, N.F., and MASSEY, H.S.W., 1965a, "Theory of Atomic Collisions" (Clarendon Press, Oxford, England) 3rd ed., Chap.2.

MOTT, N.F., and MASSEY, H.S.W., 1965b, "Theory of Atomic Collisions" (Clarendon Press, Oxford, England) 3rd ed., Chap.15

MOTT, N.F., and MASSEY, H.S.W., 1965c, "Theory of Atomic Collisions" (Clarendon Press, Oxford, England) 3rd ed., p. 508.

NEYNABER, R.H., LAWRENCE, L.M., ROTHE, E.W., and TRUJILLO, S.M., 1961, Phys. Rev. 123, 148.

NEYNABER, R.H., MARINO, L.L., ROTHE, E.W., and TRUJILLO, S.M., 1961, Phys. Rev. 124, 135.

OMIDVAR, K., 1964, NASA Technical Note TN-D-2145.

OMIDVAR, K., 1967, Phys. Rev. Letters 18, 153.

OPPENHEIMER, J.R., 1928, Phys. Rev., 32, 361.

ORNSTEIN, L.S., and LINDEMAN, H., 1933, Z. Physik, 80, 525.

PERCIVAL, I.C., and SEATON, M.J., 1957, Proc. Cambridge Phil. Soc. 53, 654.

PETERKOP, R., and VELDRE, V.Ya., 1966, in "Advances in Atomic and Molecular Physics", D.R. BATES and I.ESTERMAN, Eds. (Academic Press Inc., New York), Vol.2,p.264.

PORTEUS, J.O., 1963, in Atomic Collision Processes, M.R.C. McDOWELL, Ed. (North-Holland Publ. Co., Amsterdam, p.72. (Proceedings of the Third International Conference on the Physics of Electronic and Atomic Collisions (London, 22-26 July, 1963).

ROZSNYAI, B.F., 1967, J. Chem. Phys. 47, 4102.

RUDD, M.E., 1966, Rev. Sci, Inst. 37, 971.

SCHIFF, L.I., 1955, "Quantum Mechanics" (McGraw-Hill, New York, 2nd ed.) Chap.9, p.239.

SCOTT, B.L., 1965, Phys. Rev. 140, A.699.

SCOTT, B.L., 1968, Private Communication.

SEATON, M.J., 1962, in "Atomic and Molecular Processes", D.R. BATES, Ed. (Academic Press Inc. New York, 1962) p.398.

SIMPSON, J.A., 1961, Rev. Sci. Instr., 32, 1283.

SIMPSON, J.A., 1964, Rev. Sci. Instr. 35, 1698.

SIMPSON, J.A., 1967, in "Methods of Experimental Physics", HUGHES, V.W., and SCHULTZ, H.L., Eds, (Academic Press Inc., New York), Vol.4A, p.84.

SIMPSON, J.A., and KUYATT, C.E., 1963, Rev. Sci. Instr. 34, 265.

SLATER, J.C., 1963, "Quantum Theory of Molecules and Solids" (McGraw-Hill Book Co., Inc., New York), p.7.

SMITH, A.C.H., CAPLINGER, E., NEYNABER, R.H., ROTHE, E.W., and TRUJILLO, S.M., 1962, Phys. Rev. 127, 1647.

SMITH, S.J., 1965 in abstracts of "The Fourth International Conference on the Physics of Electronic and Atomic Collisions (Quebec, 2-6 August, 1965) (Science Bookcrafters, Inc., Hastings-on-Hudson, New York), p. 377.

ST. JOHN, R.M., LIN, C.C., STANTON, R.L., WEST, H.D., SWEENEY, J.P., and RINEHART, E.A., 1962, Rev. Sci. Instr. 33, 1089.

STEBBINGS, R.F., FITE, W.L., HUMMER, D.G., and BRACKMANN, R.T., 1961, Phys. Rev. 124, 2051.

TEUBNER, P.J.O., 1967, Thesis, University of Adelaide.

VRIENS, L., SIMPSON, J.A., and MIELCZARCK, S.R., 1968a, Phys. Rev. 165, 7.

VRIENS, L., KUYATT, C.E., and MIELCZARCK, S.R., 1968b, Phys. Rev. 170, 163.

WEBB, G.M., 1935a, Phys. Rev. 47, 379.

WEBB, G.M., 1935b, Phys. Rev. 47, 384.

WILLIAMS, J.F., and McGOWAN, J.W., 1968, Phys. Rev. 21, 719.

WILLIAMS, K.G., 1968, "Data Handling System for the Phase Sensitive Detection of Modulated Digital Signals", Internal report, University of Adelaide, Sections 4 and 5.

WINANS, J.G., and STUECKELBERG, E.C.G., 1928, Proc. Nat. Acad. Sci. 14, 867.

WU, T.Y. (1960), Can.J. Phys. 38, 1654 (1960).

WU, T.Y. and OHMURA, T., 1962, "Quantum Theory of Scattering" "Prentice Hall Inc., Englewood Cliffs, N.J.),p.xx.